

A chaotic lattice field theory in one dimension

H Liang and P Cvitanović

School of Physics, Georgia Institute of Technology, Atlanta, GA 30332-0430, USA

E-mail: predrag.cvitanovic@physics.gatech.edu

May 20, 2022

Abstract. Motivated by Gutzwiller’s semiclassical quantization, in which unstable periodic orbits of low-dimensional deterministic dynamics serve as a WKB ‘skeleton’ for chaotic quantum mechanics, we construct the corresponding deterministic skeleton for infinite-dimensional lattice-discretized scalar field theories. In the field-theoretical formulation, there is no evolution in time, and there is no ‘Lyapunov horizon’; there is only an enumeration of lattice states that contribute to the theory’s partition sum, each a global spatiotemporal solution of system’s deterministic Euler–Lagrange equations.

The reformulation aligns ‘chaos theory’ with the standard solid state, field theory, and statistical mechanics. In a spatiotemporal, crystallographer formulation, the time-periodic orbits of dynamical systems theory are replaced by periodic d -dimensional Bravais cell tilings of spacetime, each weighted by the inverse of its instability, its Hill determinant. Hyperbolic shadowing of large cells by smaller ones ensures that the predictions of the theory are dominated by the smallest Bravais cells.

The form of the partition function of a given field theory is determined by the group of its spatiotemporal symmetries, that is, by the space group of its lattice discretization, best studied on its reciprocal lattice. Already 1-dimensional lattice discretization is of sufficient interest to be the focus of this paper. In particular, from a spatiotemporal field theory perspective, ‘time’-reversal is a purely crystallographic notion, a reflection point group, leading to a novel, symmetry quotienting perspective of time-reversible theories and associated topological zeta functions.

PACS numbers: 02.20.-a, 05.45.-a, 05.45.Jn, 47.27.ed

Keywords: chaotic field theory, many-particle systems, coupled map lattices, periodic orbits, symbolic dynamics, cat maps

Submitted to: *J. Phys. A: Math. Theor.*

Dedicated to Fritz Haake 1941–2019 [87].

The year was 1988. Roberto Artuso, Erik Aurell and P.C. had just worked out the cycle expansions formulation of the deterministic and semiclassical chaotic systems [9, 10], and a Niels Bohr Institute “Quantum Chaos Symposium” was organized to introduce the newfangled theory to unbelievers (for a history, see [ChaosBook](#)

Append. A.4 Periodic orbit theory). In the first row (here figure 1) of the famed auditorium where long ago Niels Bohr and his colleagues used to nod off, sat a man with an impressive butterfly bow tie and a big smile. At the end of our presentation, Fritz –for that was Fritz Haake– stood up and exclaimed

“Amazing! I did not understand a single word!”

And indeed, there is a problem of understanding what is ‘chaos’ as encountered in different disciplines, so we start this offering to Fritz Haake’s memory by ‘a fair coin toss’ theory of chaos (section 2), as was presented in the 1988 symposium, but in a modern, field theorist’s vision. In those days ‘chaos’ was a phenomenon exhibited by low-dimensional systems. In this and companion papers [58, 93] we develop a theory of ‘chaotic’ or ‘turbulent’ infinite-dimensional deterministic field theories. Deterministic chaotic field theory is of interest on its merits, as a method of describing turbulence in strongly nonlinear deterministic field theories, such as Navier-Stokes or Kuramoto-Sivashinsky [91, 93], or as a Gutzwiller WKB ‘skeleton’ for a chaotic quantum field theory [48, 98] or a stochastic field theory [55, 56, 59, 60, 124]. Lattice reformulation aligns ‘chaos’ with standard solid state, field theory and statistical mechanics, but the claims are radical: we’ve been doing ‘turbulence’ all wrong. In “explaining” chaos we talk the talk as though we have never moved beyond Newton; here is an initial state of a system, at an instant in time, and here are the differential equations that evolve it forward in time. But when we -all of us- walk the walk, we do something altogether different (see the references preceding eq. (67)), much closer to the 20th century spacetime physics. Our papers realign the theory to what we actually *do* when solving ‘chaos equations’, using not much more than linear algebra. In the field-theoretical formulation, there is no evolution in time, and there is no ‘Lyapunov horizon’; every contributing *lattice state* is a robust global solution of a spatiotemporal fixed point condition, and there is no dynamicist’s exponential blowup of initial state perturbations.

To a field theorist, the fundamental object is *global*, the partition function sum over probabilities of all possible spacetime field configurations. To a dynamicist, the fundamental notion is *local*, an ordinary or partial differential time-evolution equation. From the field-theoretic perspective, the spacetime formulation is fundamental, elegant and computationally powerful, while moving in step-lock with time is only one of the methods, a ‘transfer matrix’ for construction of the partition sum, a method at times awkward and computationally unstable.

We start our introduction to chaotic field theory (section 1) by rewriting the two most elementary examples of deterministic chaos, the forward-in-time first order difference equation for the Bernoulli map (section 2), and the forward-in-time second order difference equation for a 1-dimensional lattice of coupled rotors (section 3) as, respectively, the ‘temporal Bernoulli’ two-term discrete lattice recurrence relation, and the ‘temporal cat’ three-term discrete lattice recurrence relation. We then apply the approach to the simplest nonlinear field theories, the 1-dimensional discretized scalar ϕ^3 and ϕ^4 theories (sections 4.1 and 4.2).

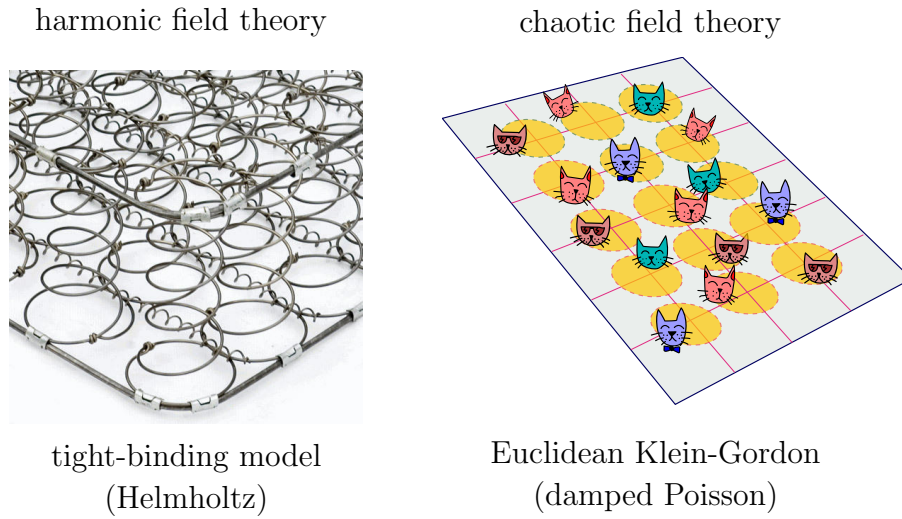


Figure 1. (Color online) The simplest of all chaotic field theories is the ‘spatiotemporal cat’, a deterministic Klein-Gordon field theory on a hypercubic lattice, with an unstable, “anti-harmonic” rotor at each lattice site, a cat that runs away rather than pushes back. In contrast to its elliptic sibling, the Helmholtz equation and its oscillatory solutions, spatiotemporal cat’s lattice states are hyperbolic and unstable.

Their spacetime generalization, the simplest of all chaotic field theories, is the ‘spatiotemporal cat’ [58, 96, 97], a discretization of the Klein-Gordon equation, a deterministic scalar field theory on a d -dimensional hypercubic lattice, with an unstable “anti-harmonic” rotor ϕ_z at each lattice site z , a rotor that gives rather than pushes back, coupled to its nearest neighbors. Dear Fritz, if you lack inclination to plunge into what follows, please take home figure 1. In contrast to its elliptic sibling, the Helmholtz equation and its oscillatory solutions, spatiotemporal cat’s lattice states are hyperbolic and ‘turbulent’, just as in contrast to oscillations of a harmonic oscillator, Bernoulli coin flips are unstable and chaotic.

The key to constructing partition sums for deterministic field theories (section 1) are the Hill determinants of the ‘orbit Jacobian matrices’ (section 6) that describe the global stability of linearized deterministic equations. How is this global, high-dimensional orbit stability related to the stability of the conventional low-dimensional, forward-in-time evolution (section 5)? The two notions of stability are related by Hill’s formulas (section 7, Appendix B), relations that rely on higher-order derivative equations being rewritten as sets of first order ODEs, relations equally applicable to mechanical, energy conserving systems, as to viscous, dissipative systems.

In order to explain the key ideas, we focus in this paper on 1-dimensional field theories, postponing the 2-dimensional Bravais lattices’ subtleties to the sequel [58]. In section 9 we show that the partition function of a given field theory is determined by the group of its symmetries, i.e., by the space group of its lattice discretization. Lattice discretization of the theory enables us to apply solid state computational methods, such as the reciprocal lattice and space group crystallography, to what are conventionally

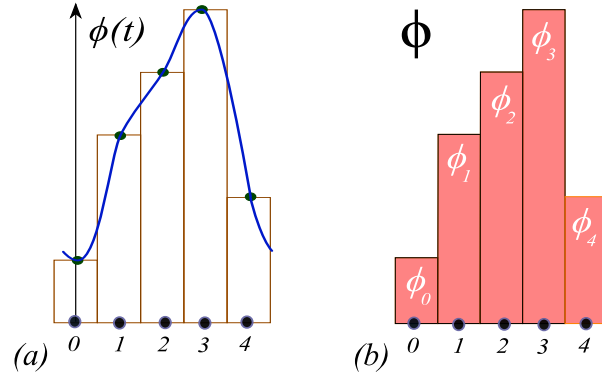




Figure 2. (Color online) Discretization of a 1-dimensional field theory. Horizontal: t coordinate, with lattice sites marked by dots and labelled by $t \in \mathbb{Z}$. (a) A periodic field $\phi(t)$, plotted as a function of continuous coordinate t . (b) A corresponding discretized period-5 Bravais cell lattice state $\Phi = \overline{\phi_0\phi_1\phi_2\phi_3\phi_4}$, with discretized field ϕ_t plotted as a bar centred at lattice site t . In what follows we use ‘lattice units’ $a = 1$. Continued in figure 6.

dynamical system problems (section 10). On the level of counting lattice states, their topological zeta functions are purely group-theoretic Lind zeta functions (section 11). As long as the only symmetry is time translation, we recover the conventional periodic orbit theory [53] (section 11.1). However, from a spatiotemporal field theory perspective, ‘time’-reversal is a purely crystallographic notion, leading to –to us very surprising– dihedral space group zeta function for the ‘time-reversible’ theories (section 11.2).

Our results are summarized and open problems discussed in section 12. The work that forms the basis of our formulation of chaotic field theory is reviewed in Appendix A. Icon  on the margin links the block of text to a supplementary online video.

1. Deterministic lattice field theory

A scalar field $\phi(x)$ over d Euclidean coordinates can be discretized by replacing the continuous space by a d -dimensional hypercubic integer lattice \mathbb{Z}^d , with lattice spacing a , and evaluating the field only on the lattice points [135, 138] 

$$\phi_z = \phi(x), \quad x = az = \text{lattice point}, \quad z \in \mathbb{Z}^d, \quad (1)$$

see figure 2. A *field configuration* (here in one spatiotemporal dimension)

$$\Phi = \cdots \phi_{-3}\phi_{-2}\phi_{-1}\phi_0\phi_1\phi_2\phi_3\phi_4\cdots, \quad (2)$$

takes any set of values $\phi_z \in \mathbb{R}$ in system’s ∞ -dimensional *state space*. A periodic field configuration Φ satisfies

$$\Phi(x + R) = \Phi(x) \quad (3)$$

for any discrete translation R in the *Bravais lattice*

$$\mathcal{L} = \left\{ \sum_{i=1}^d n_i \mathbf{a}_i \mid n_i \in \mathbb{Z} \right\} \quad (4)$$

where the d independent integer lattice vectors $\{\mathbf{a}_1, \mathbf{a}_2, \dots, \mathbf{a}_d\}$ define a *Bravais cell*.

A field configuration occurs with probability density

$$p(\Phi) = \frac{1}{Z} e^{-S[\Phi]}, \quad Z = Z[0]. \quad (5)$$

Here Z is a normalization factor, given by the *partition function*, the integral over probabilities of all configurations,

$$Z[\mathbf{J}] = \int d\Phi e^{-S[\Phi] + \Phi \cdot \mathbf{J}}, \quad d\Phi = \prod_z^{\mathcal{L}} d\phi_z, \quad (6)$$

where $\mathbf{J} = \{j_z\}$ is an external source j_z that one can vary site by site, and $S[\Phi]$ is the action that defines the theory (discussed in more detail in section 4). The dimension of the partition function integral equals the number of lattice sites $N_{\mathcal{L}}$.

Motivated by WKB semi-classical, saddle-point approximations [98] to the partition function (6), in this paper we describe their deterministic underpinning, the corresponding *deterministic* field theory, with partition function built from solutions to the variational saddle-point condition

$$F[\Phi_c]_z = \frac{\delta S[\Phi_c]}{\delta \phi_z} = 0, \quad (7)$$

with a global deterministic solution Φ_c satisfying this local extremal condition on every lattice site. We shall refer to the defining condition (7) as system's '*Euler-Lagrange equation*', keeping in mind that the field theories studied here might have a Lagrangian formulation (for example, scalar ϕ^k field theories of section 4), or be dissipative (for example, temporal Bernoulli, spatiotemporal Hénon for non-area preserving parameter values, Kuramoto-Sivashinsky or Navier-Stokes equations).

In order to distinguish a *solution* to the Euler-Lagrange equations (7) from an arbitrary *field configuration* (2), we refer to the solutions as *lattice states*, each a set of lattice site field values

$$\Phi_c = \{\phi_{c,z}\}, \quad (8)$$

that satisfies the condition (7) globally, over all lattice sites. For a finite lattice \mathcal{L} one needs to specify the boundary conditions (bc's). The companion article [96] tackles the Dirichlet bc's, a difficult, time-translation symmetry breaking, and from the periodic orbit theory perspective, a wholly unnecessary, self-inflicted pain. All that one needs to solve a field theory are the n -periodic, time-translation enforced bc's that we shall use here.

An example is the 1 spatiotemporal dimension block of fields of period $n = 5$ Bravais cell sketched in figure 2(b),

$$\Phi_c = \phi_0 \phi_1 \phi_2 \phi_3 \phi_4, \quad (9)$$

with its infinite repetition sketched in figure 7(1). The first field value ϕ_0 in the block is evaluated on the lattice site 0, the second ϕ_1 on the lattice site 1, the $(n+1)$ th $\phi_n = \phi_0$ on the lattice site n , with k th lattice site field value $\phi_k = \phi_\ell$, where $\ell = k \pmod n$.

What we call here a chaotic ‘field’ at a discretized spacetime lattice site z , a solid state physicist would call a ‘particle’ at crystal site z , coupled to its nearest neighbors. A solid state physicist endeavours to understand N -particle chaotic systems in many-body or ‘large N ’ settings, where in practice N not much larger than 2 can be ‘large’. Chaotic field theory is *ab initio* formulated for infinite time and infinite space lattice, but its periodic theory description is –thanks to hyperbolicity– often accurate already for $N = 2, 3, \dots$, where N is the number of sites in a Bravais cell that tiles the spacetime.

Each lattice state is a distinct deterministic solution Φ_c to the discretized Euler–Lagrange equations (7), so its probability density is a $N_{\mathcal{L}}$ -dimensional Dirac delta function (that’s what we mean by the system being *deterministic*), a delta function per site ensuring that Euler–Lagrange equation (7) is satisfied everywhere,

$$p_c(\Phi) = \frac{1}{Z} \delta(F[\Phi]), \quad \Phi \in \mathcal{M}_c, \quad (10)$$

where \mathcal{M}_c is a small neighborhood of lattice state Φ_c . In section 7 we verify that this definition agrees with the forward-in-time Perron-Frobenius probability density evolution [54]. However, we find field-theoretical formulation vastly preferable to the forward-in-time formulation, especially when it comes to higher spatiotemporal dimensions [58].

As is case for a WKB approximation [98], the deterministic field theory partition sum has support only on lattice field values that are solutions to the Euler–Lagrange equations (7), and the partition function (5) is now a sum over configuration state space (2) *points*, what in theory of dynamical systems is called the ‘deterministic trace formula’ [53],

$$Z[0] = \sum_c \int_{\mathcal{M}_c} d\Phi \delta(F[\Phi]) = \sum_c \frac{1}{|\text{Det } \mathcal{J}_c|}, \quad (11)$$

and we refer to the $[N_{\mathcal{L}} \times N_{\mathcal{L}}]$ matrix of second derivatives

$$(\mathcal{J}_c)_{z'z} = \frac{\delta F_{z'}[\Phi_c]}{\delta \phi_z} = S[\Phi_c]_{z'z} \quad (12)$$

as the *orbit Jacobian matrix*, and to its determinant $\text{Det } \mathcal{J}_c$ as the *Hill determinant*. Support being on state space *points* means that we do not need to worry about potentials being even or odd (thus unbounded), or the system being energy conserving or dissipative, as long as its nonwandering lattice states Φ_c set is bounded in state space. In what follows, we shall deal only with deterministic field theory and mostly omit the subscript ‘ c ’ in Φ_c .

How is a deterministic chaotic field theory different from a conventional field theory? By “spontaneous breaking of the symmetry” in a conventional theory one means that a solution does not satisfy a symmetry such as $\phi \rightarrow -\phi$; we always work in the “broken-symmetry” regime, as almost every ‘turbulent’, spatiotemporally chaotic deterministic solution breaks all symmetries. We work ‘beyond perturbation theory’, in the anti-integrable, strong coupling regime, in contrast to much of the literature that focuses on weak coupling expansions around a ‘ground state’. And, in contrast to [14, 95, 131, 160,

[186](#)], our ‘far from equilibrium’ field theory has no added dissipation, and is not driven by external noise. All chaoticity is due to the intrinsic unstable deterministic dynamics, and our trace formulas [\(11\)](#) are exact, not merely saddle points approximations to the exact theory.

1.1. Lattice Laplacian

Lattice free field theory is defined by action [\[162\]](#)

$$S_0[\Phi] = \frac{1}{2} \Phi^\top (-\square + \mu^2 \mathbf{1}) \Phi, \quad (13)$$

where the ‘discrete Laplace operator’, ‘central difference operator’, or the ‘graph Laplacian’ [\[41, 88, 136, 149, 156, 157\]](#)

$$\square \phi_z = \sum_{\|z'-z\|=1} (\phi_{z'} - \phi_z) \quad \text{for all } z, z' \in \mathcal{L} \quad (14)$$

is the average of the lattice field variation $\phi_{z'} - \phi_z$ over the sites nearest to the site z . For example, for a hypercubic lattice in one and two dimensions this discretized Laplacian is given by

$$\square \phi_t = \phi_{t+1} - 2\phi_t + \phi_{t-1} \quad (15)$$

$$\square \phi_{j,t} = \phi_{j,t+1} + \phi_{j+1,t} - 4\phi_{j,t} + \phi_{j,t-1} + \phi_{j-1,t}. \quad (16)$$

For the free field theory action [\(13\)](#) the Euler–Lagrange equation [\(7\)](#) is the discretized screened Poisson equation [\[80\]](#), also known as the Yukawa or Klein–Gordon equation, where $\mu^2 > 0$ is the Klein–Gordon mass-squared.

1.2. 1-dimensional lattice field theories

Discrete time evolution is frequently recast into a 1-dimensional temporal lattice field theory form, by anyone who rewrites a dynamical systems discrete time evolution problem as a k -term recurrence, for example in [\[55, 56, 60, 79\]](#). As already in one spatiotemporal dimension there is much to be learned about the role symmetries play in solving lattice field theories, that is what we will focus on in this paper (time-reversal sections [9](#) and [11](#)), with 2-dimensional spatiotemporal field theories studied in the sequel [\[58\]](#).

We start with the first order difference equation that we call ‘temporal Bernoulli’ (section [2](#)),

$$-\phi_{t+1} + (s\phi_t - m_t) = 0 \quad (17)$$

in order to motivate the 2-component field formulation [\(B.1\)](#) of second-order difference Euler–Lagrange equations [\(51\)](#) that we call, in the cases considered here, the ‘temporal cat’ (section [3.2](#)), ‘temporal ϕ^3 theory’ (section [4.1](#)), and ‘temporal ϕ^4 theory’ (section [4.2](#)), respectively:

$$-\phi_{t+1} + 2\phi_t - \phi_{t-1} + \mu^2 \phi_t - m_t = 0 \quad (18)$$

$$-\phi_{t+1} + 2\phi_t - \phi_{t-1} + \mu^2 (1/4 - \phi_t^2) = 0 \quad (19)$$

$$-\phi_{t+1} + 2\phi_t - \phi_{t-1} + \mu^2 (\phi_t - \phi_t^3) = 0. \quad (20)$$

Qualifier ‘temporal’ is used here to emphasize that we view 1-dimensional examples as special cases of ‘spatiotemporal’ field theories; much of our methodology for d -dimensional deterministic field theories can be profitably explained by working out 1-dimensional field theories. Lurking here is the totality of the map-iteration dynamical systems theory, but the reader will find it more profitable, and less confusing, to think of these simply as lattice problems, and forget that the subscript t often stands for ‘time’.

So, what is a ‘chaotic’, or ‘turbulent’ field theory? As we shall see in section 10, all of the above, as well as their higher-dimensional spatiotemporal siblings are ‘chaotic’ for sufficiently large ‘stretching parameter’ s , or ‘Klein-Gordon mass’ μ^2 . Our goal here is to make this ‘spatiotemporal chaos’ tangible and precise, by acquainting the reader what we believe are some of the simplest examples of chaotic field theories.

2. A fair coin toss

The very simplest example of a deterministic law of evolution that gives rise to ‘chaos’ is the *Bernoulli* map, figure 3(a), which models a **coin toss**. Starting with a random initial state, the map generates, deterministically, a sequence of tails and heads with 50-50% probability.

We introduce the model in its conventional, time-evolution dynamical formulation, than reformulate it as a lattice field theory, solved by enumeration of all admissible *lattice states*, field configurations that satisfy a global fixed point condition, and use this simple setting to motivate (1) the *fundamental fact*: for a given lattice period, the *Hill determinant* of stabilities of global solutions counts their number (section 8.1), and (2) the topological zeta function counts their translational symmetry group orbits (section 8.2).

2.1. Bernoulli map

The base-2 *Bernoulli* shift map,

$$x_{t+1} = \begin{cases} f_0(x_t) = 2x_t, & x_t \in \mathcal{M}_0 = [0, 1/2) \\ f_1(x_t) = 2x_t \pmod{1}, & x_t \in \mathcal{M}_1 = [1/2, 1) \end{cases}, \quad (21)$$

is shown in figure 3(a). If the linear part of such map has an integer-valued slope, or ‘stretching’ parameter $s \geq 2$,

$$x_{t+1} = sx_t \quad (22)$$

that maps state x_t into a state in the ‘extended state space’, outside the unit interval, the (mod 1) operation results in the base- s Bernoulli circle map,

$$\phi_{t+1} = s\phi_t \pmod{1}, \quad (23)$$

sketched as a **dice throw** in figure 3(b). The (mod 1) operation subtracts $m_t = \lfloor s\phi_t \rfloor$, the integer part of $s\phi_t$, or the circle map *winding number*, to keep ϕ_{t+1} in the unit interval $[0, 1)$, and partitions the unit interval into s subintervals $\{\mathcal{M}_m\}$,

$$\phi_{t+1} = s\phi_t - m_t, \quad \phi_t \in \mathcal{M}_{m_t}, \quad (24)$$

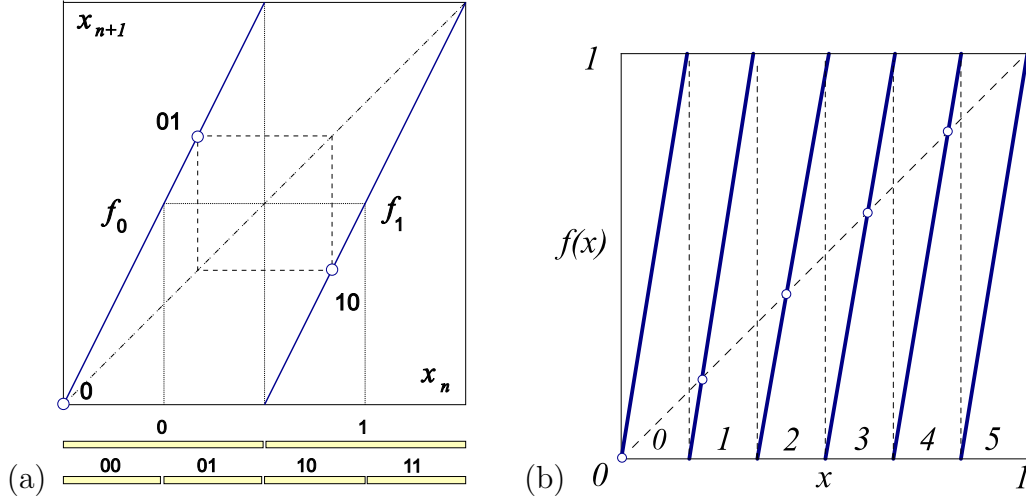


Figure 3. (Color online) (a) The ‘coin toss’ map (21), together with the $\bar{0}$ fixed point, and the $\bar{0}\bar{1}$ 2-cycle. Preimages of the critical point $x_c = 1/2$ partition the unit interval into $\{\mathcal{M}_0, \mathcal{M}_1\}$, $\{\mathcal{M}_{00}, \mathcal{M}_{01}, \mathcal{M}_{10}, \mathcal{M}_{11}\}$, \dots , subintervals. (b) The base- s Bernoulli map, here with the ‘dice throw’ stretching parameter $s = 6$, partitions the unit interval into 6 subintervals $\{\mathcal{M}_m\}$, labeled by the 6-letter alphabet (25). As the map is a circle map, $x_5 = 1 = 0 = x_0 \pmod{1}$.

where m_t takes values in the s -letter alphabet

$$m \in \mathcal{A} = \{0, 1, 2, \dots, s-1\}. \quad (25)$$

The Bernoulli map is a highly instructive example of a hyperbolic dynamical system. Its symbolic dynamics is simple: the base- s expansion of the initial point ϕ_0 is also its temporal itinerary, with symbols from alphabet (25) indicating that at time t the orbit visits the subinterval \mathcal{M}_{m_t} . The map is a ‘shift’: a multiplication by s acts on the base- s representation of $\phi_0 = .m_1m_2m_3\dots$ (for example, binary, if $s = 2$) by shifting its digits,

$$\phi_1 = f(\phi_0) = .m_2m_3\dots \quad (26)$$

Periodic points can be counted by observing that the preimages of critical points $\{\phi_{c1}, \phi_{c2}, \dots, \phi_{c,s-1}\} = \{1/s, 2/s, \dots, (s-1)/s\}$ partition the unit interval into s^n subintervals $\{\mathcal{M}_0, \mathcal{M}_1, \dots, \mathcal{M}_{s-1}\}$, s^2 subintervals $\{\mathcal{M}_{m_1m_2}\}$, \dots , s^n subintervals, each containing *one* unstable period- n periodic point $\phi_{m_1m_2\dots m_n}$, with stability multiplier s^n , see figure 3. The Bernoulli map is a full shift, in the sense that every itinerary is admissible, with one exception: on the circle, the rightmost fixed point is the same as the fixed point at the origin, $\phi_{s-1} = \phi_0 \pmod{1}$, so these fixed points are identified and counted as one, see figure 3. The total number of periodic points of period n is thus


$$N_n = s^n - 1. \quad (27)$$

2.2. Temporal Bernoulli

To motivate our formulation of a spatiotemporal chaotic field theory to be developed below, we now recast the local initial value, time-evolution Bernoulli map problem as a



temporal lattice fixed point condition, the problem of enumerating and determining all global solutions.

‘Temporal’ here refers to the lattice site field ϕ_t and the winding number m_t taking their values on the lattice sites of a 1-dimensional *temporal* integer lattice $t \in \mathbb{Z}$. Over a finite lattice segment, these can be written compactly as a *lattice state* and the corresponding *symbol block* 

$$\Phi^\top = (\phi_{t+1}, \dots, \phi_{t+n}), \quad \mathbf{M}^\top = (m_{t+1}, \dots, m_{t+n}), \quad (28)$$

where $(\dots)^\top$ denotes a transpose. The Bernoulli equation (24), rewritten as a first-order difference equation

$$-\phi_{t+1} + (s\phi_t - m_t) = 0, \quad \phi_t \in [0, 1), \quad (29)$$

takes the matrix form

$$\mathcal{J} \Phi - \mathbf{M} = 0, \quad \mathcal{J} = -\mathbf{r} + s \mathbf{1}, \quad (30)$$

where the $[n \times n]$ matrix

$$\mathbf{r}_{jk} = \delta_{j+1,k}, \quad \mathbf{r} = \begin{pmatrix} 0 & 1 & & & \\ & 0 & 1 & & \\ & & & \ddots & \\ & & & 0 & 1 \\ 1 & & & & 0 \end{pmatrix}, \quad (31)$$

implements the shift operation (26), a cyclic permutation that translates forward-in-time lattice state Φ by one site, $(\mathbf{r}\Phi)^\top = (\phi_2, \phi_3, \dots, \phi_n, \phi_1)$. The time evolution law (24) must be of the same form for all times, so the operator \mathbf{r} has to be time-translation invariant, with $\mathbf{r}_{n+1,n} = \mathbf{r}_{1n} = 1$ matrix element enforcing its periodicity.

As the temporal Bernoulli condition (30) is a linear relation, a given block \mathbf{M} , or ‘code’ in terms of alphabet (25), corresponds to a unique temporal lattice state $\Phi_{\mathbf{M}}$. That is why Percival and Vivaldi [149] refer to such symbol block \mathbf{M} as a *linear code*. The temporal Bernoulli, however, is *not* a linear dynamical system: as illustrated by figure 3, it is a set of piecewise-linear s -stretching maps and their compositions, one for each state space region $\mathcal{M}_{\mathbf{M}}$.

2.3. Bernoulli as a continuous time dynamical system

The discrete time derivative of a lattice configuration Φ evaluated at the lattice site t is given by the difference operator [75]

$$\dot{\phi}_t = \left[\frac{\partial \Phi}{\partial t} \right]_t = \frac{\phi_{t+1} - \phi_t}{\Delta t}. \quad (32)$$

The temporal Bernoulli condition (30) can be thus viewed as forward Euler method, a time-discretized, first-order ODE dynamical system

$$\dot{\Phi} = v(\Phi, \mathbf{M}), \quad (33)$$

where the ‘velocity’ vector field v is given by

$$v(\Phi, \mathbf{M}) = (s - 1) \Phi - \mathbf{M},$$

with the time increment set to $\Delta t = 1$, and perturbations that grow (or decay) with rate $(s - 1)$. By inspection of figure 3(a), it is clear that for *shrinking*, $s < 1$ parameter values the orbit is stable forward-in-time, with a single linear branch, 1-letter alphabet $\mathcal{A} = \{0\}$, and the only lattice states being the single fixed point $\phi_0 = 0$, and its repeats $\Phi = (0, 0, \dots, 0)$. However, for *stretching*, $s > 1$ parameter values, the Bernoulli system (more generally, Rényi’s beta transformations [159]) that we study here, every lattice state $\Phi_{\mathbf{M}}$ is unstable, and there is a lattice state for each admissible symbol block \mathbf{M} .

A fair coin toss, summarized. We refer to the *global* temporal lattice condition (30) as the ‘*temporal* Bernoulli’, in order to distinguish it from the 1-time step Bernoulli evolution *map* (23), in preparation for the study of *spatiotemporal* systems to be undertaken in [58]. In the lattice formulation, a *global* temporal lattice state $\Phi_{\mathbf{M}}$ is determined by the requirement that the *local* temporal lattice condition (29) is satisfied at every lattice site. In spatiotemporal formulation there is no need for forward-in-time, close recurrence searches for the returning periodic points. Instead, one determines each global temporal lattice state $\Phi_{\mathbf{M}}$ at one go, by solving the fixed point condition (7). The most importantly for what follows, the spatiotemporal field theory of [58], this calculation requires no recourse to any *explicit coordinatization and partitioning of system’s state space*.

3. A kicked rotor

Temporal Bernoulli is the simplest example of a chaotic lattice field theory. Our next task is to formulate a deterministic spatiotemporally chaotic field theory, Hamiltonian and energy conserving, because (a) that is physics, and (b) one cannot do quantum theory without it. We need a system as simple as the Bernoulli map, but mechanical. So, we move on from running in circles, to a mechanical rotor to kick.

The 1-degree of freedom maps that describe kicked rotors subject to discrete time sequences of angle-dependent force pulses $P(q_t)$, $t \in \mathbb{Z}$,

$$q_{t+1} = q_t + p_{t+1} \pmod{1}, \tag{34}$$

$$p_{t+1} = p_t + P(q_t), \tag{35}$$

with $2\pi q$ the angle of the rotor, p the momentum conjugate to the angular coordinate q , and the angular pulse $P(q_t) = P(q_{t+1}) = -V'(q_t)$ lattice periodic with period 1, play a key role in the theory of deterministic and quantum chaos in atomic physics, from the Taylor, Chirikov and Greene standard map [38, 121], to the cat maps that we turn to now. The equations are of the Hamiltonian form: eq. (34) is $\dot{q} = p/m$ in terms of discrete time derivative (32), i.e., the configuration trajectory starting at q_t reaches $q_{t+1} = q_t + p_{t+1}\Delta t/m$ in one time step Δt . Eq. (35) is the time-discretized

$\dot{p} = -\partial V(q)/\partial q$: at each kick the angular momentum p_t is accelerated to p_{t+1} by the force pulse $P(q_t)\Delta t$, with the time step and the rotor mass set to $\Delta t = 1$, $m = 1$.

3.1. Cat map

The simplest kicked rotor is subject to force pulses $P(q) = \mu^2 q$ proportional to the angular displacement q : in that case, the map (34,35) is of form

$$\begin{pmatrix} q_{t+1} \\ p_{t+1} \end{pmatrix} = \mathbb{J} \begin{pmatrix} q_t \\ p_t \end{pmatrix} \pmod{1}, \quad \mathbb{J} = \begin{pmatrix} \mu^2 + 1 & 1 \\ \mu^2 & 1 \end{pmatrix}. \quad (36)$$

The $(\text{mod } 1)$ makes the map a discontinuous ‘sawtooth,’ unless μ^2 is a positive integer. The map is then a Continuous Automorphism of the Torus known as the Thom-Anosov-Arnol’d-Sinai ‘cat map’ [7, 63, 173], extensively studied as the simplest example of a chaotic Hamiltonian system.

The determinant of the one-time-step Jacobian is $\det \mathbb{J} = 1$, i.e., the forward-in-time mapping is area-preserving. Let $s = \text{tr } \mathbb{J} = \mu^2 + 2$ be the trace of the Jacobian. For $|s| > 2$ the \mathbb{J} characteristic equation

$$\Lambda^2 - s\Lambda + 1 = 0, \quad (37)$$

has real roots (Λ, Λ^{-1}) and a positive Lyapunov exponent $\lambda > 0$,

$$\Lambda = e^\lambda = \frac{1}{2}(s + \sqrt{(s-2)(s+2)}), \quad s = \text{tr } \mathbb{J} = \Lambda + \Lambda^{-1}. \quad (38)$$

The eigenvalues are functions of the stretching parameter s , and for $|s| > 2$ the cat map (36) is a fully chaotic Hamiltonian dynamical system.

3.2. Temporal cat

In order to motivate our formulation of d -dimensional spatiotemporal chaotic field theories, to be developed in [58], we now recast the *local* initial value, Hamiltonian time-evolution as a *global* solution to the Euler–Lagrange equations.

The 2-component field at the temporal lattice site t , $\phi_t = (q_t, p_t) \in (0, 1] \times (0, 1]$ is kicked rotor’s the angular position and momentum. Hamilton’s equations (34,35) induce forward-in-time evolution on a 2-torus (q_t, p_t) *phase space*. Eliminating the momentum by Hamilton’s discrete time velocity eq. (34),

$$(q_t, p_t) = \left(q_t, \frac{q_t - q_{t-1}}{\Delta t} \right), \quad (39)$$

setting the time step to $\Delta t = 1$, and forgetting for a moment the $(\text{mod } 1)$ condition, the forward-in-time Hamilton’s first order difference equations are brought to the second order difference, 3-term recurrence Euler–Lagrange equations for scalar field $\phi_t = q_t$,

$$\phi_{t+1} - 2\phi_t + \phi_{t-1} + V'(\phi_t) = 0. \quad (40)$$

But that is Newton’s Second Law: “acceleration equals force,” so Percival and Vivaldi [149] refer to this formulation as ‘Newtonian’. Here we follow Allroth [2], Mackay,

Meiss, Percival, Kook & Dullin [71, 115, 129, 130, 132], and Li and Tomsovic [119] in referring to it as ‘Lagrangian’.


For the cat map (36), the Lagrangian passage (39) to the scalar field ϕ_t leads to the Percival-Vivaldi ‘two-configuration representation’ [149]

$$\begin{pmatrix} \phi_t \\ \phi_{t+1} \end{pmatrix} = \mathbb{J}_{PV} \begin{pmatrix} \phi_{t-1} \\ \phi_t \end{pmatrix} - \begin{pmatrix} 0 \\ m_t \end{pmatrix}, \quad \mathbb{J}_{PV} = \begin{pmatrix} 0 & 1 \\ -1 & s \end{pmatrix}, \quad (41)$$

with matrix \mathbb{J}_{PV} acting on the 2-dimensional space of successive configuration points $(\phi_{t-1}, \phi_t)^\top$. As was case for the Bernoulli map (29), the cat map (mod 1) condition (36) is enforced by integers $m_t \in \mathcal{A}$, where for a given integer stretching parameter s the alphabet \mathcal{A} ranges over $|\mathcal{A}| = s+1$ possible values for m_t ,

$$\mathcal{A} = \{\underline{1}, 0, \dots, s-1\}, \quad (42)$$

necessary to keep ϕ_t for all times t within the unit interval $[0, 1)$. (We find it convenient to have symbol \underline{m}_t denote m_t with the negative sign, i.e., ‘ $\underline{1}$ ’ stands for symbol ‘ -1 ’.)

Written out as a second-order difference equation, the Percival-Vivaldi map (41) takes a particularly elegant form, that we shall refer to as the *temporal cat* (18), 


$$-\phi_{t+1} + (s\phi_t - m_t) - \phi_{t-1} = 0, \quad (43)$$

or, in terms of a lattice state Φ , the corresponding symbol block \mathbf{M} (28), and the $[n \times n]$ time translation operator \mathbf{r} (31),

$$(-\mathbf{r} + s\mathbb{1} - \mathbf{r}^{-1})\Phi = \mathbf{M}, \quad (44)$$

very much like the temporal Bernoulli condition (30), with the winding numbers \mathbf{M} taking their values on the lattice sites of a 1-dimensional *temporal* lattice $t \in \mathbb{Z}$.

As was the case for temporal Bernoulli (30), the condition (41) is a linear relation: a given ‘code’ $\{m_t\}$ in terms of alphabet (42) corresponds to a unique temporal sequence $\{\phi_t\}$. That is why Percival and Vivaldi [149] refer to such symbol block \mathbf{M} as a *linear code*. As for the Bernoulli system, m_t can also be interpreted as ‘winding numbers’ [113], or, as they shepherd stray points back into the unit torus, as ‘stabilising impulses’ [149]. The cat map, however, is *not* a linear dynamical system: it is a set of piecewise-linear maps and their convolutions, one for each state space region $\mathcal{M}_{\mathbf{M}}$.

The lattice formulation (43) lends itself immediately to d -dimensional generalizations. An example is the Gutkin and Osipov [97] spatiotemporal cat in $d = 2$ dimensions [58], an Arnold cat map-inspired Euclidean scalar field theory of form (13) for which the Euler-Lagrange equation (7) is a 5-term recurrence relation 

$$-\phi_{j,t+1} - \phi_{j,t-1} + (2s\phi_{jt} - m_{jt}) - \phi_{j+1,t} - \phi_{j-1,t} = 0, \quad (45)$$

where we refer to parameter s , related to the Klein-Gordon mass in (13) by $\mu^2 = d(s-2)$, as the ‘stretching parameter’.


3.3. Temporal cat as a continuous time dynamical system

Recall that the Bernoulli first-order difference equation could be viewed as a time-discretization of the first-order linear ODE (33). The second-order difference equation (43) can be interpreted as the second order discrete time derivative d^2/dt^2 , or the temporal lattice Laplacian (15),

$$\square \phi_t \equiv \phi_{t+1} - 2\phi_t + \phi_{t-1} = (s-2)\phi_t - m_t, \quad (46)$$

with the time step set to $\Delta t = 1$. In other words, if we include the cat map forcing pulse (35) $P(\phi_t) = -V'(\phi_t) = (s-2)\phi - m_t$ into the definition of the on-site potential, the force is linear in the angular displacement ϕ , so the temporal cat Euler–Lagrange equation takes form (see free action (13))

$$(-\square + \mu^2 \mathbb{1}) \Phi = \mathbf{M}, \quad (47)$$

where the Klein-Gordon mass μ is related to the cat-map stretching parameter s by $\mu^2 = s - 2$. 

Here we study the strong stretching, $s > 2$ case, known as the discrete screened Poisson equation [69, 80, 89, 105, 106, 157], whose solutions are hyperbolic. We refer to the Euler–Lagrange equation (47) as the ‘temporal cat’, both to distinguish it from the forward-in-time Hamiltonian cat map (36), and in the anticipation of the *spatiotemporal cat* to be discussed in the sequel [58]. The field ϕ_t compactification to unit circle makes the spatiotemporal cat a strongly *nonlinear* deterministic field theory, with nontrivial symbolic dynamics.

Temporal cat, summarized. In the spatiotemporal formulation a *global* temporal lattice state

$$\Phi^\top = (\phi_t, \phi_{t+1}, \dots, \phi_{t+k}) \quad (48)$$

is not determined by a forward-in-time ‘cat map’ evolution (36), but rather by the fixed point condition (7) that the *local*, 3-term discrete temporal lattice Euler–Lagrange equations (43) are satisfied at every lattice point. This temporal 1-dimensional lattice reformulation is the bridge that takes us from the single cat map (36) to the higher-dimensional coupled “multi-cat” spatiotemporal lattices [58, 96, 97].

4. Nonlinear field theories


The ‘mod 1’ in the definition of the ‘linear’ kicked rotor, makes the cat map (36) a highly nonlinear, discontinuous map. In contrast, discretized scalar d -dimensional Euclidean ϕ^k theories [137] are defined by smooth, polynomial actions (6) given as lattice sums over the Lagrangian density

$$S[\Phi] = \sum_z \left\{ \frac{1}{2} \sum_{\mu=1}^d (\partial_\mu \phi)_z^2 + V(\phi_z) \right\}, \quad (49)$$



with nonlinear self-interaction [185]

$$V(\phi) = \frac{\mu^2}{2} \phi^2 - \frac{g}{k!} \phi^k, \quad k \geq 3, \quad (50)$$

where $V(\phi)$ is a local nonlinear potential [4–6, 72, 82, 120], the same for every lattice site z , $\mu^2 \geq 0$ is the Klein-Gordon mass-squared, $g \geq 0$ is the strength of the self-coupling, and we set lattice constant to unity, $a = 1$, throughout. The signs of the terms of (50) reflect our focus on deterministic spatiotemporal chaos, i.e., we shall study systems for whom all solutions are unstable. 

The discrete Euler–Lagrange equations (7) now take form of 3-term recurrence, second-order difference equations

$$-\square \phi_z + V'(\phi_z) = 0. \quad (51)$$

4.1. A ϕ^3 field theory


The simplest such nonlinear action turns out to correspond to the paradigmatic dynamicist’s model of a 2-dimensional nonlinear dynamical system, the Hénon map [101]

$$\begin{aligned} x_{t+1} &= 1 - a x_t^2 + b y_t \\ y_{t+1} &= x_t. \end{aligned} \quad (52)$$

For the contraction parameter value $b = -1$ this is a Hamiltonian map (see (66) below).

The Hénon map is the simplest map that captures chaos that arises from the smooth stretch & fold dynamics of nonlinear return maps of flows such as Rössler [161]. Written as a 2nd-order inhomogeneous difference equation [72], (52) takes the *temporal Hénon* 3-term recurrence form, time-translation and time-reversal invariant Euler–Lagrange equation (19),

$$-\phi_{t+1} + (a \phi_t^2 - 1) - \phi_{t-1} = 0. \quad (53)$$

Just as the kicked rotor (34,35), the map can be interpreted as a kicked driven anaharmonic oscillator [100], with the nonlinear, cubic Biham-Wenzel [23] lattice site potential (50) 

$$V(\phi) = \frac{1}{2} \mu^2 \phi^2 - \frac{1}{3!} g \phi^3, \quad (54)$$

giving rise to kicking pulse (35), so we refer to this field theory as ϕ^3 theory. As discussed in detail in [183], one of the parameters can be rescaled away by translations and rescalings of the field ϕ , and the Euler–Lagrange equation of the system can brought to various equivalent forms, such as the Hénon form (53), or the anti-integrable form (19),

$$-\frac{1}{d} \sum_{||z'-z||=1} (\phi_{z'} - \phi_z) + \mu^2 (1/4 - \phi_z^2) = 0. \quad (55)$$

For a sufficiently large ‘stretching parameter’ a , or ‘mass parameter’ μ^2 , the lattice states of this ϕ^3 theory are in one-to-one correspondence to the unimodal Hénon map Smale

horseshoe repeller, cleanly split into the ‘left’, positive stretching and ‘right’, negative stretching lattice site field values. A plot of this horseshoe, given in, for example, [ChaosBook Example 15.4](#) is helpfull in understanding that state space of deterministic solutions of strongly nonlinear field theories has fractal support. Devaney, Nitecki, Sterling and Meiss [64, 169, 170] have shown that the Hamiltonian Hénon map has a complete Smale horseshoe for ‘stretching parameter’ a values above

$$a > 5.699310786700 \dots . \quad (56)$$

In numerical [53] and analytic [77] calculations we fix (arbitrarily) the stretching parameter value to $a = 6$, in order to guarantee that all 2^n periodic points $\phi = f^n(\phi)$ of the Hénon map (52) exist, see table D1. The symbolic dynamics is binary, as simple as the Bernoulli map of figure 3(a), in contrast to the temporal cat which has nontrivial pruning, see table D2.

4.2. $A \phi^4$ field theory

If a symmetry forbids the odd-power potentials such as (54), one starts instead with the Klein-Gordon [5, 21, 22, 27, 29] quartic potential (50)

$$V(\phi) = \frac{1}{2} \mu^2 \phi^2 - \frac{1}{4!} g \phi^4, \quad (57)$$

leading, after some translations and rescalings [183], to the Euler–Lagrange equation for the lattice scalar ϕ^4 field theory (20),

$$-\frac{1}{d} \sum_{||z'-z||=1} (\phi_{z'} - \phi_z) + \mu^2(\phi_t - \phi_t^3) = 0. \quad (58)$$

Topology of the state space of ϕ^4 theory is very much like what we had learned for the unimodal Hénon map ϕ^3 theory, except that the repeller set is now bimodal. As long as μ^2 is sufficiently large, the repeller is a full 3-letter shift. Indeed, while Smale’s first horseshoe [167], his fig. 1, was unimodal, he also sketched the ϕ^4 bimodal repeller, his fig. 5.

4.3. Computing lattice states for nonlinear theories

Unlike the temporal Bernoulli (17) and the temporal cat (18), for which the lattice state fixed point condition (7) is linear and easily solved, for nonlinear lattice field theories the lattice states are roots of polynomials of arbitrarily high order. While Friedland and Milnor [82], Endler and Gallas [76, 77] and others [32, 168] have developed a powerful theory that yields Hénon map periodic orbits in analytic form, it would be unrealistic to demand such explicit solutions for general field theories on multi-dimensional lattices. We take a pragmatic, numerical route [92, 183], and search for the fixed-point solutions (7) starting with the deviation of an approximate trajectory from the 3-term recurrence (51), given by the lattice deviation vector

$$v_t = -\square \phi_t + V'(\phi_t), \quad (59)$$

and minimizing this error term by any suitable variational or optimization method, possibly in conjunction with a high-dimensional variant of the Newton method [57, 92, 116, 147, 181].

5. Forward-in-time stability

Consider a temporal lattice with a d -component field on each lattice site t , with time evolution given by a d -dimensional map (1st order difference equation)

$$\phi_t - f(\phi_{t-1}) = 0, \quad \phi_t = \{\phi_{t,1}, \phi_{t,2}, \dots, \phi_{t,d}\}. \quad (60)$$

A small deviation $\Delta\phi_t$ from ϕ_t satisfies the linearized equation

$$\Delta\phi_t - \mathbb{J}_{t-1} \Delta\phi_{t-1} = 0, \quad (\mathbb{J}_t)_{ij} = \frac{\partial f(\phi_t)_i}{\partial \phi_{t,j}}, \quad (61)$$

where $\mathbb{J}_t = \mathbb{J}(\phi_t)$ is the 1-time step $[d \times d]$ Jacobian matrix, evaluated on lattice site t . The formula for the linearization of n th iterate of the map

$$\mathbb{J}^n = \mathbb{J}_{n-1} \mathbb{J}_{n-2} \cdots \mathbb{J}_1 \mathbb{J}_0 \quad (62)$$

in terms of 1-time step Jacobian matrix (61) follows by chain rule for iterated functions. For a period- n Bravais cell lattice state Φ_c we refer to this forward-in-time $[d \times d]$ matrix as the Floquet (or monodromy) matrix.

If the only symmetry of the system is time translation (the map (60) is the same at all temporal lattice sites, but not invariant under a lattice reflection), a lattice state Φ_p is *prime* if it is not a repeat of a shorter period lattice state. Evaluated at lattice site t_0 , its Floquet matrix is

$$\mathbb{J}_p = \mathbb{J}_{n_p-1} \mathbb{J}_{n_p-2} \cdots \mathbb{J}_1 \mathbb{J}_0. \quad (63)$$

Consider a lattice state Φ which is m th repeat of a period- n prime lattice state Φ_p (for a sketch, see figure 7(1)). Due to the multiplicative structure (62) of Jacobian matrices, the Floquet matrix for the m th repeat of a prime period- n lattice state Φ_p is

$$\mathbb{J}^{mn}(\phi_0) = \mathbb{J}^n(\phi_{(m-1)n}) \cdots \mathbb{J}^n(\phi_n) \mathbb{J}^n(\phi_0) = \mathbb{J}_p^m. \quad (64)$$

Hence it suffices to restrict our considerations to the Floquet matrix of prime lattice states.

For example, for the Hamiltonian, $b = -1$ Hénon map (52), the 1-time step Jacobian matrix (61) is

$$\mathbb{J}_t = \begin{pmatrix} -2a\phi_t & -1 \\ 1 & 0 \end{pmatrix}, \quad (\phi_t, \varphi_t) = f^t(\phi_0, \varphi_0). \quad (65)$$

So, once we have a determined a temporal Hénon lattice state Φ_p , we have its Floquet matrix \mathbb{J}_p . When \mathbb{J}_p is hyperbolic, only the expanding eigenvalue $\Lambda_1 = 1/\Lambda_2$ needs to be determined, as the determinant of the Hénon 1-time step Jacobian matrix (65) is unity,


$$\det \mathbb{J}_p = \Lambda_1 \Lambda_2 = 1. \quad (66)$$

The map is Hamiltonian in the sense that it preserves areas in the $[\phi, \varphi]$ plane.

6. Orbit stability

The discretized Euler–Lagrange $F[\Phi_c] = 0$ fixed point condition (7) is central to the theory of robust global methods for finding periodic orbits. In global multi-shooting, collocation [39, 68, 90], and Lindstedt-Poincaré [178–180] searches for periodic orbits, one discretizes a periodic orbit into n sites temporal lattice configuration [57, 66, 67, 116], and lists the field value at a point of each segment

$$\Phi^\top = (\phi_0, \phi_1, \dots, \phi_{n-1}). \quad (67)$$

Starting with an initial guess for Φ , a zero of function $F[\Phi_c]$ can then be found by Newton iteration, which requires an evaluation of the $[n \times n]$ orbit Jacobian matrix 

$$\mathcal{J}_{tt'} = \frac{\delta F[\Phi_c]_t}{\delta \phi_{t'}}. \quad (68)$$

The temporal Bernoulli condition (30) and the temporal cat discretized Euler–Lagrange equation (44) can be viewed as searches for zeros of the vector of n functions

$$F[\Phi_M] = \mathcal{J}\Phi - M = 0 \quad (69)$$

$$\text{temporal Bernoulli:} \quad \mathcal{J} = -r + s \mathbb{1} \quad (70)$$

$$\text{temporal cat:} \quad \mathcal{J} = -r + s \mathbb{1} - r^{-1}, \quad (71)$$

with the entire periodic *lattice state* Φ_M treated as a single fixed *point* $(\phi_0, \phi_1, \dots, \phi_{n-1})$ in the n -dimensional state space unit hypercube $\Phi \in [0, 1]^n$.

For uniform stretching systems, such as the temporal Bernoulli and the temporal cat, $[n \times n]$ orbit Jacobian matrix \mathcal{J} is a circulant, time-translation invariant matrix. Written out as matrices they are, respectively, temporal Bernoulli (70)

$$\mathcal{J} = \begin{pmatrix} s & -1 & 0 & 0 & \dots & 0 & 0 \\ 0 & s & -1 & 0 & \dots & 0 & 0 \\ 0 & 0 & s & -1 & \dots & 0 & 0 \\ \vdots & \vdots & \vdots & \vdots & \ddots & \vdots & \vdots \\ 0 & 0 & 0 & 0 & \dots & s & -1 \\ -1 & 0 & 0 & 0 & \dots & 0 & s \end{pmatrix}, \quad (72)$$

and temporal cat (71)

$$\mathcal{J} = \begin{pmatrix} s & -1 & 0 & 0 & \dots & 0 & -1 \\ -1 & s & -1 & 0 & \dots & 0 & 0 \\ 0 & -1 & s & -1 & \dots & 0 & 0 \\ \vdots & \vdots & \vdots & \vdots & \ddots & \vdots & \vdots \\ 0 & 0 & 0 & 0 & \dots & s & -1 \\ -1 & 0 & 0 & 0 & \dots & -1 & s \end{pmatrix}. \quad (73)$$

While in Lagrangian mechanics matrices such as (73) are often called “Hessian”, here we refer to them collectively as ‘orbit Jacobian matrices’, to emphasize that they describe the stability of any dynamical system, be it energy-conserving, or a dissipative system without a Lagrangian formulation.

Solutions of a nonlinear field theory, such as the lattice state sketched in figure 2(b), are in general not translation invariant, so the orbit Jacobian matrix (68) (or the ‘discrete Schrödinger operator’ [28, 166])

$$\mathcal{J}_c = \begin{pmatrix} s_0 & -1 & 0 & 0 & \cdots & 0 & -1 \\ -1 & s_1 & -1 & 0 & \cdots & 0 & 0 \\ 0 & -1 & s_2 & -1 & \cdots & 0 & 0 \\ \vdots & \vdots & \vdots & \vdots & \ddots & \vdots & \vdots \\ 0 & 0 & 0 & 0 & \cdots & s_{n-2} & -1 \\ -1 & 0 & 0 & 0 & \cdots & -1 & s_{n-1} \end{pmatrix} \quad (74)$$

is not a circulant matrix: each lattice state Φ_c has its own orbit Jacobian matrix $\mathcal{J}_c = \mathcal{J}[\Phi_c]$, with the ‘stretching factor’ $s_t = V''(\phi_t) + 2$ at the lattice site t a function of the site field ϕ_t .

The orbit Jacobian matrix of a period- (mn) lattice state Φ , which is a m th repeat of a period- n prime lattice state Φ_p , has a tri-diagonal block circulant matrix form that follows by inspection from (74):

$$\mathcal{J} = \begin{pmatrix} \mathbf{s}_p & -\mathbf{r} & & & -\mathbf{r}^\top \\ -\mathbf{r}^\top & \mathbf{s}_p & -\mathbf{r} & & \\ & \ddots & \ddots & \ddots & \\ & & -\mathbf{r}^\top & \mathbf{s}_p & -\mathbf{r} \\ -\mathbf{r} & & & -\mathbf{r}^\top & \mathbf{s}_p \end{pmatrix}, \quad (75)$$

where block matrix \mathbf{s}_p is a $[n \times n]$ symmetric Toeplitz matrix

$$\mathbf{s}_p = \begin{pmatrix} s_0 & -1 & & & 0 \\ -1 & s_1 & -1 & & \\ & \ddots & \ddots & \ddots & \\ & & -1 & s_{n-2} & -1 \\ 0 & & & -1 & s_{n-1} \end{pmatrix}, \quad \mathbf{r} = \begin{pmatrix} 0 & \cdots & 0 \\ & \ddots & \vdots \\ 1 & & 0 \end{pmatrix}, \quad (76)$$

and \mathbf{r} and its transpose enforce the periodic bc’s. This period- (mn) lattice state Φ orbit Jacobian matrix is as translation-invariant as the temporal cat (73), but now under Bravais lattice translations by multiples of n . As discussed in section 9, one can visualize this lattice state as a tiling of the integer lattice \mathbb{Z} by a generic lattice state field decorating a tile of length n . The orbit Jacobian matrix \mathcal{J} is now a block circulant matrix which can be brought into a block diagonal form by a unitary transformation, with a repeating $[n \times n]$ block along the diagonal, see section 10.2.1.

7. Stability of an orbit vs. its time-evolution stability

The orbit Jacobian matrix $\mathcal{J}[\Phi_c]_{z'z}$ is a high-dimensional linear stability matrix for the extremum condition $F[\Phi_c] = 0$, evaluated on the lattice state Φ_c . How is the stability so computed related to the dynamical systems’ forward-in-time stability?

As we shall show now, the two notions of stability are related by *Hill’s formula*



$$|\text{Det } \mathcal{J}_c| = |\det(\mathbb{1} - \mathbb{J}_c)| \quad (77)$$

which relates the characteristic polynomial of the forward-in-time evolution periodic orbit Floquet matrix (monodromy matrix) \mathbb{J}_c to the determinant of the global orbit Jacobian matrix \mathcal{J}_c .

While first discovered in a Lagrangian setting, Hill’s formulas apply equally well to dissipative dynamical systems, from the Bernoulli map of section 2 to Navier-Stokes and Kuramoto-Sivashinsky systems [91, 93], with the Lagrangian formalism of [26, 115, 129, 177] mostly getting in the way of understanding them. We find the discrete spacetime derivations given below a good starting point to grasp their simplicity.

Why do we need them? Let’s say that an n -periodic $\phi_{t+n} = \phi_t$ lattice state Φ_c is known ‘numerically exactly’, that is to say, to a high (but not infinite) precision. One way to present the solution is to list the field value ϕ_0 at a single temporal lattice site $t = 0$, and instruct the reader to reconstruct the rest by stepping forward in time, $\phi_t = f^t(\phi_0)$. However, for a linearly unstable orbit a single field value ϕ_0 does not suffice to present the solution, because there is always a finite ‘Lyapunov time’ horizon t_{Lyap} beyond which $f^t(\phi_0)$ has lost all memory of the entire lattice state Φ_c . This problem is particularly vexing in searches for ‘exact coherent structures’ embedded in turbulence, where even the shortest period solutions have to be computed to the (for a working fluid dynamicist excessive) machine precision [85, 86, 184], in order to complete the first return to the initial state. And so the “... sensitivity to ...” incantations of introductory chaos courses [1, 53, 99, 146, 172] bear no relation to what we actually *do* in practice.

In practice, instead of relaying on forward-in-time numerical integration, *global methods* for finding periodic orbits [39] view them as equations for the vector fields $\dot{\phi}$ on spaces of closed curves, or, as we shall see [57, 58, 93, 96, 116], on D -tori spacetime tilings. In numerical implementations (67) one discretizes a periodic orbit into sufficiently many short segments [39, 66–68, 90], and lists one field value for each segment $(\phi_1, \phi_2, \dots, \phi_n)$. For a n -dimensional discrete time map f obtained by cutting the flow by n local Poincaré sections, with the periodic orbit now of discrete period n , every trajectory segment can be reconstructed by short time integration, and satisfies

$$\phi_{t+1} = f_t(\phi_t), \quad (78)$$

to high accuracy, as for sufficiently short times the exponential instabilities are numerically controllable. That is why a very rough, but topologically correct global guess can robustly lead to a solution that forward-in-time methods fail to find.

7.1. Hill’s formula for a 1st order difference equation

As Hill’s formula is fundamental to our formulation of the spatiotemporal chaotic field theory, we rederive it now in three ways, relying on nothing more than elementary linear algebra. Here is its first, ‘multi-shooting’ derivation (where the reader is invited to take care of the convergence of the formal series used).

Consider a temporal lattice with a d -component field (60). It suffices to work out a temporal period $n = 3$ example to understand the calculation for any period. In terms of the $[3d \times 3d]$ generalized (31) block shift matrix \mathbf{r}

$$\mathbf{r} = \begin{pmatrix} 0 & \mathbb{1}_d & 0 \\ 0 & 0 & \mathbb{1}_d \\ \mathbb{1}_d & 0 & 0 \end{pmatrix}, \quad (79)$$

where $\mathbb{1}_d$ is the d -dimensional identity matrix, the orbit Jacobian matrix (68) has a block matrix form

$$\mathcal{J}_c = \mathbb{1} - \mathbf{r}^{-1} \mathbb{J}, \quad \mathbb{J} = \begin{pmatrix} \mathbb{J}_0 & 0 & 0 \\ 0 & \mathbb{J}_1 & 0 \\ 0 & 0 & \mathbb{J}_2 \end{pmatrix}, \quad (80)$$

where $\mathbb{J}_t = \mathbb{J}(\phi_t)$ is the 1-time step $[d \times d]$ Jacobian matrix (61). Next, consider

$$\mathbf{r}^{-1} \mathbb{J} = \begin{pmatrix} 0 & 0 & \mathbb{J}_2 \\ \mathbb{J}_0 & 0 & 0 \\ 0 & \mathbb{J}_1 & 0 \end{pmatrix}, \quad (\mathbf{r}^{-1} \mathbb{J})^2 = \begin{pmatrix} 0 & \mathbb{J}_2 \mathbb{J}_1 & 0 \\ 0 & 0 & \mathbb{J}_0 \mathbb{J}_2 \\ \mathbb{J}_1 \mathbb{J}_0 & 0 & 0 \end{pmatrix}, \quad (81)$$

and note that the $n = 3$ repeat of $\mathbf{r}^{-1} \mathbb{J}$ is block-diagonal

$$(\mathbf{r}^{-1} \mathbb{J})^3 = \begin{pmatrix} \mathbb{J}_2 \mathbb{J}_1 \mathbb{J}_0 & 0 & 0 \\ 0 & \mathbb{J}_0 \mathbb{J}_2 \mathbb{J}_1 & 0 \\ 0 & 0 & \mathbb{J}_1 \mathbb{J}_0 \mathbb{J}_2 \end{pmatrix}, \quad (82)$$

with $[d \times d]$ blocks along the diagonal cyclic permutations of each other. The trace of the $[nd \times nd]$ matrix for a period n lattice state Φ_c

$$\text{Tr}(\mathbf{r}^{-1} \mathbb{J})^k = \sum_{m=1}^{\infty} \delta_{k, mn} n \text{tr} \mathbb{J}_c^m, \quad \mathbb{J}_c = \mathbb{J}_{n-1} \mathbb{J}_{n-2} \cdots \mathbb{J}_1 \mathbb{J}_0 \quad (83)$$

is non-vanishing only if k is a multiple of n , where \mathbb{J}_c is the forward-in-time $[d \times d]$ Floquet matrix of the period- n lattice state Φ_c , evaluated at lattice site 0. Evaluate the Hill determinant $\text{Det} \mathcal{J}_c$ by expanding

$$\begin{aligned} \ln \text{Det} \mathcal{J}_c &= \text{Tr} \ln(\mathbb{1} - \mathbf{r}^{-1} \mathbb{J}) = - \sum_{k=1}^{\infty} \frac{1}{k} \text{Tr}(\mathbf{r}^{-1} \mathbb{J})^k \\ &= - \text{tr} \sum_{m=1}^{\infty} \frac{1}{m} \mathbb{J}_c^m = \ln \det(\mathbb{1}_d - \mathbb{J}_c), \end{aligned} \quad (84)$$

where ‘Tr, Det’ refer to the big, $[nd \times nd]$ global matrices, while ‘tr, det’ refer to the small, $[d \times d]$ time-stepping matrices.

The orbit Jacobian matrix \mathcal{J}_c evaluated on a lattice state Φ_c that is a solution of the temporal lattice first-order difference equation (60), and the dynamical, forward-in-time Jacobian matrix \mathbb{J}_c are thus connected by *Hill’s formula* (77) which relates the global orbit stability to the Floquet, forward-in-time evolution stability. This version of Hill’s formula applies to all first-order difference equations, i.e., systems whose evolution laws are first order in time.

Perhaps the simplest example of Hill's formula is afforded by the temporal Bernoulli lattice (30). The site field ϕ_t is a scalar, so $d = 1$, the 1-time step $[1 \times 1]$ time-evolution Jacobian matrix (61) is the same at every lattice point t , $\mathbb{J}_t = s$, the orbit Jacobian matrix (30) is the same for all lattice states of period n , and (see section 8.1) in this case the Hill's formula (77) counts the numbers of lattice states

$$\text{temporal Bernoulli: } N_n = |\text{Det } \mathcal{J}| = s^n - 1, \quad (85)$$

in agreement with the time-evolution count (27); all itineraries are allowed, except that the periodicity of $r^n = \mathbb{1}$ accounts for $\bar{0}$ and $\overline{s-1}$ fixed points (see figure 3) being a single periodic point.

7.2. Hill's formula for the trace of an evolution operator

Our second derivation redoes the first, but now in the **ChaosBook evolution operator formulation** of the deterministic transport of state space orbits densities [54], setting up the generalization of the time-periodic orbit theory to the spacetime-periodic orbit theory [58].

For a d -dimensional deterministic map (60) the Perron-Frobenius operator

$$\mathcal{L} \rho(\phi_{t+1}) = \int_{\mathcal{M}} d^d \phi_t \mathcal{L}(\phi_{t+1}, \phi_t) \rho(\phi_t) \quad (86)$$

maps a state space density distribution $\rho(\phi_t)$ one step forward-in-time. Applied repeatedly, its kernel, the d -dimensional Dirac delta function

$$\mathcal{L}(\phi_{t+1}, \phi_t) = \delta(\phi_{t+1} - f(\phi_t)), \quad (87)$$

satisfies the semigroup property

$$\mathcal{L}^2(\phi_{t+2}, \phi_t) = \int_{\mathcal{M}} d^d \phi_{t+1} \mathcal{L}(\phi_{t+2}, \phi_{t+1}) \mathcal{L}(\phi_{t+1}, \phi_t) = \delta(\phi_{t+2} - f^2(\phi_t)). \quad (88)$$

The time-evolution periodic orbit theory [53] relates the long time chaotic averages to the traces of Perron-Frobenius operators

$$\text{tr } \mathcal{L}^n = \int_{\mathcal{M}} d^d \phi \mathcal{L}^n(\phi, \phi) = \int_{\mathcal{M}} d^d \phi \delta(\phi - f^n(\phi)), \quad (89)$$

and their weighted evolution operator generalizations, with support on all deterministic period- n temporal lattice states $\phi_c = f^n(\phi_c)$. Usually one evaluates this trace by restricting the d -dimensional integral over \mathcal{M} to an infinitesimal open neighborhood c around a lattice site field $\phi_{c,0}$,

$$\text{tr}_c \mathcal{L}^n = \int_c d^d \phi_0 \delta(\phi_0 - f^n(\phi_0)) = \frac{1}{|\det(\mathbb{1} - \mathbb{J}_c)|}, \quad (90)$$

where \mathbb{J}_c is the forward-in-time $[d \times d]$ Floquet matrix (83) evaluated at the period- n Bravais cell temporal site field $\phi_{c,0}$.

Alternatively, one can use the group property (88) to insert integrations over all n temporal lattice site fields, and rewrite \mathcal{L}^n as a product of one-time-step operators \mathcal{L} :

$$\text{tr } \mathcal{L}^n = \int d\Phi \prod_{t=0}^{n-1} \delta(\phi_{t+1} - f(\phi_t)), \quad d\Phi = \prod_{t=0}^{n-1} d^d \phi_t, \quad (91)$$

where $\phi_n = \phi_0$. The lattice site field ϕ_t is a d -component field (60), so a period- n Bravais cell lattice state Φ is (nd) -dimensional, with the (nd) -dimensional Dirac delta function of the deterministic field theory form (11),

$$\text{tr } \mathcal{L}^n = \int d\Phi \delta(\mathbf{r}\Phi - f(\Phi)), \quad (92)$$

where \mathbf{r} is the cyclic $[nd \times nd]$ version of the time translation operator (79), and $f(\Phi)$ acts within d -dimensional blocks (60) along the diagonal. We recognize the argument (60) of this (nd) -dimensional Dirac delta function as the Euler–Lagrange equation (7) of the system,

$$F[\Phi_c] = \mathbf{r}\Phi_c - f(\Phi_c) = 0,$$

with lattice state Φ_c satisfying the local Euler–Lagrange equation (60) lattice site by site. Now evaluate the trace by integrating over the d components of the n lattice site fields,

$$\text{tr}_c \mathcal{L}^n = \int_{\mathcal{M}_c} d\Phi \delta(F[\Phi]) = \frac{1}{|\text{Det } \mathcal{J}_c|}, \quad (93)$$

where $\mathcal{J}_c = \mathcal{J}[\Phi_c]$ is the $[nd \times nd]$ orbit Jacobian matrix (68) of a period- n lattice state Φ_c , and \mathcal{M}_c is an (nd) -dimensional infinitesimal open neighborhood of Φ_c . By comparing the trace evaluations (90) and (93), we see that we have again proved Hill’s formula (77) for first-order, forward-in-time difference equations, this time without writing down any explicit matrices such as (80-82).

In dynamical systems theory, one often replaces higher order derivatives (for example, Euler–Lagrange equations) by multi-component fields satisfying first order equations (for example, Hamilton’s equations), and the same is true for discrete time systems, where a k th order difference equation is the discrete-time analogue of a k th order differential equation [75]. For example, the cat map and Hénon map are usually presented as discrete time evolution over a 2-component phase space (36) and (52), rather than the 3-term scalar field recurrence conditions (43) and (53).

One could compute a Hill determinant for such system using the forward-in-time Hill’s formula for the k -component lattice site field, with the corresponding $[kn \times kn]$ orbit Jacobian matrix determinant (93), or use the recurrence relation to reduce the dimension of the orbit Jacobian matrix. For example, in section 3.2, in passage from the Hamiltonian to the Lagrangian formulation, the $k = 2$ component phase space field (q_t, p_t) is replaced by 1 component scalar field ϕ_t . And using the 1 component scalar field one can compute the $[n \times n]$ orbit Jacobian matrices such as (72-74), whose Hill determinant equals the forward-in-time $[2 \times 2]$ phase space $|\det(\mathbf{1} - \mathbb{J}_c)|$. Appendix B, our third derivation of a Hill’s formula, is an example of such relation.

8. Hill determinants

Having shown that the inverse of Hill determinant $1/|\text{Det } \mathcal{J}_c|$ gives us the lattice state’s probability (10) in the deterministic partition function, our next task is to compute it.

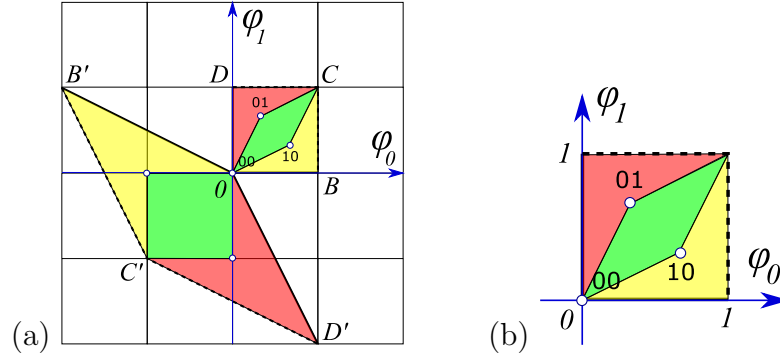


Figure 4. (Color online) (a) The Bernoulli map (21) periodic points $\Phi_M = (\phi_0, \phi_1)$ of period 2 are the $\bar{0} = (0,0)$ fixed point, and the 2-cycle $\Phi_{01} = (1/3, 2/3)$, see figure 3(a). They all lie within the unit square $[0BCD]$, which is mapped by the orbit Jacobian matrix $-\mathcal{J}$ (96) into the fundamental parallelepiped $[0B'C'D']$. Periodic points Φ_M are mapped by \mathcal{J} onto the integer lattice, $\mathcal{J}\Phi_M \in \mathbb{Z}^n$, and are sent back into the origin by integer translations \mathbf{M} , in order to satisfy the fixed point condition (69). Note that this fundamental parallelepiped is covered by 3 unit area quadrilaterals, hence $|\text{Det } \mathcal{J}| = 3$. (b) Conversely, in the flow conservation sum rule (106) sum over all lattice states \mathbf{M} of period n , the inverse of the Hill determinant defines the ‘neighborhood’ of a lattices state as the corresponding fraction of the unit hypercube volume.

As we shall see in section 10.2, that is often best done on the reciprocal lattice. But first we show that on hypercubic lattices we can visualize a Hill determinant geometrically, as the volume of the associated fundamental parallelepiped.

8.1. Fundamental fact

Consider temporal Bernoulli and temporal cat. The orbit Jacobian matrix \mathcal{J} stretches the state space unit hypercube $\Phi \in [0,1]^n$ into the n -dimensional *fundamental parallelepiped*, and maps each periodic lattice state Φ_M into an integer lattice \mathbb{Z}^n site, which is then translated by the winding numbers \mathbf{M} into the origin, in order to satisfy the fixed point condition (69). Hence N_n , the total number of the solutions of the fixed point condition equals the number of integer lattice points within the fundamental parallelepiped, a number given by what Baake *et al* [13] call the ‘*fundamental fact*’,

$$N_n = |\text{Det } \mathcal{J}|, \quad (94)$$

i.e., fact that the number of integer points in the fundamental parallelepiped is equal to its volume, or, what we refer to as its Hill determinant.

The action of the orbit Jacobian matrix \mathcal{J} for period-2 lattice states (periodic points) of the Bernoulli map of figure 3(a), suffices to convey the idea. In this case, the $[2 \times 2]$ orbit Jacobian matrix (30), the unit square basis vectors, and their images are

$$\mathcal{J} = \begin{pmatrix} 2 & -1 \\ -1 & 2 \end{pmatrix},$$

$$\begin{aligned}\Phi^{(B)} &= \begin{pmatrix} 1 \\ 0 \end{pmatrix} \rightarrow \Phi^{(B')} = \mathcal{J} \Phi^{(B)} = \begin{pmatrix} 2 \\ -1 \end{pmatrix}, \\ \Phi^{(D)} &= \begin{pmatrix} 0 \\ 1 \end{pmatrix} \rightarrow \Phi^{(D')} = \mathcal{J} \Phi^{(D)} = \begin{pmatrix} -1 \\ 2 \end{pmatrix},\end{aligned}\tag{95}$$

i.e., the columns of the orbit Jacobian matrix are the edges of the fundamental parallelepiped,

$$\mathcal{J} = \left(\Phi^{(B')} \Phi^{(D')} \right), \tag{96}$$

see figure 4(a), and $N_2 = |\text{Det } \mathcal{J}| = 3$, in agreement with the periodic orbit count (27).

In general, the unit vectors of the state space unit hypercube $\Phi \in [0, 1]^n$ point along the n axes; orbit Jacobian matrix \mathcal{J} stretches them into a fundamental parallelepiped basis vectors $\Phi^{(j)}$, each one a column of the $[n \times n]$ matrix

$$\mathcal{J} = \left(\Phi^{(1)} \Phi^{(2)} \dots \Phi^{(n)} \right). \tag{97}$$

The Hill determinant

$$\text{Det } \mathcal{J} = \text{Det} \left(\Phi^{(1)} \Phi^{(2)} \dots \Phi^{(n)} \right), \tag{98}$$

is then the volume of the fundamental parallelepiped whose edges are basis vectors $\Phi^{(j)}$. Note that the unit hypercubes and fundamental parallelepipeds are half-open, as indicated by dashed lines in figure 4(a), so that their translates form a partition of the extended state space (22). For another example of fundamental parallelepipeds, see figure 5.

For temporal cat the total number of lattice states is again, as for the Bernoulli system, given by the fundamental fact (94). However, while for the temporal Bernoulli every sequence of alphabet letters (25) but one is admissible, for temporal cat the condition (43) constrains admissible winding numbers blocks \mathbf{M} .

For period-1, constant field lattice states $\phi_{t+1} = \phi_t = \phi_{t-1}$ it follows from (43) that

$$(s - 2)\phi_t = m_t,$$

so the orbit Jacobian matrix is a $[1 \times 1]$ matrix, and there are

$$N_1 = s - 2 \tag{99}$$

period-1 lattice states. This is easy to verify by counting the admissible m_t values. Since $\phi_t \in [0, 1)$, the range of m_t is $m_t \in [0, s - 2)$. So three of the (42) temporal cat letters are not admissible: $\underline{1}$ is below the range, and $s - 2$ and $s - 1$ are above it.

The action of the temporal cat orbit Jacobian matrix can be hard to visualize, as a period-2 lattice field is a 2-torus, period-3 lattice field a 3-torus, etc.. Still, the fundamental parallelepiped for the period-2 and period-3 lattice states, figure 5, should suffice to convey the idea. The fundamental parallelepiped basis vectors are the columns of \mathcal{J} . The $[2 \times 2]$ orbit Jacobian matrix (73) and its Hill determinant are

$$\mathcal{J} = \begin{pmatrix} s & -2 \\ -2 & s \end{pmatrix}, \quad N_2 = \text{Det } \mathcal{J} = (s - 2)(s + 2), \tag{100}$$

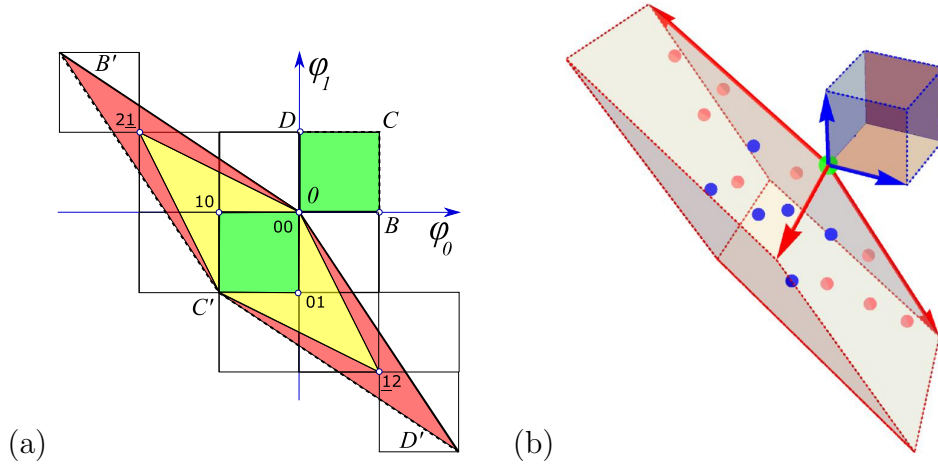


Figure 5. (Color online) (a) For $s = 3$, the temporal cat (44) has 5 period-2 lattice states $\Phi_M = (\phi_0, \phi_1)$: Φ_{00} fixed point and period-2 lattice states $\{\Phi_{01}, \Phi_{10}\}$, $\{\Phi_{12}, \Phi_{21}\}$. They lie within the unit square $[0BCD]$, and are mapped by the $[2 \times 2]$ orbit Jacobian matrix $-\mathcal{J}$ (100) into the fundamental parallelepiped $[0B'C'D']$, as in, for example, Bernoulli figure 4. The images of periodic points Φ_M land on the integer lattice, and are sent back into the origin by integer translations $M = m_0 m_1$, in order to satisfy the fixed point condition $\mathcal{J}\Phi_M + M = 0$. (b) A 3-dimensional [blue basis vectors] unit-cube stretched by $-\mathcal{J}$ (101) into the [red basis vectors] fundamental parallelepiped. For $s = 3$, the temporal cat (44) has 16 period-3 lattice states: a Φ_{000} fixed point at the vertex at the origin, [pink dots] 3 period-3 orbits on the faces of the fundamental parallelepiped, and [blue dots] 2 period-3 orbits in its interior. An n -dimensional state space unit hypercube $\Phi \in [0, 1]^n$ and the corresponding fundamental parallelepiped are half-open, as indicated by dashed lines, so the integer lattice points on the far corners, edges and faces do not belong to it.

(compare with the lattice states count (D.5)), with the resulting fundamental parallelepiped shown in figure 5(a). Period-3 lattice states for $s = 3$ are contained in the half-open fundamental parallelepiped of figure 5(b), defined by the columns of $[3 \times 3]$ orbit Jacobian matrix

$$\mathcal{J} = \begin{pmatrix} s & -1 & -1 \\ -1 & s & -1 \\ -1 & -1 & s \end{pmatrix}, \quad N_3 = \text{Det } \mathcal{J} = (s - 2)(s + 1)^2, \quad (101)$$

again in agreement with the periodic orbit count (D.5). The 16 period-3, $s = 3$ lattice states $\Phi_M = (\phi_0, \phi_1, \phi_2)$ are the Φ_{000} fixed point at the vertex at the origin, 3 period-3 orbits on the faces of the fundamental parallelepiped, and 2 period-3 orbits in its interior.

In this example there is no need to go further with the fundamental fact Hill determinant evaluations, as the explicit formula for the numbers of periodic lattice states is well known [108, 113]. The temporal cat equation (43) is a linear 2nd-order inhomogeneous difference equation (3-term recurrence relation) with constant coefficients that can be solved by standard methods [75] that parallel the theory of linear differential equations. Inserting a solution of form $\phi_t = \Lambda^t$ into the $m_t=0$ homogenous

2nd-order temporal cat condition (43) yields the characteristic equation (37) with roots $\{\Lambda, \Lambda^{-1}\}$. The result is that the number of temporal lattice states of period n is

$$N_n = |\text{Det } \mathcal{J}| = \Lambda^n + \Lambda^{-n} - 2, \quad (102)$$

often written as

$$N_n = 2 T_n(s/2) - 2, \quad (103)$$


where $T_n(s/2)$ is the Chebyshev polynomial of the first kind (this discussion continues in section 10.2).

Note that in the temporal lattice reformulation, both temporal Bernoulli and temporal cat happen to involve two distinct lattices:

- (i) In the latticization (1) of a time continuum, one replaces a time-dependent field $\phi(t)$ at time $t \in \mathbb{R}$ of *any* dynamical system by a discrete set of its values $\phi_t = \phi(at)$, at time instants $t \in \mathbb{Z}$. Here the subscript ‘ t ’ indicates a *coordinate* over which the field ϕ lives.
- (ii) A peculiarity of the temporal Bernoulli and temporal cat is that the *field* ϕ_t , (23) and (41), is confined to the unit interval $[0, 1)$, imparting an integer lattice structure onto the intermediate calculational steps in the extended state space (22) on which the orbit Jacobian matrix \mathcal{J} acts. Nothing like that applies to general nonlinear field theories of section 4.

8.2. Periodic orbit theory

How come that a Hill determinant (94) counts lattice states?

For a general, nonlinear fixed point condition $F[\Phi] = 0$, expansion (84) in terms of traces is a cycle expansion [9, 47, 53], with support on *periodic orbits*. Ozorio de Almeida and Hannay [3] were the first to relate the number of periodic points to a Jacobian matrix generated volume; in 1984 they used such relation as an illustration of their ‘principle of uniformity’: “periodic points of an ergodic system, counted with their natural weighting, are uniformly dense in phase space.” In periodic orbit theory [47, 52]  this principle is stated as a **flow conservation** sum rule, where the sum is over all lattice states \mathbf{M} of period n ,

$$\sum_{|\mathbf{M}|=n} \frac{1}{|\det(\mathbb{1} - \mathbb{J}_{\mathbf{M}})|} = 1, \quad (104)$$

or, by Hill’s formula (77),

$$\sum_{|\mathbf{M}|=n} \frac{1}{|\text{Det } \mathcal{J}_{\mathbf{M}}|} = 1. \quad (105)$$

For the Bernoulli and temporal cat systems the ‘natural weighting’ takes a particularly simple form, as the Hill determinant of the orbit Jacobian matrix is the same for all

periodic points of period n , $\text{Det } \mathcal{J}_M = \text{Det } \mathcal{J}$, whose number is thus given by (85). For example, the sum over the $n = 2$ lattice states is,

$$\frac{1}{|\text{Det } \mathcal{J}_{00}|} + \frac{1}{|\text{Det } \mathcal{J}_{01}|} + \frac{1}{|\text{Det } \mathcal{J}_{10}|} = 1, \quad (106)$$


see figure 4(b). Furthermore, for any piece-wise linear system all curvature corrections [50] for orbits of periods $k > n$ vanish, leading to explicit lattice state-counting formulas of kind reported in this paper.

In the case of temporal Bernoulli or temporal cat, the hyperbolicity is the same everywhere and does not depend on a particular solution Φ_c , counting periodic orbits is all that is needed to solve a cat-map dynamical system completely; once periodic orbits are counted, all cycle averaging formulas [51] follow.

Fritz, this is the ‘periodic orbit theory’. And if you don’t know, *now you know*.

9. Translations and reflections

Though this exposition is nominally about ‘evolution in time’, ‘time’ is such a loaded notion, a straightjacket hard to escape, that it is best to forget about ‘time’ for time being, and think instead like a crystallographer, about lattices and the space groups that describe their symmetries.

Of necessity, there are many group-theoretic notions a crystallographer must juggle (see *ChaosBook sect. 11.2*), but only a few key things to understand. For a 1-dimensional lattice, there are only two kinds of qualitatively different symmetry transformations, 

- (i) translations (109) and reflections (111), which reverse the direction of translation.
- (ii) There are two kinds of reflections (121), across a lattice site, and across a mid-point between lattice sites, figure 6.
- (iii) While the lattice \mathcal{L} and its space group G are both infinite, *orbits* of lattice states are finite and described by finite cyclic and dihedral groups, figure 7.
- (iv) A lattice state has one of the 4 possible symmetries, figure 9. They are the building blocks of zeta functions of section 11.

Should the reader find symmetries of infinite lattices too obtruse: to understand all that one needs to know about translations and reflections, it suffices to understand the symmetries of a triangle and a square, figure 8.

9.1. Internal symmetries

In addition to the spacetime symmetries, a field theory might have an *internal* symmetry, a group of transformations that leaves the Euler–Lagrange equations invariant, but acts only on a lattice site field, not on the spacetime lattice.

The ϕ^4 action (57) is invariant under the D_1 reflection $\phi_z \rightarrow -\phi_z$. The temporal Bernoulli (29) and temporal cat (43) Euler–Lagrange equations are invariant under D_1 inversion of the field though the center of the $0 \leq \phi_z < 1$ unit interval:

$$\bar{\phi}_z = 1 - \phi_z \pmod{1}. \quad (107)$$

If $\Phi = \{\phi_z\}$ is a lattice state of the system, its inversion $\bar{\Phi} = \{\bar{\phi}_z\}$ is also a lattice state. So every lattice state of the temporal Bernoulli and the temporal cat either belongs to a pair of asymmetric lattice states $\{\Phi, \bar{\Phi}\}$, or is symmetric under the inversion. Figures 10 and 13 illustrate such symmetries.

In principle, the internal symmetries should also be quotiented, but to keep things as simple as possible, they are not quotiented in this paper.

9.2. Symmetries of 1-dimensional lattices, sublattices

A space group G is the set of all translations and rotations that puts a crystallographic structure \mathcal{L} in coincidence with itself. To make the exposition as simple as possible, here we focus on 1-dimensional crystals, with sites labeled by integer lattice $\mathcal{L} = \mathbb{Z}$. Their space groups crystallographers [70] call *line groups*. There are only two **1-dimensional space groups** G : $p1$, or the *infinite cyclic group* C_∞ of all lattice translations, and $p1m$, the *infinite dihedral group* D_∞ of all translations and reflections [114],

$$D_\infty = \{\cdots, r_{-2}, \sigma_{-2}, r_{-1}, \sigma_{-1}, 1, \sigma, r_1, \sigma_1, r_2, \sigma_2, \cdots\}. \quad (108)$$

A half of the elements are translations ('shifts'; for finite period lattices, 'rotations'). $r_0 = 1$ denotes the identity, and the $r_1 = r$, $r_2 = r^2$, \cdots , $r_k = r^k$, \cdots , denote translations by $1, 2, \cdots, k, \cdots$ lattice points. They form the *infinite cyclic group*

$$C_\infty = \{\cdots, r_{-2}, r_{-1}, 1, r_1, r_2, r_3, \cdots\}, \quad (109)$$

a subgroup of D_∞ , in crystallography called the translation group.

The other half of elements are reflections $\sigma_k^2 = 1$ ('inversions', 'time reversals', 'flips'), defined by first translating by k steps, and then reflecting over the 0th lattice point, resulting in a 'translate-reflect' operation

$$\sigma_k = \sigma r_k. \quad (110)$$

The defining property of translate & reflect groups ('dihedral' groups, 'flip systems' [114]) is that any reflection reverses the direction of the translation

$$\sigma_k r = r^{-1} \sigma_k. \quad (111)$$

The group multiplication (or 'Cayley') table for successive group actions $g_i g_j$ follows:

$$\begin{array}{c|cc} & r_j & \sigma_j \\ \hline r_i & r_{i+j} & \sigma_{j-i} \\ \sigma_i & \sigma_{i+j} & r_{j-i} \end{array}. \quad (112)$$

Multiplication either adds up translations, or shifts and then reverses their direction. The order in which the elements $g_i g_j$ act is right to left, i.e., a group element acts on the expression to its right.

A crystallographer organizes the *subgroups* of a space group G by means of *Bravais lattices* $\mathcal{L}_{\mathbf{a}}$ (4), sublattices of the lattice \mathbb{Z} , each defined here by a 1-dimensional *Bravais cell of period* n , given by a lattice vector \mathbf{a} of integer length n ,

$$\mathcal{L}_{\mathbf{a}} = \{j\mathbf{a} \mid j \in \mathbb{Z}\}, \quad (113)$$

with the lattice generated by the infinite translation group of all discrete translations replaced by

$$\mathbf{r}_j \rightarrow \mathbf{r}_{j\mathbf{a}}$$

multiples of \mathbf{a} , resulting in

$$H_{\mathbf{a}} = \{\cdots, \mathbf{r}_{-2\mathbf{a}}, \mathbf{r}_{-\mathbf{a}}, 1, \mathbf{r}_{\mathbf{a}}, \mathbf{r}_{2\mathbf{a}}, \cdots\}, \quad (114)$$

infinite translation subgroup of C_{∞} . You can visualize a lattice state invariant under subgroup $H_{\mathbf{a}}$ as a tiling of the lattice \mathbb{Z} by a generic lattice state over tile of length n .

Another family of subgroups of D_{∞} is obtained by substituting elements of D_{∞} (108) by

$$\mathbf{r}_j \rightarrow \mathbf{r}_{j\mathbf{a}}, \quad \sigma \rightarrow \sigma_k \quad 0 \leq k < n,$$

resulting in n infinite dihedral subgroups

$$H_{\mathbf{a},k} = \{\cdots, \mathbf{r}_{-2\mathbf{a}}, \sigma_k \mathbf{r}_{-2\mathbf{a}}, \mathbf{r}_{-\mathbf{a}}, \sigma_k \mathbf{r}_{-\mathbf{a}}, 1, \sigma_k, \mathbf{r}_{\mathbf{a}}, \sigma_k \mathbf{r}_{\mathbf{a}}, \mathbf{r}_{2\mathbf{a}}, \sigma_k \mathbf{r}_{2\mathbf{a}}, \cdots\}, \quad (115)$$

each given by a Bravais cell of period n , with reflection across a symmetry point shifted k half-steps, see (124).

9.3. Classes

Definition: A class is the set of elements left invariant by conjugation with all elements g of the group G , where an element b is conjugate to element a if

$$b = g a g^{-1}. \quad (116)$$

By (111), a conjugation by any reflection reverses the direction of translation

$$\sigma_i \mathbf{r}_j \sigma_{-i} = \mathbf{r}_{-j}, \quad (117)$$

so every translation pairs up with the equal counter-translation to form

$$\text{identity class} \quad \{1\}, \quad j = 0 \quad (118)$$

$$\text{translation classes} \quad \{\mathbf{r}_j, \mathbf{r}_{-j}\}, \quad j = 1, 2, 3, \cdots. \quad (119)$$

The $\mathbf{r}_0 = 1$ commutes with all group elements, and is thus always a class by itself.

From the multiplication table (112) it follows that a conjugate of a reflection

$$\mathbf{r}_i \sigma_j \mathbf{r}_i^{-1} = \sigma_{j-2i}, \quad \sigma_i \sigma_j \sigma_i^{-1} = \sigma_{2i-j}. \quad (120)$$

is a reflection related to it by a $2i$ translation. Hence the even subscript reflections belong to one class, and the odd subscript reflections to the other:

$$\begin{aligned} \text{even} & \quad \{\sigma_{2m}\}, \quad m \in \mathbb{Z} \\ \text{odd} & \quad \{\sigma_{2m+1}\}. \end{aligned} \quad (121)$$

By (120) $\mathbf{r} H_{n,k} \mathbf{r}^{-1} = H_{n,k-2}$, so for odd n , all subgroups $H_{n,k}$ are conjugate subgroups, and for even n , $H_{n,k}$ separate into 2 sets of conjugate subgroups,

$$\begin{aligned} \text{even} & \quad \{H_{2m,2j}\}, \quad 0 \leq j < m \\ \text{odd} & \quad \{H_{2m,2j+1}\}, \end{aligned} \quad (122)$$

each containing m subgroups.

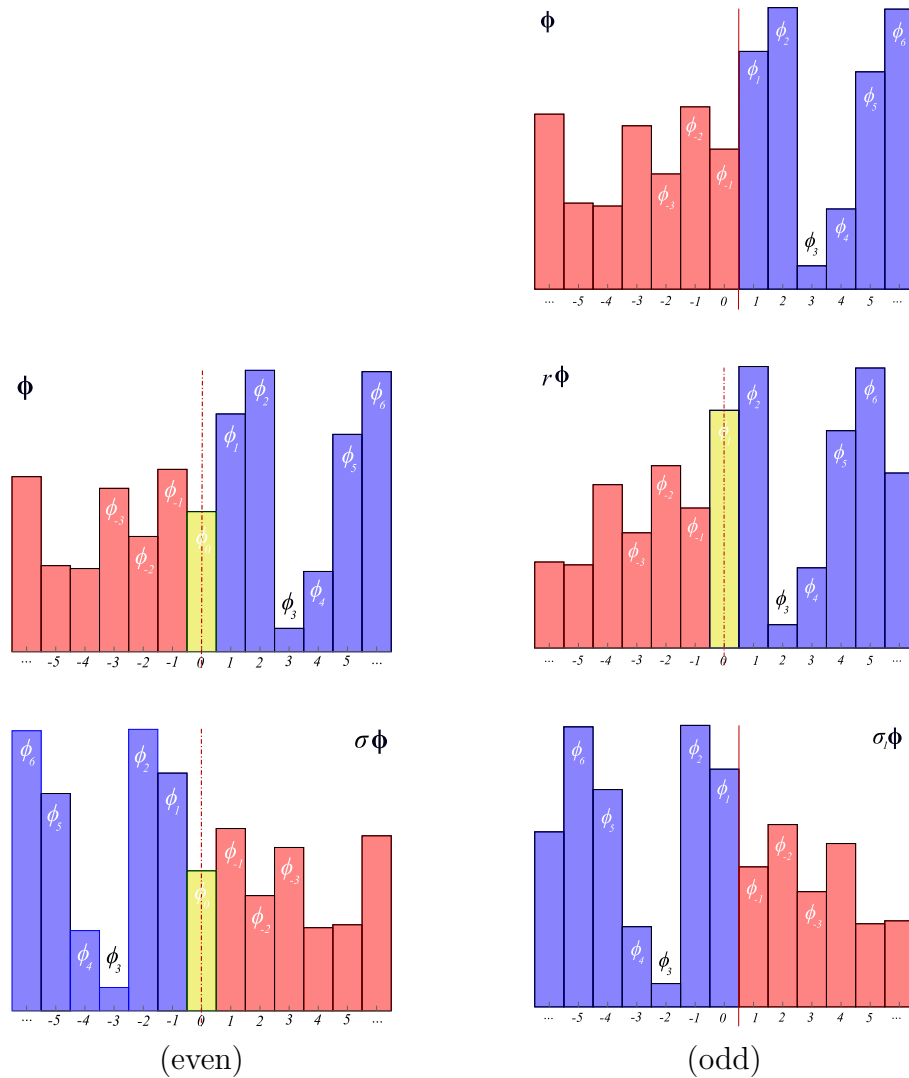


Figure 6. (Color online) There are two classes of lattice state reflections, even (123) and odd (124). (Even) reflection σ exchanges (blue ϕ_j) \leftrightarrow (red ϕ_{-j}) marked by dashed line reflection axis, with lattice site 0 fixed. (Odd) reflection $\sigma_1 = \sigma r$ swaps the ‘blues’ and the ‘reds’ by a lattice translation $\Phi \rightarrow r\Phi$, followed by a reflection σ . The result is a reflection across the midpoint of the $[01]$ interval, marked by full line reflection axis. See figure 2(b) for the notation. Continued in figure 7.

9.4. Reflections

What’s the difference between an ‘odd’ and an ‘even’ reflection? Every element in a class is equivalent to any other of its elements. So, to understand what everybody in a given class does, it suffices to work out what a single representative does: it suffices to analyse the $H_{n,0}$ and $H_{n,1}$ to account for all $H_{n,k}$.

So far, we have only discussed the abstract structure of the space group D_∞ and its subgroups. But the difference between an ‘odd’ and an ‘even’ is easiest to grasp by working out the action of σ_k on a lattice state.

Even class. Take $\sigma = \sigma_0$ as a representative of all even reflections σ_{2m} , and act on a lattice state (8):

$$\begin{aligned}\Phi &= \cdots \phi_{-3} \phi_{-2} \phi_{-1} \phi_0 \phi_1 \phi_2 \phi_3 \phi_4 \cdots \\ \sigma \Phi &= \cdots \phi_5 \phi_4 \phi_3 \phi_2 \phi_1 \boxed{\phi_0} \phi_{-1} \phi_{-2} \phi_{-3} \cdots,\end{aligned}\tag{123}$$


with $\boxed{\phi_0}$ indicating that the field at the lattice site 0 is unchanged by the reflection, see figure 6 (even).

Odd class. Take σ_1 as a representative of all odd reflections σ_{2m+1} . The result is:

$$\begin{aligned}\Phi &= \cdots \phi_{-3} \phi_{-2} \phi_{-1} \underline{\phi_0} \phi_1 \phi_2 \phi_3 \phi_4 \cdots \\ r\Phi &= \cdots \phi_{-3} \phi_{-2} \phi_{-1} \phi_0 \underline{\phi_1} \phi_2 \phi_3 \phi_4 \phi_5 \cdots \\ \sigma_1 \Phi = \sigma r\Phi &= \cdots \phi_6 \phi_5 \phi_4 \phi_3 \phi_2 \underline{\phi_1} | \phi_0 \phi_{-1} \phi_{-2} \phi_{-3} \cdots,\end{aligned}\tag{124}$$

where $\underline{\phi_j}$ indicates the field value at the lattice site 0, and $|$ indicates a reflection across midpoint between lattice sites 0 and 1, see figure 6 (odd).

More generally, one can say that the subscript k in the ‘translate-reflection’ (110) operation $\sigma_k = \sigma r_k$ advances the reflection point by $k/2$ steps, and then reflects across it.

If you do not find the two kinds of reflections intuitive, the distinction becomes crystal clear once you have a look at the smallest Bravais lattices, lattices of periods 3 and 4, figure 8. 

9.5. Symmetries of a system and of its solutions

What’s the deal about classes? A ‘class’ is a refinement of our intuitive notion that “rotations are rotations, and translations are translations.” Translated into a more familiar language, conjugation (116) is central to all of physics: a ‘law’ $F(\Phi)$ is invariant if it retains its form in all symmetry related coordinate frames,

$$F(\Phi) = g^{-1} F(g \Phi),\tag{125}$$

where g is a representation of group element $g \in G$. If this holds, we say that G is the *symmetry* of the system.

For example, the ‘temporal Bernoulli’ Euler–Lagrange equation (30) retains its form under conjugation by any C_∞ translation (109),

$$r_i(s1 - r_1) r_i^{-1} \Phi = (s1 - r_1) \Phi,\tag{126}$$

while the Euler–Lagrange second-order difference equations (51), ‘temporal cat’, ‘temporal Hénon’, and ‘temporal ϕ^4 theory’ Euler–Lagrange equations (18), (19) and (20) retain their form also under any D_∞ reflection.

Given that G is the symmetry of the system does not mean that G is also the symmetry of its solutions, or what we here call *lattice states*. They can satisfy all of system’s symmetries, a subgroup of them, or have no symmetry at all. For example, a generic lattice state (8) sketched in figure 6 has no symmetry beyond the identity, so

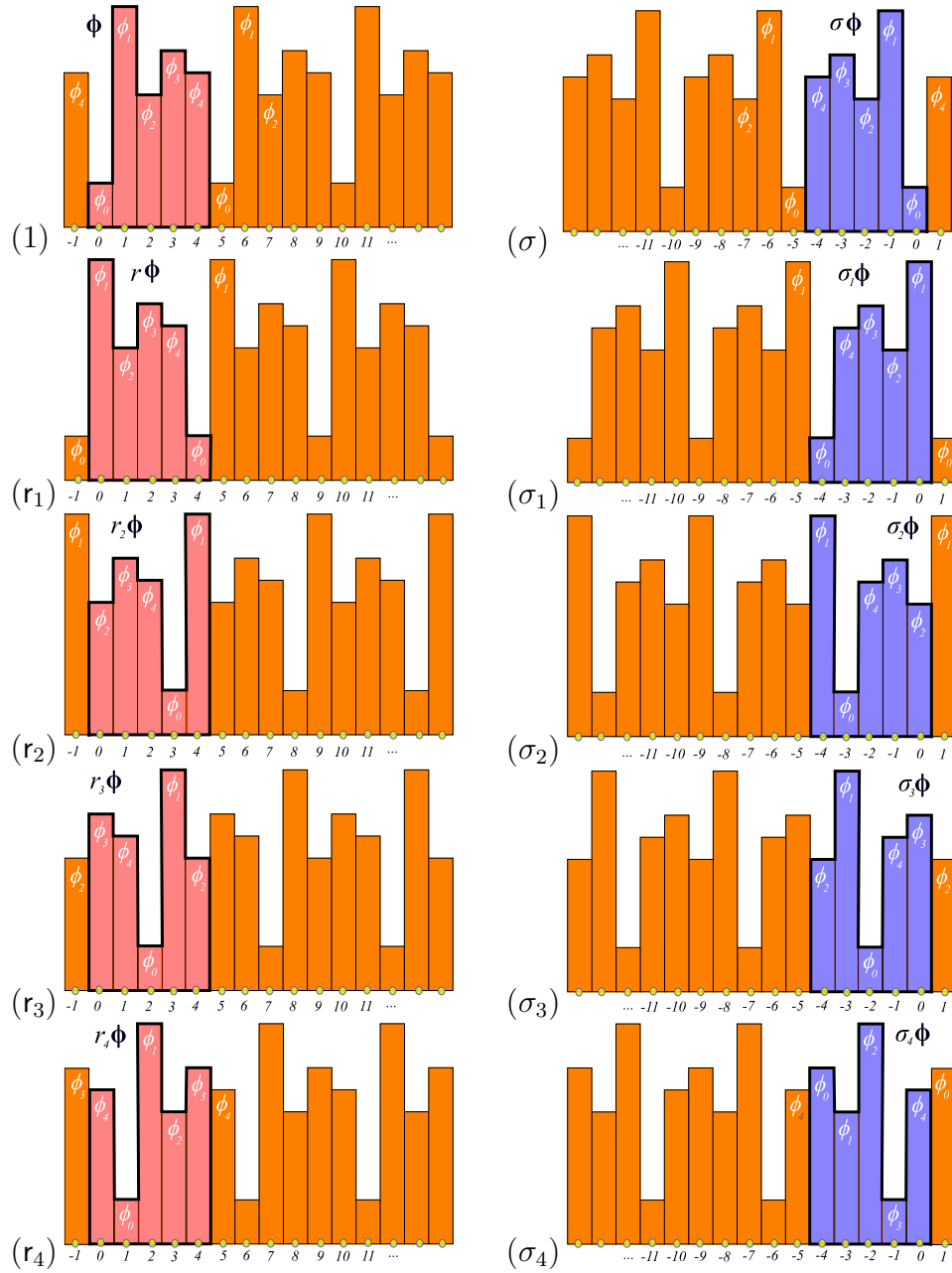


Figure 7. (Color online) (1) A Bravais cell \mathbf{a} with asymmetric lattice state $\Phi = \phi_0\phi_1\phi_2\phi_3\phi_4$, no reflection symmetry, outlined in bold, is invariant under the translation subgroup H_5 . Its C_∞ orbit are the $n = 5$ distinct lattice states (1) to (r_4) , obtained by all of the C_5 translations. Its D_∞ -orbit are $2n = 10$ distinct lattice states, 5 translations (1) to (r_4) and 5 translate-reflections (σ) to (σ_4) , obtained by all of the D_5 actions. See figure 2 (b) for the notation. Continued in figure 8.

its symmetry group is the trivial subgroup $\{e\}$; any translation r_j or reflection σ_k maps it into a different, distinct lattice state, as shown in figure 7. At the other extreme, the constant lattice state $\phi_j = \phi$ is invariant under any translation or reflection - its symmetry group is the full G , the symmetry of the system. In between, there are lattice states whose symmetry is a subgroup of G .

9.6. What are 'lattice states'? Orbits?

For evolution-in-time, every period- n periodic point is a fixed point of the n th iterate of the 1 time-step map. In the lattice formulation, the totality of finite-period lattice states is the *set of fixed points* of all $H_{\mathbf{a}}$ and $H_{\mathbf{a},k}$ subgroups of D_{∞} .

You can visualize a lattice state invariant under ('fixed by') subgroup $H_{\mathbf{a},k}$ as a tiling of the lattice \mathbb{Z} by a lattice state tile of length n , symmetric under reflection σ_k , see figure 9 (b-c).

Definition: Orbit or G -orbit of a lattice state Φ is the set of all lattice states

$$\mathcal{M}_{\Phi} = \{g\Phi \mid g \in G\} \quad (127)$$

into which Φ is mapped under the action of group G . We label the orbit \mathcal{M}_{Φ} by any lattice state Φ belonging to it.

As an example, the D_{∞} orbit of the period-5 lattice state is shown in figure 7.

Definition: Symmetry of a solution. We shall refer to the maximal subgroup $G_{\Phi} \subseteq G$ of actions which permute lattice states within the orbit \mathcal{M}_{Φ} , but leave the orbit invariant, as the symmetry G_{Φ} of the orbit \mathcal{M}_{Φ} ,

$$G_{\Phi} = \{g \in G \mid g\mathcal{M}_{\Phi} = \mathcal{M}_{\Phi}\}. \quad (128)$$

An orbit \mathcal{M}_{Φ} is G_{Φ} -symmetric (symmetric, set-wise symmetric, self-dual) if the action of elements of G_{Φ} on the set of lattice states \mathcal{M}_{Φ} reproduces the orbit.

Definition: Index of orbit \mathcal{M}_{Φ} is given by

$$m_{\Phi} = |G|/|G_{\Phi}|. \quad (129)$$

(See Wikipedia [182] and Dummit and Foote [73].)

And now, a pleasant surprise, obvious upon an inspection of figures 7 and 9: what happens in the Bravais cell, stays in the Bravais cell. Even though the lattices \mathcal{L} , $\mathcal{L}_{\mathbf{a}}$ are infinite, and their symmetries D_{∞} , $H_{\mathbf{a}}$, $H_{\mathbf{a},k}$ are *infinite* groups, the Bravais lattice states' *orbits* are *finite*, described by the finite group permutations of the infinite lattice curled up into a Bravais cell periodic n -site ring.

Indeed, to grasp everything one needs to know about translations r_j (for regular polygons, 'rotations'), and reflections σ_k , it suffices to understand the symmetries of an equilateral triangle (dihedral group D_3) and a square (dihedral group D_4), depicted in figure 8. It is clear by inspection that an n -sided regular polygon has n -fold translational

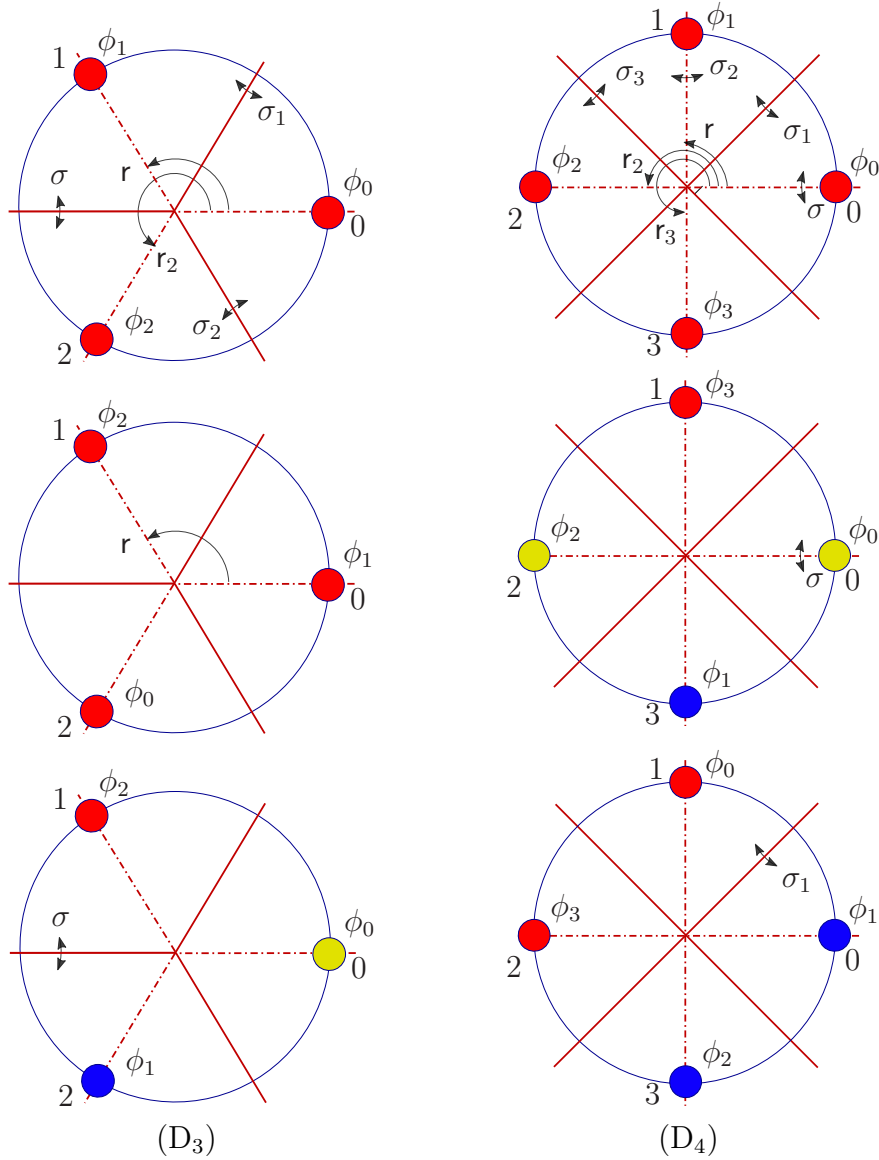


Figure 8. (Color online) Consider a period- n Bravais cell tiling of a 1-dimensional lattice \mathcal{L} . With \mathcal{L} curled into a ring of n lattice sites, actions of the infinite dihedral group D_∞ reduce to translational and reflection symmetries of (D_3) an equilateral triangle, $n = 3$ lattice sites; (D_4) a square, $n = 4$ lattice sites; all group operations that overlie an n -sided regular polygon onto itself. The n translations r_j permute the sites cyclically. The n dihedral group D_n translate-reflect σ_k elements (130) reflect the sites across reflection axes, exchanging red and blue sites. For even n , an even reflection (dashed line reflection axis), here σ , leaves a pair of opposite sites fixed (marked yellow), while an odd reflection axis (full line), here σ_1 , bisects the opposite edges, and flips all sites. For odd n , every reflection half-axis leaves a site fixed (dashed line), and bisects the opposite edge (full line). This periodic ring visualization makes it obvious that any symmetric lattice state is reflection invariant across two points on the lattice, see figure 9.

symmetry and n reflection symmetry axes. The group of such symmetries is the finite dihedral group

$$D_n = \{1, \sigma, \mathbf{r}, \sigma_1, \mathbf{r}_2, \sigma_2, \dots, \mathbf{r}_{n-1}, \sigma_{n-1}\} \quad (130)$$

of order $2n$. A half of its elements are the n cyclic group C_n translations \mathbf{r}_j . The other half are the n reflections σ_k , one for the reflection across each symmetry axis. The group multiplication table is the same as the D_∞ (112), but with all subscripts mod n . As in (117), conjugation by any reflection reverses the direction of translation

$$\sigma_i \mathbf{r}_j \sigma_{-i} = \mathbf{r}_{n-j}, \quad 0 < j < n, \quad (131)$$

so every translation pairs up with the equal counter-translation to form a 2-element class (119).

The distinction between the classes of even and odd reflections (121) is visually self-evident by inspection of figure 8: the symmetry axes either connect opposite lattice sites, or bisect the edges, or both, if n is odd (a triangle, for example). One can say that k in the ‘translate-reflection’ (110) operation σ_k advances the reflection point by k $1/2$ steps, and then reflects across it.

For a polygon with an *odd* number of lattice sites (a triangle, for example), we see by contemplating the triangle of figure 8, as well as by taking mod n of the conjugation relation (120), that all reflections are in the same conjugacy class $\{\sigma_j\}$: there is no splitting into odd and even cases, in contrast to the infinite lattice case (121).

For a polygon with an *even* number of lattice sites (a square, for example), one must distinguish the ‘long’ axes that connect lattice sites (we label them by even numbers $0, 2, \dots$) from the ‘short’ symmetry axes that bisect opposite edges (labelled by odd numbers $1, 3, \dots$). The corresponding reflections belong to different D_n (subclasses of (121)),

$$\begin{aligned} \text{even reflections} & \quad \{\sigma, \sigma_2, \sigma_4, \dots, \sigma_{n/2}\} \\ \text{odd reflections} & \quad \{\sigma_1, \sigma_3, \dots, \sigma_{n/2+1}\}. \end{aligned} \quad (132)$$

9.7. Symmetries of lattice states

A Bravais lattice state Φ has one of the four symmetries:



$$\begin{aligned} & \text{asymmetric, no reflection symmetry} \\ (a) \quad & \overline{\phi_0 \phi_1 \phi_2 \phi_3 \dots \phi_{n-1}} \\ & \text{index } m_\Phi = 2n \end{aligned} \quad (133)$$

lattice state invariant under the translation group H_n . Its G -orbit, generated by all actions of D_∞ , results in $2n$ distinct, D_n related lattice states. This is illustrated by the H_5 -invariant lattice state Φ of figure 7. Its D_5 orbit are $2n = 10$ lattice states, 5 translations and 5 translate-reflections.

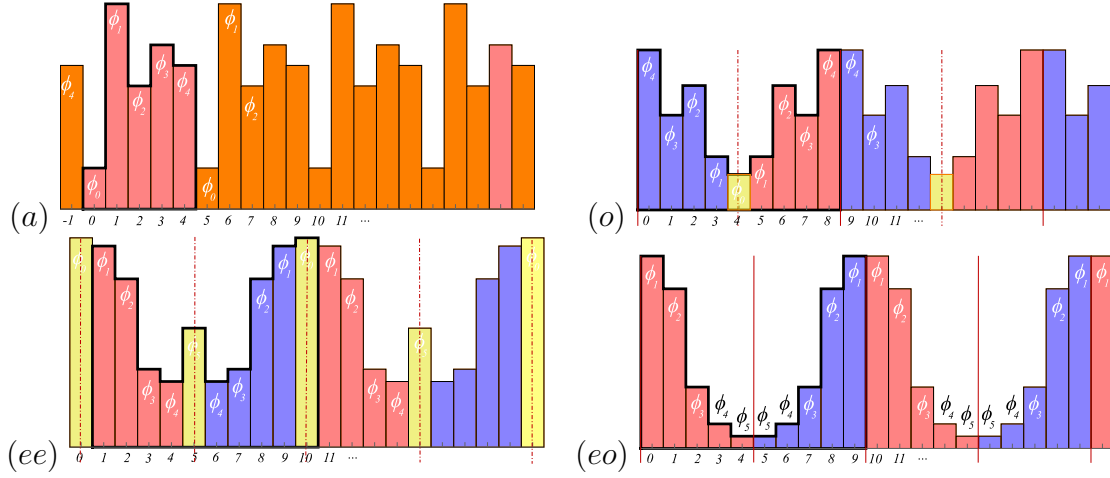


Figure 9. (Color online) A Bravais lattice state Φ has one of the 4 possible symmetries, illustrated by: (a) *No reflection symmetry*: an H_5 invariant period-5 lattice state (133). For its G -orbit, see figure 7. (o) *Odd period, reflection-symmetric*: an $H_{9,8}$ invariant period-9 lattice state (134), reflection symmetric over the lattice sites interval [8-9] midpoint and over the lattice site 4. (ee) *Even period, even reflection-symmetric*: an $H_{10,0}$ invariant period-10 lattice state (135), reflection symmetric over lattice sites 0 and 5. (eo) *Even period, odd reflection-symmetric*: an $H_{10,9}$ invariant period-10 lattice state (136), reflection symmetric over the [4-5] and [9-10] interval midpoints. Horizontal: lattice sites labelled by $t \in \mathbb{Z}$. Vertical: value of field ϕ_t , plotted as a bar centred at lattice site t . Time reversed blocks indicated in blue, boundary sites in yellow. Even reflection axes dashed, odd reflections full line.

Next, the reflection-symmetric lattice states. As illustrated in figures 6 and 8, there are two classes (121) of lattice state reflections: even, across a lattice site, and odd, across the mid-point between a pair of adjacent lattice sites. However, as is evident by inspection of figure 8, curling up the lattice \mathcal{L} into a Bravais cell periodic n -site ring implies that an axis cuts the ring twice, and constrains the possible reflection points to three configurations:

$$\begin{aligned}
 &\text{odd period } n = 2m + 1 \\
 (o) \quad &\overline{\phi_0 \phi_1 \phi_2 \cdots \phi_m | \phi_m \cdots \phi_2 \phi_1} \\
 &\text{index } m_\Phi = n
 \end{aligned} \tag{134}$$

lattice state invariant under the dihedral group $H_{n,k}$, illustrated by the $H_{9,8}$ invariant lattice state Φ of figure 9(o).

$$\begin{aligned}
 &\text{even period } n = 2m + 2, \text{ even reflection } k \\
 (ee) \quad &\overline{\phi_0 \phi_1 \phi_2 \cdots \phi_m | \phi_{m+1} \phi_m \cdots \phi_2 \phi_1} \\
 &\text{index } m_\Phi = n
 \end{aligned} \tag{135}$$

lattice state invariant under the dihedral group $H_{n,k}$, k even, illustrated by the $H_{10,0}$ invariant lattice state Φ of figure 9(ee).

$$\text{even period } n = 2m, \text{ odd reflection } k$$

$$(eo) \quad \overline{\phi_1 \phi_2 \phi_3 \cdots \phi_m | \phi_m \cdots \phi_2 \phi_1 |} \quad (136)$$

index $m_\Phi = n$

lattice state invariant under the dihedral group $H_{n,k}$, k odd, illustrated by the $H_{10,9}$ invariant lattice state Φ of figure 9(eo).

The lattice state symmetry G_Φ (128) of the above (o)–(eo) reflection-symmetric lattice states Φ is the reflection group $D_1 = \{1, \sigma_k\}$. This symmetry means two things:

- (1) The D_∞ orbits of reflection-symmetric lattice states contain only translations, as any reflection amounts to a cyclic group C_n translation. (Reflect a lattice state in figure 9(b-d) over any lattice site or mid-interval: the result is its translation.)
- (2) The prime lattice state is a ‘half’ of the Bravais cell, the length m orbit,

$$\tilde{\Phi} = (\phi_1 \phi_2 \phi_3 \cdots \phi_m), \quad (137)$$

give or take some boundary sites.

To develop intuition about how one reconstructs the period- n orbit from this length- m block it is helpful to have a look at explicit matrix representation of the dihedral group D_n actions.

9.8. Permutation representation

A lattice state Φ over a Bravais cell \mathbf{a} can be assembled into an n -dimensional vector whose components are lattice site fields

$$\Phi^\top = (\phi_0, \phi_1, \phi_2, \phi_3, \cdots, \phi_{n-1}). \quad (138)$$

Matrices that reshuffle the components of such vectors form the *permutation representation* of a finite group G . They give us a different perspective on the above three kinds of symmetric solutions.

The permutation representation of 1-step lattice translation \mathbf{r} acts on a Bravais lattice state by the off-diagonal $[n \times n]$ matrix (31). This is a cyclic C_n permutation that translates the lattice state Φ “forward-in-time” by one site,

$$(\mathbf{r}\Phi)^\top = (\phi_1, \phi_2, \cdots, \phi_{n-1}, \phi_0).$$

A permutation representation of a D_n translate-reflect operation is essentially an anti-diagonal matrix that reverses the order of site fields, up to a cyclic permutation

$$(\sigma_k \Phi)^\top = (\phi_{n-1}, \cdots, \phi_2, \phi_1, \phi_0).$$

Even periods: The shortest even period symmetric lattice state is the period-2 lattice state $\Phi_p^\top = (\phi_0, \phi_1)$ such as the temporal cat (100). For example, for temporal Hénon (53) there is only one period-2 prime orbit, consisting of lattice state

$$\Phi_p = \frac{1}{a} \begin{pmatrix} -1 - \sqrt{a-3} \\ -1 + \sqrt{a-3} \end{pmatrix}, \quad (139)$$

and its translation $\mathbf{r}\Phi_p$. Its symmetry, $\Phi_p^\top = (\boxed{\phi_0}\boxed{\phi_1})$ is of (ee) type (135), indicated as yellow lattice sites fields in figure 9(ee). Its orbit Jacobian matrix is of the nonlinear field theory form (74)

$$\mathcal{J} = \begin{pmatrix} s_0 & -2 \\ -2 & s_1 \end{pmatrix}. \quad (140)$$

This lattice state is ‘all boundary points’, too short to illustrate a symmetry reduction to a D_n prime orbit. Still, as we show in figure 12(b), its relation to the block circulant structure of repeated-tile orbit Jacobian matrix (75) and its contribution to ϕ^3 field theory spectrum is instructive.

Odd periods: In odd dimensions, the n translate-reflect matrices of D_n are related by translations (120). For example, for a period-3 lattice state without symmetry $\Phi^\top = (\phi_0, \phi_1, \phi_2)$, they are

$$\sigma = \begin{pmatrix} 1 & 0 & 0 \\ 0 & 0 & 1 \\ 0 & 1 & 0 \end{pmatrix}, \quad \sigma_1 = \begin{pmatrix} 0 & 1 & 0 \\ 1 & 0 & 0 \\ 0 & 0 & 1 \end{pmatrix}, \quad \sigma_2 = \begin{pmatrix} 0 & 0 & 1 \\ 0 & 1 & 0 \\ 1 & 0 & 0 \end{pmatrix}.$$

In agreement with (134), figure 8 and figure 9(o), these reflections keep one lattice site fixed (for each permutation matrix σ_k there is only one ‘1’ on the diagonal), swap the rest.

To get some insight into the length- m prime lattice state $\tilde{\Phi}$ (137), consider next a period-5 reflection symmetric lattice states that tile the infinite lattice \mathcal{L} with a reflection-fixed $\boxed{\phi_0}$, and a length-2 block $\tilde{\Phi} = (\phi_1, \phi_2)$,

$$\Phi^\top = (\boxed{\phi_0}\phi_1\phi_2|\phi_2\phi_1). \quad (141)$$

Actions of D_5 permutation representation illustrates that the fixed lattice states Φ of σ_k are related by cyclic translations:

$$\begin{aligned} \sigma\Phi &= \begin{pmatrix} 1 & 0 & 0 & 0 & 0 \\ 0 & 0 & 0 & 0 & 1 \\ 0 & 0 & 0 & 1 & 0 \\ 0 & 0 & 1 & 0 & 0 \\ 0 & 1 & 0 & 0 & 0 \end{pmatrix} \begin{pmatrix} \boxed{\phi_0} \\ \phi_1 \\ \phi_2 \\ \phi_2 \\ \phi_1 \end{pmatrix} = \begin{pmatrix} \boxed{\phi_0} \\ \phi_1 \\ \phi_2 \\ \phi_2 \\ \phi_1 \end{pmatrix} \\ \sigma_4(\mathbf{r}_{-2}\Phi) &= \begin{pmatrix} 0 & 0 & 0 & 0 & 1 \\ 0 & 0 & 0 & 1 & 0 \\ 0 & 0 & 1 & 0 & 0 \\ 0 & 1 & 0 & 0 & 0 \\ 1 & 0 & 0 & 0 & 0 \end{pmatrix} \begin{pmatrix} \phi_2 \\ \phi_1 \\ \boxed{\phi_0} \\ \phi_1 \\ \phi_2 \end{pmatrix} = \begin{pmatrix} \phi_2 \\ \phi_1 \\ \boxed{\phi_0} \\ \phi_1 \\ \phi_2 \end{pmatrix}. \end{aligned} \quad (142)$$

What is the orbit stability of such lattice state? The symmetry conditions are the Bravais lattice state 5-periodicity mod 5, and the even reflection across $\boxed{\phi_0}$:

$$\phi_i = \phi_{i+5}, \quad \phi_{-i} = \phi_i. \quad (143)$$

A lattice state satisfies the Euler–Lagrange equation (51)

$$-\phi_{t-1} + 2\phi_t - \phi_{t+1} + V'(\phi_t) = 0, \quad (144)$$

on the period-5 Bravais cell,

$$\begin{aligned}
-\phi_1 + 2\phi_0 - \phi_1 + V'(\phi_0) &= 0 \\
-\phi_0 + 2\phi_1 - \phi_2 + V'(\phi_1) &= 0 \\
-\phi_1 + 2\phi_2 - \phi_2 + V'(\phi_2) &= 0 \\
-\phi_1 + 2\phi_2 - \phi_2 + V'(\phi_2) &= 0 \\
-\phi_0 + 2\phi_1 - \phi_2 + V'(\phi_1) &= 0,
\end{aligned} \tag{145}$$

where we have used (143). The result are symmetry reduced equations, modified by the two reflection bc's,

$$\begin{aligned}
-2\phi_1 + 2\phi_0 + V'(\phi_0) &= 0 \\
-\phi_0 + 2\phi_1 - \phi_2 + V'(\phi_1) &= 0 \\
-\phi_1 + \phi_2 + V'(\phi_2) &= 0,
\end{aligned} \tag{146}$$

with an asymmetric 3-dimensional orbit Jacobian matrix (74)

$$\mathcal{J}_o = \begin{pmatrix} s_0 & -2 & 0 \\ -1 & s_1 & -1 \\ 0 & -1 & s_2 - 1 \end{pmatrix}. \tag{147}$$

So, for a reflection-symmetric lattice state of odd period, one has to impose the even $\boxed{\phi_0}$ and odd | reflection bc's in order to define the orbit Jacobian matrix for the prime orbit $\tilde{\Phi}$ (137).

The form of orbit Jacobian matrices for all bc's of section 9.7, specialized to temporal cat but easily generalized to general nonlinear field theories, is given in Appendix C.

Why bother? ChaosBook.org [53] bemoans more than 20 times that in it the time-reversal symmetric orbits are not accounted for (here that is accomplished in section 11). But for long periods, almost all lattice states are of asymmetric type (133). Why do we obsess about symmetric lattice states so much? How important are they?

The reason is that periodic orbit expansions are dominated by short orbits, with the longer ones only providing exponentially small corrections. But almost all short-period lattice states are symmetric; for example, for the ϕ^3 field theory, the first two asymmetric lattice states are of period 6.

10. Reciprocal lattice

If the orbit Jacobian matrix is invariant under time translation, its eigenvalue spectrum and Hill determinant can be efficiently computed using tools of crystallography, such as the discrete Fourier transform, a discretization approach that goes all the way back to Hill's 1886 paper [102].

Think of a solution of a discrete time dynamical system as a 1-dimensional lattice state with the field on each site labeled by integer time. A time period- n lattice state

lives on a discrete 1-torus (a ring or chain or necklace) of period- n , and if system's law is time-invariant, its orbit, the set of lattice states related to it by cyclic translations, are physically equivalent (figure 7). The symmetry is the cyclic group C_n , and one only needs to count and distinguish C_n orbits, compute only one lattice state per each orbit.

The smart way to do this is by a discrete Fourier transform. Were the lattice d -dimensional (4), defined by Bravais cell vectors $\{\mathbf{a}\}$, a crystallographer would immediately move to the *reciprocal* lattice, $\tilde{\mathcal{L}}_{\mathbf{b}} = \{k\mathbf{b} | k \in \mathbb{Z}\}$, with reciprocal lattice basis vectors $\{\mathbf{b}\}$ satisfying $\mathbf{b}\mathbf{a} = 2\pi$. On the reciprocal lattice translations are quotiented out, and calculations are restricted to a finite Brillouin zone (Bloch's theorem of solid state physics). Here we work on a 1-dimensional lattice with unit lattice spacing 1, so the reciprocal lattice spacing is $2\pi/1 = 2\pi$, with the (first) Brillouin zone from $k = -\pi$ to $k = \pi$ (we give an example in figure 12).

The cyclic group C_n elements are generated by the $[n \times n]$ shift matrix (31) which translates a lattice state (9) forward-in-time by one site, $(\mathbf{r}\Phi)^\top = (\phi_1, \phi_2, \dots, \phi_{n-1}, \phi_0)$. After n shifts, the lattice state returns to the initial state, yielding the characteristic equation for the matrix \mathbf{r}

$$\mathbf{r}^n - \mathbb{1} = 0, \quad (148)$$

whose eigenvalues are n th roots of unity, with the n complex eigenvectors also built from roots of unity

$$\begin{aligned} \{\lambda_k\} &= \{1, \omega, \omega^2, \dots, \omega^{n-1}\}, & \omega &= e^{2\pi i/n} \\ \tilde{e}_k &= \frac{1}{\sqrt{n}}(1, \omega^k, \omega^{2k}, \dots, \omega^{k(n-1)}), & k &= 0, 1, \dots, n-1. \end{aligned} \quad (149)$$

10.1. Reciprocal lattice states

In the $\{\tilde{e}_k\}$ Fourier basis, a real n -dimensional lattice state vector Φ is mapped onto a n -dimensional complex reciprocal lattice vector

$$\tilde{\Phi} = (\tilde{\phi}_0, \tilde{\phi}_1, \tilde{\phi}_2, \dots, \tilde{\phi}_{n-1}), \quad (150)$$

with the k th Fourier mode of magnitude $|\tilde{\phi}_k|$ and phase $e^{i\theta_k}$.

On the reciprocal lattice, the shift matrix is diagonal, $\mathbf{r}_{jk} = \omega^k \delta_{jk}$, and the 'time' dynamics is breathtakingly simple: no matter what the dynamical system is, in one time step $\Phi \rightarrow \mathbf{r}\Phi$, the k th Fourier mode phase is incremented by a fraction of the circle,

$$\begin{aligned} (\tilde{\phi}_0, \tilde{\phi}_1, \tilde{\phi}_2, \dots, \tilde{\phi}_{n-1}) &\rightarrow (\tilde{\phi}_0, \omega\tilde{\phi}_1, \omega^2\tilde{\phi}_2, \dots, \omega^{n-1}\tilde{\phi}_{n-1}) \\ e^{i\theta_k} &\rightarrow e^{i(\theta_k + 2\pi k/n)}, \end{aligned} \quad (151)$$

so reciprocal lattice states literally run in circles; for non-zero k and $|\tilde{\phi}_k|$, all reciprocal lattice states lie on vertices of regular complex plane n -gons, inscribed in circles of radius $|\tilde{\phi}_k|$, one circle for each orbit.

As a concrete example, consider the period-3 lattice states of the temporal Bernoulli (29) for stretching parameter $s = 2$. It is a linear problem and all lattice states are easily computed by hand, one for each symbol block \mathbf{M} . There is always the fixed point lattice

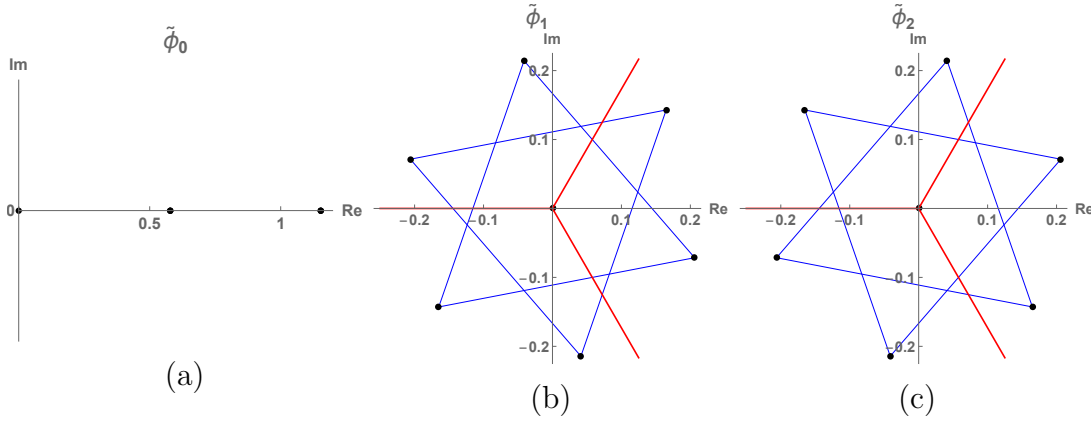


Figure 10. (Color online) The reciprocal lattice $(\tilde{\phi}_0, \tilde{\phi}_1, \tilde{\phi}_2)$ Fourier components of the 7 C_3 -equivariant period-3 lattice states, $s = 2$ temporal Bernoulli system (29). In $\tilde{\phi}_1$ and $\tilde{\phi}_2$ complex planes, reciprocal lattice states lie on vertices of the 2 equilateral triangles, one for each C_3 orbit, while the component at the origin is the fixed point $\Phi = (0, 0, 0)$. The C_3 fundamental domain indicated by red border lines contains non-zero reciprocal lattice states whose phases lie in the $[-2\pi/6, 2\pi/6)$ wedge, one reciprocal lattice state for each distinct C_3 orbit.

state $(0, 0, 0)$ at the origin, and the remaining lattice states belong to $M_3 = 2$ period-3 orbits, where M_n is the number of orbits of period n . Discrete Fourier transform maps these 2 orbits into reciprocal lattice $(\tilde{\phi}_0, \tilde{\phi}_1, \tilde{\phi}_2)$ triangles, see figure 10. The time-step r acts on the $\tilde{\phi}_1, \tilde{\phi}_2$ components by complex $1/3$ -circle phase rotations $\exp(2\pi i/3)$ and $\exp(4\pi i/3)$, respectively: reciprocal lattice states connected by blue lines in figure 10 lie on a circle and belong to the same orbit. In this example the two orbits happen to lie on the same circle, as they are related by the *internal* $D_1 : \phi_i \rightarrow 1 - \phi_i$ symmetry of the Bernoulli system, see section 9.1.

10.1.1. C_n fundamental domain. Divide each $k > 0$ complex $\tilde{\phi}_k$ plane of a period- n reciprocal lattice state into n equal wedges, and call one of them the ‘fundamental domain’, for example the wedge bordered by $[-\pi/n, \pi/n)$. Under n discrete rotations the fundamental domain completely tiles the complex plane. We exclude the fixed point lattice state $\tilde{\phi}_k = 0$ at the origin from the domain, as it belongs to a time invariant subspace.

As is clear by inspection of figure 10, every k th complex plane regular n -gon has precisely one vertex, i.e., a single reciprocal lattice state per each orbit, in the interior of the fundamental domain, or on its border. For the period-3 reciprocal lattice states shown in figure 10, there are 2 points in both $k = 2$ and $k = 3$ complex plane fundamental domain, one lattice state for each period-3 orbit.

Consider next the 121 period-5 reciprocal lattice states of the $s = 3$ temporal cat (43), figure 11 (a,b,c). Excluding the fixed point $\tilde{\phi}_k = 0$ lattice state at the origin, there are $M_5 = 24$ reciprocal lattice states in the figure 11 (d,e,f) fundamental domain, each representing $n = 5$ lattice states in its orbit, so the total number of lattice states is

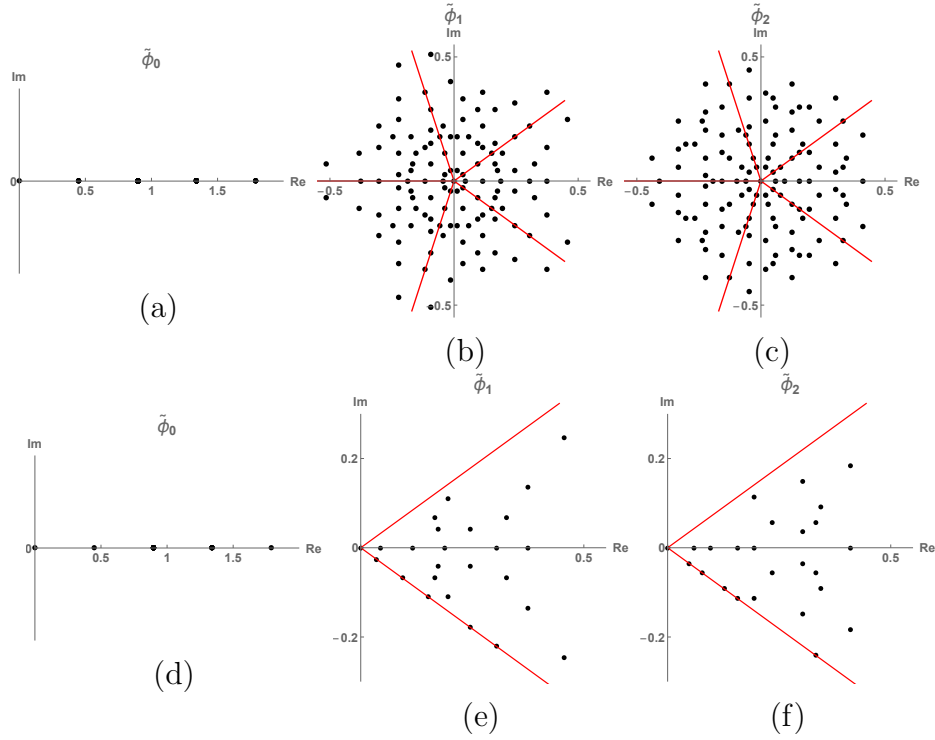



Figure 11. (Color online) The 121 period-5 reciprocal lattice states of the $s = 3$ temporal cat (43). (a,b,c) The reciprocal lattice $\tilde{\phi}_0, \tilde{\phi}_1, \tilde{\phi}_2$ complex planes. The state at the origin is the fixed point $(0, 0, 0, 0, 0)$. As in figure 10, all non-zero reciprocal lattice states lie on vertices of regular pentagons (not drawn here) that form orbits under C_5 cyclic permutations. (d,e,f) The C_5 fundamental domain contains $M_5 = 24$ non-zero reciprocal lattice states whose phases lie in the $[-2\pi/10, 2\pi/10)$ wedge, one reciprocal lattice state for each distinct C_5 orbit.

$N_5 = 1 + 5 M_5 = 1 + 5 \times 24 = 121$, in agreement with table D2.

The set of period-5 reciprocal lattice states of Figure 11 clearly exhibits symmetries beyond the cyclic C_5 , in particular under reflections across the axes drawn in red. It also turns out that for the temporal cat the $\tilde{\phi}_1$ complex plane looks the same as the $\tilde{\phi}_4$ complex plane, and $\tilde{\phi}_2$ the same as $\tilde{\phi}_3$, so we do not plot them here. Furthermore, for period n not a prime number, some $|\tilde{\phi}_k|$ might vanish. We shall return to these symmetries in section 10.3.

10.2. Spectra of orbit Jacobian matrices

As the period of a lattice state gets longer, the orbit Jacobian matrix becomes larger and the Hill determinant becomes harder to compute. For a period- n lattice state, \mathcal{J} is a matrix with n eigenvalues and eigenvectors. What are they? What are the magnitudes of these eigenvalues? 

10.2.1. Spectra of translationally invariant orbit Jacobian matrices. Orbit Jacobian matrices of the temporal Bernoulli (70) and temporal cat (71) consist of only identity

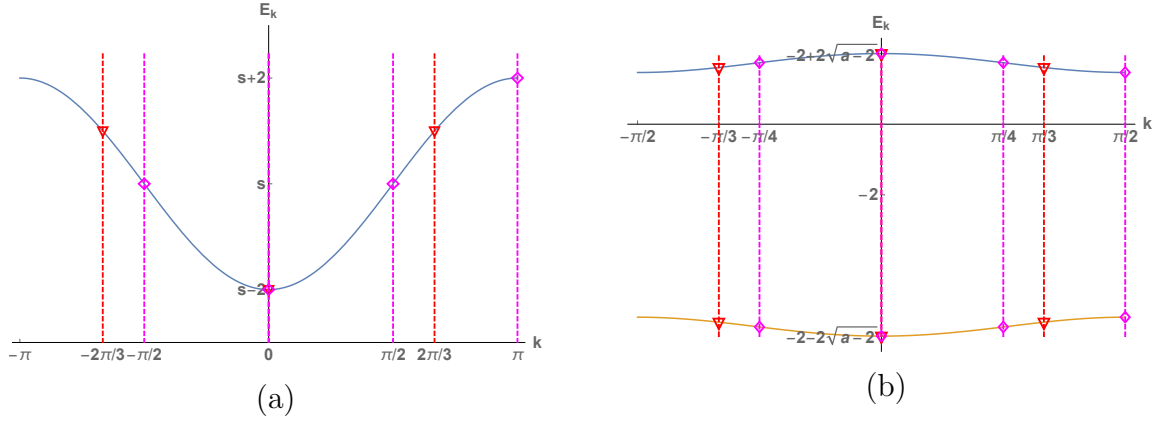


Figure 12. (Color online) Infinite lattice orbit Jacobian matrix first Brillouin zone spectra, as functions of the reciprocal lattice wavenumber k . For time-reversal invariant systems the spectra are $k \rightarrow -k$ symmetric. (a) The temporal cat $E(k)$ spectrum (158). Any period- n lattice state spectrum consists of n discrete points embedded into $E(k)$, for example period-3 (red triangles) and period-4 (magenta diamonds) lattice states eigenvalues (161). There are only 4 reciprocal lattice states, as $k = \pi$ and $k = -\pi$ differ by a reciprocal lattice translation, and are counted only once. (b) The temporal Hénon $E(k)_{\pm}$ spectrum (164) of the infinite lattice tiled by the period-2 lattice state, together with the eigenvalues of repeats (165) for 1st repeat, 3rd repeat (red triangles) and 4th repeat (magenta diamonds).

matrix and cyclic shift matrix, whose eigenvectors are discrete Fourier basis (149), so they are diagonalized by discrete Fourier transform. In the space of reciprocal lattice states, orbit Jacobian matrices (70) and (71) are diagonal, each diagonal element an eigenvalues of orbit Jacobian matrices, for the temporal Bernoulli

$$(s \mathbb{1} - r) \tilde{e}_k = (s - \omega^k) \tilde{e}_k, \quad (152)$$

and for the temporal cat

$$(-r + s \mathbb{1} - r^{-1}) \tilde{e}_k = \left[s - 2 \cos \left(\frac{2\pi k}{n} \right) \right] \tilde{e}_k. \quad (153)$$

Determinants are products of eigenvalues, so the temporal Bernoulli Hill determinant for any period- n lattice state is

$$\text{Det}(s \mathbb{1} - r) = \prod_{k=0}^{n-1} (s - \omega^k) = s^n - 1, \quad (154)$$

in agreement with the time-evolution count (27) and Hill's formula calculation (85). The temporal cat Hill determinant is

$$\text{Det}(-r + s \mathbb{1} - r^{-1}) = \prod_{k=0}^{n-1} \left[s - 2 \cos \left(\frac{2\pi k}{n} \right) \right] = 2 T_n(s/2) - 2, \quad (155)$$

confirming the 2nd-order inhomogeneous difference equation calculation (103).

The orbit Jacobian matrix (68) of a period- n lattice state is an $[n \times n]$ matrix. For an infinite lattice state, the orbit Jacobian matrix is an infinite-dimensional linear operator.

For example, the temporal cat infinite-dimensional orbit Jacobian matrix has the form (71), where the time translation operator \mathbf{r} implements the translation on the infinite lattice. The orbit Jacobian matrix commutes with the time translation operator, so its symmetry is the infinite cyclic group of integer lattice translations (109). By Bloch's theorem an eigenstate of the linear operator \mathcal{J} is of form

$$\psi_k(t) = e^{ikt} u_k(t), \quad (156)$$

where $u_k(t)$ is a period-1 periodic function. The orbit Jacobian matrix only acts on the field over the integer lattice, on which the periodic function $u_k(t)$ is a constant. The eigenstates

$$(\psi_k)_t = \psi_k(t) = e^{ikt}, \quad t \in \mathbb{Z}, \quad (157)$$

are plane waves on the lattice. The wavenumber k of the eigenstate ψ_k can always be restricted to the first Brillouin zone, $k \in [-\pi, \pi)$. Action of the orbit Jacobian matrix (71) on the wavenumber k eigenstate (157) yields eigenvalue

$$E(k)\psi_k = \mathcal{J}\psi_k = (s - 2\cos k)\psi_k, \quad (158)$$

plotted in the first Brillouin zone in figure 12(a). The infinite lattice spectrum contains all eigenvalues of orbit Jacobian matrices for any period- n lattice state. The period- n boundary condition is

$$\psi_k(t+n) = \psi_k(t), \quad (159)$$

hence the wavenumber k is restricted to the n first Brillouin zone values $k = 2\pi l/n$, where l is an integer, with eigenvalues

$$E_k\psi_k = \mathcal{J}\psi_k = (s - 2\cos k)\psi_k, \quad k = \frac{2\pi l}{n}, \quad l \in \mathbb{Z}, \quad (160)$$

in agreement with (153). For example, for the period-1, period-3 and the period-4 lattice states the wavenumbers and corresponding eigenvalues are, respectively

$$\begin{aligned} (k_0) &= (0), \quad (\lambda_0) = (s - 2) \\ (k_{-1}, k_0, k_1) &= \left(-\frac{2\pi}{3}, 0, \frac{2\pi}{3}\right) \\ (\lambda_{-1}, \lambda_0, \lambda_1) &= (s + 1, s - 2, s + 1) \\ (k_{-1}, k_0, k_1, k_2) &= \left(-\frac{\pi}{4}, 0, \frac{\pi}{4}, \frac{\pi}{2}\right) \\ (\lambda_{-1}, \lambda_0, \lambda_1, \lambda_2) &= (s, s - 2, s, s + 2), \end{aligned} \quad (161)$$

plotted in figure 12(a).

In summary: for a field theory with translationally invariant, uniform stretching parameter s orbit Jacobian matrices, eigenvalues of any lattice state are embedded in a single first Brillouin zone spectrum $E(k)$, the blue curve in figure 12(a). As long as the Klein-Gordon mass $\mu^2 = s - 2 > 0$ is positive, all lattice states are unstable, and the field theory is chaotic.

10.2.2. Spectra of nonlinear field theories. For a nonlinear field theory, the orbit Jacobian matrix (74) of a general prime lattice state is not translationally invariant. The orbit Jacobian matrix of a repeat of a period- n prime lattice state, however, is a tri-diagonal block circulant matrix (75), which commutes with the translation operator r^n . For an infinite lattice state tiled by repeats of a period- n prime lattice state Φ_p (see figure 7 (1) for a sketch), the infinite-dimensional orbit Jacobian matrix is invariant under r^n translation subgroup (114). Now we can apply Bloch's theorem to Bravais lattice $n\mathbb{Z}$, with an eigenstate of the orbit Jacobian matrix a plane wave times a periodic function (156), where $u_k(t)$ is a periodic function with period n . The wavenumber k is restricted in the first Brillouin zone of the Bravais lattice $n\mathbb{Z}$, $k \in [-\pi/n, \pi/n)$. Using the Bloch's theorem (156) we can find the eigenvalue spectrum of the orbit Jacobian matrix of a prime lattice state Φ_p 's repeats.

This infinite lattice spectrum contains eigenvalues of orbit Jacobian matrix of the infinite repeat of the prime lattice state Φ_p . To find eigenvalues of the orbit Jacobian matrix of the m th repeat of Φ_p (75), we need to only use the period- (mn) eigenstates, which satisfy:

$$\psi_k(t + mn) = \psi_k(t). \quad (162)$$

The wavenumber k must exist on the reciprocal lattice of the Bravais lattice spanned by (mn) , i.e., $k = 2\pi l/(mn)$, where l is an integer.

As an example, consider the temporal Hénon period-2 lattice state Φ_p (139), with a 2-dimensional repeating block (140) orbit Jacobian matrix. The orbit Jacobian matrix of an infinite lattice state tiled by repeats of Φ_p is the infinite-dimensional linear operator

$$\mathcal{J} = \begin{pmatrix} \ddots & \ddots & & & \\ & \ddots & s_1 & -1 & \\ & & -1 & s_0 & -1 \\ & & & -1 & s_1 & \ddots \\ & & & & \ddots & \ddots \end{pmatrix}, \quad \begin{pmatrix} s_0 \\ s_1 \end{pmatrix} = \begin{pmatrix} -2 - 2\sqrt{a-3} \\ -2 + 2\sqrt{a-3} \end{pmatrix} \quad (163)$$

whose eigenstates are plane waves of form (156), where $u_k(t)$ is periodic with period 2. Now there are two families of \mathcal{J} eigenvalues:

$$E(k)^\pm \psi_k = \mathcal{J} \psi_k = -2(1 \pm \sqrt{a-3 + \cos^2 k}) \psi_k, \quad (164)$$

plotted in the first Brillouin zone $k \in [-\pi/2, \pi/2)$ in figure 12 (b).

The eigenvalues of the orbit Jacobian matrices of the m th repeat of Φ_p are $2m$ points in the spectrum (164), at $k = 2\pi l/(2m)$, where l is an integer. For example, for the single repeat (see orbit Jacobian matrix (140)), the 3rd repeat and the 4th repeat the wavenumbers and corresponding eigenvalues are, respectively

$$\begin{aligned} (k_0) &= (0), \quad (\lambda_0^\pm) = (-2 \pm 2\sqrt{a-2}) \\ (k_{-1}, k_0, k_1) &= (-\frac{\pi}{3}, 0, \frac{\pi}{3}) \\ (\lambda_{-1}^\pm, \lambda_0^\pm, \lambda_1^\pm) &= (-2 \pm \sqrt{4a-11}, -2 \pm 2\sqrt{a-2}, -2 \pm \sqrt{4a-11}) \end{aligned}$$

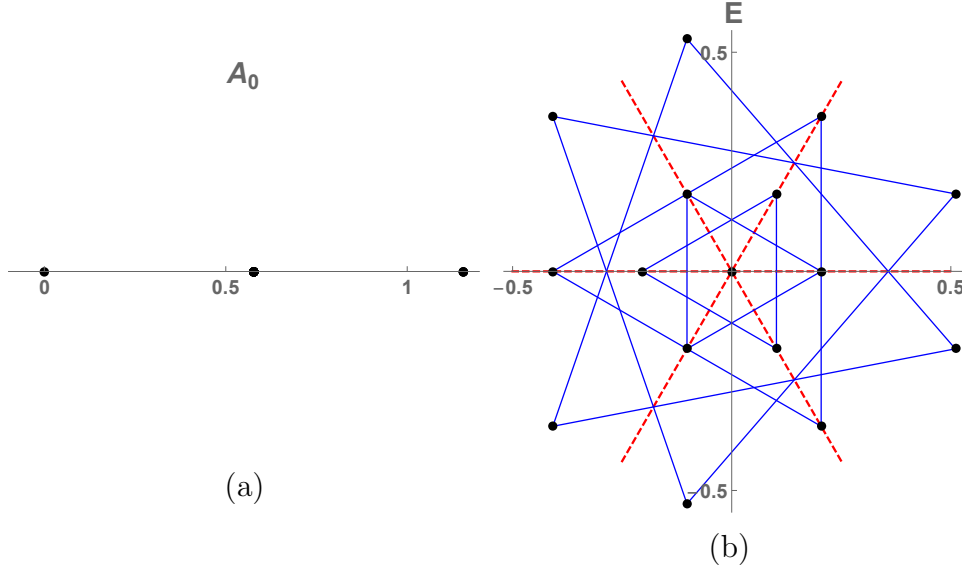


Figure 13. (Color online) Period-3 reciprocal lattice states of the $s = 3$ temporal cat, plotted in the D_3 permutation representation irreducible subspaces $A_0 + E$. (a) A_0 representation is the one-dimensional, time invariant ‘center of mass’ of the orbit. (b) In contrast to the C_n complex irreps of figure 10, the 2-dimensional irreps E_k of D_n are real. In the E_k planes reciprocal lattice states related by cyclic permutations and reflections lie on vertices of n -gons or pairs of n -gons. For D_3 they lie on triangles, with cyclic sets connected by blue lines. The 2 big triangles are a single D_3 6-lattice states orbit, what for C_3 is a pair of 3-lattice states orbits, with time reversal symmetry ignored. The remaining 3 smaller triangles are 3 time-reversal symmetric orbits. The small pair in the center would be two distinct radius D_3 orbits, where they not related by the internal symmetry $D_1 : \phi_i \rightarrow 1 - \phi_i$ specific to the spatiotemporal cat (see section 9.1). The state in the center is the fixed point $\phi_0 = 0$. Red dashed lines are the reflection axes of the D_3 group. Note that there are 4 reciprocal lattice states on each reflection axis.

$$\begin{aligned}
 (k_{-1}, k_0, k_1, k_2) &= \left(-\frac{\pi}{4}, 0, \frac{\pi}{4}, \pi/2\right) \\
 (\lambda_{-1}^{\pm}, \lambda_0^{\pm}, \lambda_1^{\pm}, \lambda_2^{\pm}) &= (-2 \pm \sqrt{4a - 10}, -2 \pm 2\sqrt{a - 2}, \\
 &\quad -2 \pm \sqrt{4a - 10}, -2 \pm 2\sqrt{a - 3}),
 \end{aligned} \tag{165}$$

plotted in figure 12(b).

In summary: for a nonlinear field theory, each period- n prime lattice state Φ_p has up to n distinct eigenvalues $\{\lambda^{(j)}\}$, each with its own infinite lattice spectrum family $E(k)^{(j)}$ into which eigenvalues of all repeats of Φ_p are embedded.

10.3. Reciprocal lattice visualization of system’s symmetries

When we block-diagonalize the permutation representation of section 9.8 into D_n irreps, the lattice states are projected into the irrep subspaces. An example are the period-3 reciprocal lattice states of $s = 3$ temporal cat shown in figure 13. The permutation representation is block diagonalized by basis vectors: $e_0 = 1/\sqrt{3}(1, 1, 1)$, $e_1 = \sqrt{2/3}(1, \cos(2\pi/3), \cos(4\pi/3))$ and $e_2 = \sqrt{2/3}(0, \sin(2\pi/3), \sin(4\pi/3))$. The basis

vector e_0 spans the subspace of the symmetric 1-dimensional irrep A_0 , invariant under D_3 actions. In the 2-dimensional irrep E subspace spanned by basis vectors (e_1, e_2) the translation operator r rotates the reciprocal lattice states clockwise by $2\pi/3$, while the reflection operator σ reflects the lattice states across the horizontal axis. In figure 13 lattice states that are related by translations are connected by blue lines. The red dashed lines are reflection operators' reflection axes. The 2 big triangles are related by reflection, and thus form a 6 reciprocal lattice states D_3 -orbit. The remaining 3 triangles are 3 orbits of symmetric lattice states, self dual under reflection.

10.3.1. D_n fundamental domain. If the space of the field configuration has D_n symmetry, the subspace of the 2-dimensional irrep E_1 can be divided into $2n$ copies by the irrep. One can choose the fundamental domain to be the region with polar angle between 0 and π/n , assuming that the horizontal axis is one of the reflection axis of the irrep E_1 . Each orbit only appears once in the fundamental domain, as shown in figure 13. Note that the two translational orbits related by the time reflection are a single orbit of the dihedral group.

What happens when lattice states appear on the boundary of the fundamental domain? There are two possible situations. The first situation is that the lattice state belongs to an orbit with index less than the order of the symmetry group. For example, in figure 13 subspace of E , there are 3 points in the fundamental domain with polar angle equal to 0 or $\pi/3$. These 3 points are representative lattice states of orbits with time reflection symmetry. The indices of these orbits are 3 instead of 6.

The second situation is that the index of the orbit of the lattice state is equal to the order of the symmetry group but the component in the subspace is 0. For example,

$$\Phi = \frac{1}{104}(17, 51, 49, 43, 25, 75)$$

is a period-6 lattice state of the $s = 3$ temporal Bernoulli (17). Using the discrete Fourier transform this lattice state becomes:

$$\tilde{\phi} = \left(\frac{5}{2\sqrt{6}}, 0, \frac{-5 - 3i\sqrt{3}}{13\sqrt{6}}, -\frac{\sqrt{3}}{4\sqrt{2}}, \frac{-5 + 3i\sqrt{3}}{13\sqrt{6}}, 0 \right).$$


This is a period-6 lattice state. It belongs to an orbit that contains 6 different lattice states. The $k = 1$ component of this lattice state is 0, which is on the boundary of the fundamental domain. To put this kind of lattice states into the fundamental domain one needs to divide other subspaces. For this lattice state the $k = 2$ and $k = 3$ components are not 0. The irreps divide the $k = 2$ subspace into 3 copies and the $k = 3$ subspace into 2 copies. One way to choose the fundamental domain in these subspaces is: the argument of the component in the $k = 1$ subspace is $0 \leq \arg(\tilde{\phi}_1) < \pi/3$; if the $k = 1$ component is 0, the arguments of the components in the $k = 2$ and $k = 3$ subspaces are $0 \leq \arg(\tilde{\phi}_2) < 2\pi/3$ and $0 \leq \arg(\tilde{\phi}_3) < \pi$. Each orbit is guaranteed to visit this fundamental domain exactly once.

Time-reversal invariant field configurations are confined to subspaces of the system's ∞ -dimensional state space, as only 'half' of the Bravais cell field values are independent,

the other half being a repeat in the reverse order. The orbit Jacobian matrix of the corresponding prime lattice state is evaluated in a time-reversal invariant subspace. An example of such prime lattice state orbit Jacobian matrix was given in (147). Appendix C lists all orbit Jacobian matrices of the temporal cat prime lattice state with time-reversal symmetry. The corresponding Hill determinants, together with the fundamental fact of section 8.1, are then used to count the time-reversal symmetric lattice states.

11. Lind zeta function

For a discrete time dynamical system $\phi_{t+1} = f(\phi_t)$, period- n solutions (in present context, the period- n Bravais cell lattice states) are *fixed points* of the n th iterate map f^n . While the symmetry of a time-invariant dynamical ‘law’ f is the infinite cyclic group C_∞ , the group of all temporal lattice translations, for a period- n solution the symmetry is n -steps translation subgroup H_n .

This observation motivates definition of a general group-theoretic *fixed-points counting* generating function that relates the number of lattice states to the number of prime orbits for any state space map $f : \mathcal{M} \rightarrow \mathcal{M}$ with a symmetry group G , a counting function that applies equally well to multi-dimensional lattice field theories [58] as to the 1-dimensional theories considered here. 

Let G be a group whose action $\alpha : G \times \mathcal{M} \rightarrow \mathcal{M}$ permutes elements of a set \mathcal{M} . The Lind zeta function [123] is then defined as

$$\zeta_{Lind}(t) = \exp \left(\sum_H \frac{N_H}{|G/H|} t^{|G/H|} \right), \quad (166)$$

where the sum is over all subgroups H of G of index $|G/H| < \infty$, and N_H is the number of states in \mathcal{M} invariant under action of (i.e., fixed points of) subgroup H ,

$$N_H = |\{\Phi \in \mathcal{M} : \text{all } h \in H \quad \alpha(h, \Phi) = \Phi\}|. \quad (167)$$

The index $|G/H|$ is best explained by working out a few examples.

In the lattice field theory setting, \mathcal{M} is the set of all lattice states. For 1-dimensional lattice field theories, the group G is either the infinite cyclic group C_∞ of all lattice translations (109), or the infinite dihedral group D_∞ of all translations and reflections (108). Their finite-index subgroups H are, respectively, infinite translation subgroups $H_{\mathbf{a}}$ (114), or $H_{\mathbf{a}}$ and infinite dihedral subgroups $H_{\mathbf{a},k}$ (115).

11.1. C_∞ or Artin-Mazur zeta function

Assume that the symmetry group of a given discrete time dynamical system is the group of temporal lattice translations C_∞ , i.e., that the system’s defining law is time invariant. The infinite translation subgroup $H_{\mathbf{a}}$ (114) leaves Bravais cell of period n (113) invariant, so the sum over H in (166) can be replaced by the sum over periods n , with N_n the number of lattice states of period n . For C_∞ subgroups H_n (contemplate the C_∞ column of figure 7) the index is

$$|C_\infty/H_n| = n. \quad (168)$$

The Lind zeta function (166) now takes form of the Artin-Mazur zeta function [8, 50]

$$\zeta_{\text{AM}}(z) = \exp \left(\sum_{n=1}^{\infty} \frac{N_n}{n} z^n \right), \quad (169)$$

which, from symmetry perspective, is the statement that the law governing the dynamical system is time invariant.

The number of *prime* orbits of period n can be computed recursively by subtracting repeats of shorter prime orbits [50],

$$M_n = \frac{1}{n} \left(N_n - \sum_{d|n, d < n} d M_d \right), \quad (170)$$


where d 's are all divisors of n .

In what sense is $\zeta_{\text{AM}}(z)$ a lattice state counts generating function? Given the $\zeta_{\text{AM}}(z)$, the number of periodic points of period n is given by its logarithmic derivative (see [ChaosBook](#) [50])

$$\sum_{n=1}^{\infty} N_n z^n = \frac{1}{\zeta_{\text{AM}}} z \frac{d}{dz} \zeta_{\text{AM}}. \quad (171)$$

Examples of $\zeta_{\text{AM}}(z)$ lattice state counts for scalar lattice field theories studied here are given in [Appendix D.1](#).

11.2. D_{∞} or Kim-Lee-Park zeta function

If the assumed symmetry G is not the maximal symmetry group, let's say we assume only $G = C_{\infty}$ whereas the full symmetry is D_{∞} , Lind zeta function (166) reduces to the Artin-Mazur zeta (D.4) which counts reflection symmetry-related lattice states as belonging to separate 'prime orbits', a problem that repeatedly bedevils the [ChaosBook.org](#) exposition of periodic orbit theory. 

So our next task is to evaluate Lind zeta function when the symmetry group G of temporal lattice of a given dynamical system is the infinite dihedral group D_{∞} , the group of all translations and reflections, i.e., system's defining law is time and time-reversal invariant. For the infinite translation $H_{\mathbf{a}}$ subgroup (114) the index is (as illustrated by figure 7)

$$|D_{\infty}/H_n| = 2n. \quad (172)$$

As explained in section 9.7, the D_{∞} orbits of reflection-symmetric lattice states contain only translations, so the index of each infinite dihedral subgroup $H_{\mathbf{a},k}$ (115) is

$$|D_{\infty}/H_{n,k}| = n. \quad (173)$$

The Lind zeta function (166) now has contributions from periodic lattice states, whose index is (172), and symmetric periodic lattice states, index (173):

$$\zeta_{D_{\infty}}(t) = \exp \left(\sum_{n=1}^{\infty} \frac{N_n}{2} \frac{t^{2n}}{n} + \sum_{n=1}^{\infty} \sum_{k=1}^{n-1} N_{n,k} \frac{t^n}{n} \right). \quad (174)$$

N_n counts the number of lattice states invariant under the translation group H_n , while $N_{n,k}$ counts the the number of lattice states invariant under the dihedral group $H_{n,k}$. So the first sum yields the square root of the Artin-Mazur zeta function $\sqrt{\zeta_{\text{AM}}(t^2)}$. The zeta function is factorized into:

$$\zeta_{\text{D}_\infty}(t) = \sqrt{\zeta_{\text{AM}}(t^2)} \zeta_s(t). \quad (175)$$

The second factor $\zeta_s(t)$ is the contribution from the time-reversal symmetric lattice states.

$$\zeta_s(t) = \exp \left(\sum_{n=1}^{\infty} \sum_{k=0}^{n-1} \frac{N_{n,k}}{n} t^n \right). \quad (176)$$

The number of reflection-symmetric lattice states does not depend on the location of the reflection point k , only on the type of symmetry (see the class counts (122) and (132)), so

$$N_{n,k} = \begin{cases} N_{n,0} & \text{if } n \text{ odd} \\ N_{n,0} & \text{if } n \text{ and } k \text{ are even} \\ N_{n,1} & \text{if } n \text{ even and } k \text{ is odd,} \end{cases} \quad (177)$$

and the Lind zeta function takes the form that we refer to as the Kim-Lee-Park [114] zeta function

$$\zeta_{\text{D}_\infty}(t) = \sqrt{\zeta_{\text{AM}}(t^2)} e^{h(t)}, \quad (178)$$

where

$$h(t) = \sum_{m=1}^{\infty} \left\{ N_{2m-1,0}^s t^{2m-1} + (N_{2m,0}^s + N_{2m,1}^s) \frac{t^{2m}}{2} \right\}. \quad (179)$$

11.2.1. Euler product form of Kim-Lee-Park zeta function. The state space \mathcal{M} of a D_∞ invariant dynamical system is the union

$$\mathcal{M} = \mathcal{M}_a \cup \mathcal{M}_s, \quad (180)$$

where \mathcal{M}_a is the set of pairs of asymmetric orbits (133), each element of the set a forward-in-time orbit and the time-reversed orbit, and \mathcal{M}_s is the set of time reversal symmetric orbits, invariant under reflections (134–136). Kim *et al* [114] show that the contribution of a single prime orbit p to the Kim-Lee-Park zeta function is:

$$1/\zeta_{\text{D}_\infty}(t)|_p = \begin{cases} 1 - t^{n_p} & \text{if } p \in \mathcal{M}_a, \\ \sqrt{1 - t^{2n_p}} \exp\left(-\frac{t^{n_p}}{1 - t^{n_p}}\right) & \text{if } p \in \mathcal{M}_s, \end{cases} \quad (181)$$

with the zeta function written as a product over prime orbits:

$$1/\zeta_{\text{D}_\infty}(t) = \prod_{p_a \in \mathcal{M}_a} (1 - t^{n_{p_a}}) \prod_{p_s \in \mathcal{M}_s} \sqrt{1 - t^{2n_{p_s}}} \exp\left(-\frac{t^{n_{p_s}}}{1 - t^{n_{p_s}}}\right), \quad (182)$$

to be expanded as a power series in t .

The Euler product form of topological zeta functions makes it explicit that they count *prime orbits*, i.e., sets of equivalent lattice states related by symmetries of the

problem. [Appendix D.2](#) verifies by explicit temporal cat calculations that the Kim-Lee-Park zeta function indeed counts infinite dihedral group D_∞ orbits and the corresponding lattice states.

12. Summary

How to think about matters spatiotemporal? As our intuition about motions of fluids is so much better than about turbulent quantum field theories, here we briefly describe the recent lack of progress in turbulence that underpins ideas developed in this paper.

While dynamics of a turbulent system might appear so complex to defy any precise description, the laws of motion drive a spatially extended system through a repertoire of recognizable unstable patterns (clouds, say), each defined over a finite spatiotemporal region [\[91, 93\]](#). The local dynamics, observed through such finite spatiotemporal windows, can be thought of as a visitation sequence of a finite repertoire of finite patterns. To make predictions, one needs to know how often a given pattern occurs, and that is a purview of periodic orbit theory [\[49\]](#). The early 2000's rapid progress in the description of turbulence in terms of such 'exact coherent structures' [\[86, 103, 112\]](#) has since slowed down to a crawl due to our inability to extend the theory and the computations to spatially large or infinite computational domains [\[34\]](#).

In dynamics, we have no fear of the infinite extent in time. That is periodic orbit theory's [\[53\]](#) *raison d'être*; the dynamics itself describes the infinite time invariant sets by a hierarchical succession of periodic orbits, of longer and longer finite periods (with no artificial external periodicity imposed along the time axis). And, since 1990's we know how to deal with spatially extended, temporally infinite regions by tiling them with spatiotemporally periodic tiles [\[40, 58, 78, 86, 93\]](#). A time periodic orbit is computed in a finite time, with period T , but it repeats "tile" the time axis for all times. Similarly, a spatiotemporally periodic "tile" or "periodic orbit" is computed on a finite spatial region L , for a finite period T , but it repeats in both time and space directions tile the infinite spacetime.

These ideas open a path to determining exact solutions on *spatially infinite* regions, and many physical turbulent flows come equipped with D spatial translational symmetries. For example, in a pipe flow at transitional Reynolds number, the azimuthal and radial directions (measured in viscosity length units) are compact, while the pipe length is infinite. If the theory is recast as a d -dimensional space-time theory, $d = D + 1$, spatiotemporally translational invariant recurrent solutions are d -tori (and *not* the 1-dimensional temporal periodic orbits of the traditional periodic orbit theory), and the symbolic dynamics is likewise d -dimensional (rather than a 1-dimensional temporal string of symbols).

This changes everything. Instead of studying time evolution of a chaotic system, one now studies the repertoire of spatiotemporal patterns compatible with a given PDE, or, in the discretized spacetime, a given partial difference equation. There is no more *time* evolution in this vision of nonlinear *dynamics*! Instead, there is a state space of all



spatiotemporal patterns, and the likelihood that a given finite spatiotemporally pattern can appear, like the mischievous grin of Cheshire cat, anywhere, anytime in the turbulent evolution of a flow. A bold vision, but how does it work?

It is in this context of working out the geometry of Hopf's [104] infinite-dimensional state spaces of turbulent fields (*not* 3-dimensional visualizations of fluids!), that we find the lessons learned from discretized field theories very helpful. Already 1-dimensional lattice discretization teaches us so much that it merits this paper by itself, with the intricacies of higher dimensional Bravais lattices reserved for the sequel [58].

We have learned that, in order to describe turbulence, one has to think globally but act locally. Turbulence is described by a catalogue of spatiotemporal patterns ('lattice states' in the present, discretized field theory context; 'tiles' in the PDE settings [58, 93]), each a numerically exact *global* solution satisfying *local* deterministic Euler–Lagrange equations lattice site by site. Stripped to its essentials, the problem is to systematically enumerate them, compute them, and determine their relative importance:

- (i) *Lattice states*. Each solution Φ_c is a zero of a global *fixed point* condition

$$F[\Phi_c] = 0.$$

Together, these solutions form the deterministic scaffold, the ∞ -dimensional state space of spatiotemporal 'patterns' explored by deterministic (or semiclassical or stochastic) turbulence.

- (ii) *Global stability* is given by the orbit Jacobian matrix

$$\mathcal{J}_{ij} = \frac{\delta F[\Phi_c]_i}{\delta \phi_j}.$$

In the field-theoretical formulation there is no evolution in time; Hill's formulas relate the two notions of stability.

- (iii) *Hill determinants*

$$\text{Det } \mathcal{J}$$

determine the numbers of spatiotemporal orbits and the weight of each. In the discrete spacetime, the time-periodic orbits of dynamical systems theory are replaced by periodic d -dimensional Bravais cell tilings (d -tori) of spacetime, each weighted by the inverse of its instability, its Hill determinant. The weighted sum over spatiotemporal patterns leads to chaotic field theory partition sums (11) much like those of solid state, field theory, and statistical mechanics.

- (iv) *Symmetries*. The reciprocal lattice states are organized by rules of crystallography. In particular, from a spatiotemporal field theory perspective, 'time'-reversal is a purely crystallographic notion, a reflection point group, leading to a dihedral symmetry quotienting of time-reversible theories and to the associated
- (v) topological *zeta functions* of, to us, surprising form. In principle, zeta functions encapsulate all the predictions of the theory. In contrast to conventional solid state

calculations, the hyperbolic shadowing of large Bravais cells by smaller ones [96, 97] ensures that the predictions of the theory are dominated by the smallest cells.

What lies ahead? We know how to enumerate 2-dimensional spacetime Bravais lattices, count and compute lattice states and their Hill determinants [58], but at present we have no dynamical zeta function analogous to the Lind zeta counting function for the 1- and higher-dimensional deterministic lattice field theories.

Acknowledgments

We are grateful to Karol Życzkowski, Sven Gnutzmann, Henning Schomerus and Thomas Guhr for including us in this remembrance and celebration of Fritz Haake.

Fritz was not the only doubter. During the 2016 Kadanoff Symposium Steve Shenker asked “What is chaos in quantum field theory?”, but as P. C. was getting ready to formulate an answer, Pavel Wiegmann butted in and settled the matter from the Soviet angle, with details elaborated by Boris Gutkin during 2015-2016 visit to Georgia Tech. But when it comes to a spacetime field theory, Yasha Sinai’s forward-in-time partitions only get in the way. The spatiotemporal chaotic field theory sketched here is our answer to Shenker’s question, the first seed of which was planted decades earlier by Wiegmann’s throwaway remark that one can have systems with several “time” dimensions, i.e., treat all translational symmetries on equal footing. Along the way we have received and misunderstood much in-person sage tutoring from Rafael De La Llave. Matt Gudorf has furthered the project more than anybody, and we have enjoyed interactions with Sidney Williams.

Further across the spacetime, the first seed of doubt was planted by Mitchell Feigenbaum, who admired Leibnitz and in 1975 asked P. C.: “Do you really believe that clouds are supercomputers in the sky?”. We have since been inspired and helped along by Robert MacKay’s 1982 work on time-reversal, MacKay and James Meiss 1983 Hill’s formula, Alessandro Torcini and Antonio Politi path breaking 1990’s chronotopic theory of spatiotemporal chaos, Serge Aubry’s 1990 anti-integrability framework, Douglas Lind’s 1996 multi-dimensional zeta functions, David Sterling and Meiss’ 1999 multi-dimensional spatiotemporal Hénon field theory, Divakar Viswanath’ 2002 Lindstedt-Poincaré theory, Carl Dettmann, Ronnie Mainieri and Gábor Vattay 1998 and Domenico Lippolis and Jeffrey Heninger 2010’s stochastic field theory, Young-One Kim, Jungseob Lee and Kyewon K. Park’s 2003 flip zeta function, Jason Gallas’ 2005 Hénon map orbit polynomials, Fabian Waleffe, Genta Kawahara, Bruno Eckhardt, John Gibson, Laurette Tuckerman, Rich Kerswell, Marc Avila, Ashley Willis, and Jonathan Halcrow 2000’s, and Mike Schatz and Roman Grigoriev 2020’s ‘exact coherent structures’, Evangelos Siminos and Burak Budanur’s 2010’s symmetry reductions, Michael Aizenman’s 2016 Ihara zeta functions, and Sara Solla, Juan Gallego, Matt Perich and Lee Miller 2018 neural manifolds. This paper thus sets up the necessary underpinnings for the quantum field theory of the spatiotemporal cat, the details of which we leave to our friends Jon Keating and Marcos Saraceno.

This research was initiated during the KITP UC Santa Barbara 2017 *Recurrent Flows: The Clockwork Behind Turbulence* program, supported in part by the National Science Foundation under Grant No. NSF PHY-1748958. The work of H. L. was fully supported by the family of late G. Robinson, Jr.. No actual cats, graduate or undergraduate were harmed during this research.

Appendix A. Historical context

Anyone who had ever thought of an integer, or looked at a crystal, or discretized a PDE, or constructed a secure cryptographic key, or truncated a Fourier series, or solved turbulence, eventually writes a paper much like this one. Our reading list is currently at 3,000 references, and there is not much here what no eye has seen, what no ear has heard, and what no human mind has conceived.

Still, we did not know that the dynamicist's Arnold cat (see [ChaosBook example 14.12](#)) is but the Klein-Gordon field theory (13) in disguise, and that the lattice form (43) of the theory is so much more elegant than the cat map (36) or the Hénon map (52). A cat is Hooke's wild, 'anti-harmonic' sister. For $s < 2$ Hooke rules, with restoring oscillations around the resting state. For $s > 2$ cats rule, with exponential runaway, wrapped globally around a state space torus. Cat is to chaos what harmonic oscillator is to order. There is no more fundamental example of chaos in mechanics.

For small stretching parameter values, $s < 2$, discretized Euler-Lagrange equation (51) describes a set of coupled penduli, with oscillatory solutions, known as the discrete Helmholtz equation in applied math [65, 80, 122], as the tight-binding model, the discrete Schrödinger equation, the Harper's or Azbel-Hofstadter model in solid state physics [45, 46, 74, 134, 148], and the critical almost Mathieu operator in mathematical physics [166], with quadratic action (13) written as Hamiltonian

$$H = \sum_{\ell} |\ell\rangle \epsilon_0 \langle \ell| + \sum_{\ell m} |\ell\rangle U_{\ell m} \langle m|, \quad U_{\ell m} = \begin{cases} U & \ell, m \text{ nearest neighbors} \\ 0 & \text{otherwise} \end{cases}$$

with the stretching factor $s = -\epsilon_0/U$ in (46). Equilibria or steady solutions of the d -dimensional Frenkel-Kontorova Hamiltonian lattice [12, 136], and discrete breather solutions [29] of the discrete nonlinear Klein-Gordon system that describe the motion of particles under the competing influence of an onsite potential field and the nearest neighbor attraction

$$\frac{d^2 \phi_z}{dt^2} - \square \phi_z + V'(\phi_z) = 0, \quad z \in \mathbb{Z}^d, \quad (\text{A.1})$$

are also examples of what we here call a 'nonlinear lattice field theory'. In contrast to the above mostly oscillatory, often weakly coupled mechanical systems, the d -dimensional spatiotemporal, everywhere hyperbolic discretized strongly coupled field theory developed here [58, 96] is a descendant of Gutkin's many-particle quantum chaos [97].

Much of the work on 1-dimensional ϕ^3 (temporal Hénon) and ϕ^4 field theories has already been carried out in 1990's, within the *anti-integrability* framework [11, 12, 169]. Our work is a continuation of Torcini, Politi and collaborators [84, 109, 117, 118, 153–155] 1990's *chronotopic approach* to spatiotemporal chaos, and the multi-dimensional spatiotemporal ϕ^3 field theory pioneered by Sterling [171] in his 1999 **PhD thesis**. Sterling studies Hénon map lattices in both Hamiltonian and Lagrangian formulations, and introduces the multidimensional ‘symbol tensor’ (Bunimovich and Sinai [35] ‘symbolic representation’, Coutinho and Fernandez [44] ‘spatiotemporal code’, Just [110] ‘symbol lattice’, MacKay [128] ‘symbol table’, Pethel, Corron and Bollt [150] ‘symbol pattern’, and, in our notation [58, 96, 97] symbol block or winding number M , see (28)). He focuses on the ‘destruction of chaos’ as one lowers the stretching parameter a , a much harder problem than what we address here. Luckily for us, the strong coupling, strong local stretching field theories’ deterministic solutions are protected by anti-integrability and live on horseshoes, safely away from the regions of intermediate stretches, where dragons live.

The reformulation of the lattice field theory 3-term recurrence (18–20) in terms of the 2-component field (B.1) is a generalization of the passage from the Lagrangian to the Hamiltonian formulation, also known as the ‘transfer matrix’ formulation of lattice field theories [135, 138] and Ising models [111, 145]. We chose to prove it here using only elementary linear algebra, not only because the Lagrangian formalism [26] is not needed for the problem at hand, but because it actually obscures the generality of Hill’s formula, which applies to all systems, the dissipative ones, such as the Hill’s formula (41) for the Bernoulli system, as well at the special cases, such as the contraction parameter value $b = -1$ for which -in general dissipative- Hénon map (52) happens to exhibit an additional symplectic, time-reversal symmetry.

For *forward-in-time evolution* (36), the $[2 \times 2]$ Jacobian matrix J^n (the monodromy matrix of a periodic orbit) describes the growth of an initial state perturbation in n steps. For the corresponding ‘Lagrangian’ system, with action S , the first variation of the action $\delta S = 0$ yields the Euler–Lagrange equations (7), (44), while the second variation, the $[n \times n]$ *orbit Jacobian matrix* (71), describes the stability of the *entire* periodic orbit. In the classical mechanics context, Bolotin and Treschev [26] refer to \mathcal{J} as the ‘Hessian operator’, but, as it is clear from our Bernoulli discussion, section 6, and the applications to Kuramoto-Sivashinsky and Navier-Stokes systems [93], the notion of global (in)stability of orbits applies to all dynamical systems, not only the Hamiltonian ones.

His 1878-1886 study [102] of the stability of planar motion of the Moon around the Earth led Hill to the Hill’s formula (77). In Lagrangian setting, orbit Jacobian matrix \mathcal{J} is the Hessian, the second variation of the action functional. The discrete-time Hill’s formula for 1-dimensional lattices with the nearest neighbor interactions that we use here was derived by Mackay and Meiss [129] in 1983 (see also Allroth [2] eq. (12)). Why Hill deserves the credit, and why celestial mechanics and quantum mechanics go hand-in-hand here, is explained in chapter 5 of Gutzwiller’s beautiful monograph [98], as well

as in Viswanath’s masterly calculation of Hill’s lunar orbit [178]. Reader conversant with celestial literature might have hard time recognizing the 3-term recurrences whose Hill determinants we compute here. What took Hill from the spatial continuum to an integer lattice is the fact that the Fourier modes for a compact orbit form a discrete set. Hill’s recurrence relations are made explicit in chapter 4 of Toda’s 1967 theory of Toda lattices [176], the classical mechanics of one-dimensional lattices (chains) of particles with nearest neighbor interaction, discrete and infinite in space, continuous in time (their unexpected symmetries are discussed in chapter 4 of Gutzwiller monograph [98]). In his lunar application Hill was lucky: $\text{Det } \mathcal{J}_c$ that he computed in a $[3 \times 3]$ Fourier modes matrix truncation turned out to be a quite good approximation. But his is a remarkable formula in the limit of $n \rightarrow \infty$ infinitesimal time steps, a formula that relates the ∞ -dimensional *functional* Hill determinant $\text{Det } \mathcal{J}_c$ to a determinant of the finite $[d \times d]$ matrix \mathbb{J}_c , and it took Poincaré [151] to prove that Hill’s truncated Fourier modes calculation is correct in the continuum limit.

While first discovered in a Lagrangian setting, Hill’s formulas apply equally well to dissipative dynamical systems, from the Bernoulli map of section 2 to Navier-Stokes and Kuramoto-Sivashinsky systems [91, 93], with the Lagrangian formalism of [26, 115, 129, 177] mostly getting in the way of understanding them. Historically, dynamicists always compute \mathbb{J}_c . However, in field theory it is the *Hill determinant* $\text{Det } \mathcal{J}_c$ that is the computationally robust quantity that one should evaluate.

The *fundamental fact* (94) which equates the number of periodic points in the fundamental parallelepiped with its volume, i.e., its Hill determinant, has a long history in the theory of integer lattices, and a key role in cryptography [16, 18, 20, 61, 133]. In two dimensions this formula is known since 1899 as *Pick’s theorem*, in higher dimensions it was stated by Nielsen [31, 144] in 1920, and rederived several times since in different contexts, for example in 1997 by Baake *et al* [13]. For the task at hand, Barvinok [17 lectures offer a clear and simple introduction to integer lattices, and a proof of the ‘fundamental fact’ (94).

Poincaré [152] was the first to recognize the fundamental role *periodic orbits* play in shaping ergodic dynamics. The first step in this program is a census of periodic orbits, addressed in [8, 25, 30, 33, 36, 37, 50, 125, 126, 187], starting with 1950’s Myrberg investigations of periodic orbits of quadratic maps, in what was arguably the first application of computers to dynamics [139–143]. Such orbit counts are most elegantly encoded by *topological zeta functions* of section 11. In 1966 Ihara [107] defined the zeta function of an undirected graph Γ by analogy to Euler’s product form of a zeta function,

$$\zeta_{\text{Ihara}}(z)_\Gamma = \prod_{[C]} \frac{1}{1 - z^{|C|}}, \quad (\text{A.2})$$

where the product is over all equivalence classes of prime (non-self retracing) loops C of Γ , and $|C|$ denotes the length of C . Ihara zeta functions [19, 42, 43, 62, 94, 107, 156, 158, 163, 164, 175, 188] are “graph-theoretic analogues of discrete Laplacians” [174] defined here in (14). Even though ‘undirected’ refers to no preferential time direction, they

do not appear related to the time-reversal, group-theoretic Kim-Lee-Park zeta function (178) deployed here. Still, as discussed in section 11.2.1, Ihara's idea that zeta function can be written as a product (A.2) over prime orbits holds.

In preparing this manuscript we have found expositions of Lagrangian dynamics for discrete time systems by MacKay, Meiss and Percival [129, 130, 132], and Li and Tomsovic [119] particularly helpful. The orbit Jacobian matrix (75) of a period- (mn) lattice state Φ was studied by Gade and Amritkar [83] in 1993. The exposition of section 9 owes much to MacKay [127] 1982 PhD thesis' chapter on reversible maps, and Endler and Gallas Hamiltonian Hénon map orbit polynomials [76, 77].

Appendix B. Hill's formula for a 2nd order difference equation

Consider a map of form $\phi_{t+1} = g(\phi_{t-1}, \phi_t)$, where ϕ_t is a scalar field (examples are the kicked rotor (40) and the 3-term recurrence relations (18-20)). Such a map can be replaced by a pair of 1st order difference equations for the 2-component field $\hat{\phi}_t = (\varphi_t, \phi_t)$ at the temporal lattice site t ,

$$\hat{\phi}_{t+1} = \hat{f}(\hat{\phi}_t) = \begin{pmatrix} \phi_t \\ g(\varphi_t, \phi_t) \end{pmatrix}. \quad (\text{B.1})$$

As in section 7.2, the trace of the n th iterate of the forward-in-time Perron-Frobenius operator can be evaluated in two ways. First, using the Dirac delta kernel of the operator \mathcal{L}^n ,

$$\text{tr } \mathcal{L}^n = \int_{\mathcal{M}} d^2 \hat{\phi}_0 \delta(\hat{\phi}_0 - \hat{f}^n(\hat{\phi}_0)). \quad (\text{B.2})$$

Restricting the integration to an infinitesimal open neighborhood of the 2-component field $(\varphi_{c,0}, \phi_{c,0})$ at lattice site 0, the period n lattice state Φ_c contribution to the trace is again $1/|\det(\mathbb{1} - \mathbb{J}_c)|$, with \mathbb{J}_c the forward-in-time $[2 \times 2]$ Floquet matrix (83), a product of the 1-time step Jacobian matrices (61)

$$\mathbb{J}_t = \begin{pmatrix} 0 & 1 \\ \frac{\partial g(\varphi_t, \phi_t)}{\partial \varphi_t} & \frac{\partial g(\varphi_t, \phi_t)}{\partial \phi_t} \end{pmatrix}, \quad (\text{B.3})$$

where $(\varphi_t, \phi_t) = \hat{f}^t(\varphi_{c,0}, \phi_{c,0})$.

Alternatively, the trace can be evaluated as $2n$ -dimensional integral over a product of one-time-step Perron-Frobenius operators (91),

$$\begin{aligned} \text{tr } \mathcal{L}^n &= \int \prod_{t=0}^{n-1} \left[d^2 \hat{\phi}_t \delta(\hat{\phi}_{t+1} - \hat{f}(\hat{\phi}_t)) \right] \\ &= \int \prod_{t=0}^{n-1} [d\varphi_t d\phi_t \delta(\varphi_{t+1} - \phi_t) \delta(\phi_{t+1} - g(\varphi_t, \phi_t))] , \end{aligned} \quad (\text{B.4})$$

with a 1-dimensional Dirac delta for each field component (B.1). With the periodic bc's $\hat{\phi}_{t+n} = \hat{\phi}_t$, the $d\varphi_t$ integration eliminates the φ_t components, resulting in the n -

dimensional scalar field integral

$$\mathrm{tr} \mathcal{L}^n = \int d\Phi \prod_{t=0}^{n-1} \delta(\phi_{t+1} - g(\phi_{t-1}, \phi_t)), \quad d\Phi = \prod_{t=0}^{n-1} d\phi_t, \quad (\text{B.5})$$

or, in the lattice state notation,

$$\mathrm{tr} \mathcal{L}^n = \int d\Phi \delta(F[\Phi]), \quad F[\Phi] = \mathbf{r}\Phi - g(\mathbf{r}^{-1}\Phi, \Phi). \quad (\text{B.6})$$

where Φ and $g(\mathbf{r}^{-1}\Phi, \Phi)$ are n -dimensional column vectors with t -th components ϕ_t and $g((\mathbf{r}^{-1}\Phi)_t, \phi_t)$, respectively, \mathbf{r} is the cyclic $[n \times n]$ time translation operator (31), and the saddle-point condition $F[\Phi_c] = 0$ is the Euler–Lagrange equation (7) of the system. The rest is as in (93); the trace is the deterministic partition sum (11) over all lattice states,

$$\mathrm{tr}_c \mathcal{L}^n = \int_{\mathcal{M}_c} d\Phi \delta(F[\Phi]) = \frac{1}{|\mathrm{Det} \mathcal{J}_c|}, \quad (\text{B.7})$$

where \mathcal{J}_c is the $[n \times n]$ orbit Jacobian matrix evaluated on the period- n lattice state Φ_c , enclosed by an infinitesimal open neighborhood \mathcal{M}_c . Comparing the traces (90) and (B.7), we see that we have again proved the Hill’s formula (77).

Note that nowhere in the derivation have we assumed that the system has a Lagrangian formulation: this version of Hill’s formula applies to any 2nd order difference equation, or 3-term recurrence of form $\phi_{t+1} = g(\phi_{t-1}, \phi_t)$, for example, any dissipative Hénon map (52) as well as its special $b = -1$ Hamiltonian case (53).

Appendix C. Orbit Jacobian matrices of \mathbf{D}_n prime orbits.

As shown in (147), the orbit Jacobian matrix in the linear space of the prime lattice state with time reversal symmetry has a different form compared to the orbit Jacobian matrix that acts on a Bravais lattice state. It only acts on ‘half’ of the Bravais cell and the cyclic translational symmetry is broken.

Consider possible symmetries of periodic lattice states of the temporal cat. If a lattice state has odd period n , reflection symmetry (o) defined by (134), the prime lattice state is a $m + 1$ -dimensional vector:

$$\tilde{\Phi}^\top = (\phi_0, \phi_1, \phi_2, \phi_3, \dots, \phi_m). \quad (\text{C.1})$$

And the $[(m + 1) \times (m + 1)]$ symmetry reduced orbit Jacobian matrix is:

$$\mathcal{J}_o = \begin{pmatrix} s & -2 & 0 & \dots & 0 & 0 \\ -1 & s & -1 & \dots & 0 & 0 \\ 0 & -1 & s & \dots & 0 & 0 \\ \vdots & \vdots & \vdots & \ddots & \vdots & \vdots \\ 0 & 0 & \dots & \dots & s & -1 \\ 0 & 0 & \dots & \dots & -1 & s - 1 \end{pmatrix}. \quad (\text{C.2})$$

If lattice states have symmetries defined by (135) or (136), the symmetry reduced orbit Jacobian matrices are $[(m+1) \times (m+1)]$ matrix:

$$\mathcal{J}_{ee} = \begin{pmatrix} s & -2 & 0 & \dots & 0 & 0 \\ -1 & s & -1 & \dots & 0 & 0 \\ 0 & -1 & s & \dots & 0 & 0 \\ \vdots & \vdots & \vdots & \ddots & \vdots & \vdots \\ 0 & 0 & \dots & \dots & s & -1 \\ 0 & 0 & \dots & \dots & -2 & s \end{pmatrix}, \quad (\text{C.3})$$

or $[m \times m]$ matrix:

$$\mathcal{J}_{eo} = \begin{pmatrix} s-1 & -1 & 0 & \dots & 0 & 0 \\ -1 & s & -1 & \dots & 0 & 0 \\ 0 & -1 & s & \dots & 0 & 0 \\ \vdots & \vdots & \vdots & \ddots & \vdots & \vdots \\ 0 & 0 & \dots & \dots & s & -1 \\ 0 & 0 & \dots & \dots & -1 & s-1 \end{pmatrix}. \quad (\text{C.4})$$

The determinants of these symmetry reduced orbit Jacobian matrices are the stabilities of the lattice states in the time-reflection symmetric subspace. Using the fundamental fact, one can compute the number of time-reversal invariant lattice states of temporal cat.

Note that even though the symmetry reduced orbit Jacobian matrices are not circulant matrices, they share eigenvalues with circulant orbit Jacobian matrices (73), because the eigenvectors of the circulant orbit Jacobian matrices are Fourier modes and can be written as symmetric and anti-symmetric vectors. The determinants of the symmetry reduced orbit Jacobian matrices are:

$$\begin{aligned} \text{Det } \mathcal{J}_o &= \prod_{j=0}^{(n-1)/2} \left(s - 2 \cos \frac{2\pi j}{n} \right) = \sqrt{(s-2) \text{Det } \mathcal{J}}, \\ \text{Det } \mathcal{J}_{ee} &= \prod_{j=0}^{(n-2)/2} \left(s - 2 \cos \frac{2\pi j}{n} \right) = \sqrt{(s-2)(s+2) \text{Det } \mathcal{J}}, \\ \text{Det } \mathcal{J}_{eo} &= \prod_{j=0}^{n/2} \left(s - 2 \cos \frac{2\pi j}{n} \right) = \sqrt{\frac{(s-2)}{(s+2)} \text{Det } \mathcal{J}}, \end{aligned} \quad (\text{C.5})$$

where $\text{Det } \mathcal{J}$ is given in (102). $\text{Det } \mathcal{J}$, $\text{Det } \mathcal{J}_o$, $\text{Det } \mathcal{J}_{ee}$ and $\text{Det } \mathcal{J}_{eo}$ count numbers of periodic lattice states that satisfy the symmetries defined by (133–136) respectively.

MacKay [127] and Endler and Gallas [76] give tables of lattice states and their orbits counts, together with the counts of symmetric lattice states and orbits.

Appendix D. Counting lattice states using zeta functions

Appendix D.1. Counting lattice states using Artin-Mazur zeta function

Let us first evaluate ζ_{AM} for scalar lattice field theories studied here.

Bernoulli. The number of Bernoulli system period- n lattice states is given in (27), so

$$1/\zeta_{\text{AM}}(z) = \exp\left(-\sum_{n=1}^{\infty} \frac{s^n - 1}{n} z^n\right) = \frac{1 - sz}{1 - z}. \quad (\text{D.1})$$

The numerator $(1 - sz)$ says that a Bernoulli system is a full shift [50]: there are s fundamental lattice states, in this case fixed points $\{\phi_0, \phi_1, \dots, \phi_{s-1}\}$, and every other lattice state is built from their concatenations and repeats. The denominator $(1 - z)$ compensates for the single overcounted lattice state, the fixed point $\phi_{s-1} = \phi_0 \pmod{1}$ of figure 3, and its repeats. If the stretching factor $s = \beta$ is not an integer, the map (23) is called the ‘ β -transformation’. For its Artin-Mazur zeta function see [81].

Counting Bernoulli prime orbits. Substituting the Bernoulli map topological zeta function (D.1) into (171) we obtain

$$\begin{aligned} \sum_{n=1} N_n z^n &= z + 3z^2 + 7z^3 + 15z^4 + 31z^5 + 63z^6 + 127z^7 \\ &\quad + 255z^8 + 511z^9 + 1023z^{10} + 2047z^{11} \dots, \end{aligned} \quad (\text{D.2})$$

in agreement with the lattice states count (85). The number of *prime* orbits of period n is given recursively by subtracting repeats of shorter prime orbits (170), hence

$$\begin{aligned} \sum_{n=1} M_n z^n &= z + z^2 + 2z^3 + 3z^4 + 6z^5 + 9z^6 + 18z^7 \\ &\quad + 30z^8 + 56z^9 + 99z^{10} + 186z^{11} \dots, \end{aligned} \quad (\text{D.3})$$

in agreement with the usual numbers of binary symbolic dynamics prime cycles [50].

Temporal cat. Substituting the number of temporal cat period- n lattice states given in (102) into the Artin-Mazur zeta (169), Isola [108] obtains

$$1/\zeta_{\text{AM}}(z) = \exp\left(-\sum_{n=1}^{\infty} \frac{\Lambda^n + \Lambda^{-n} - 2}{n} z^n\right) = \frac{1 - sz + z^2}{(1 - z)^2}. \quad (\text{D.4})$$

Conversely, given the topological zeta function, the generating function for the number of temporal lattice states of period n is given by the logarithmic derivative (171),

$$\begin{aligned} \sum_{n=0}^{\infty} N_n z^n &= \frac{2 - sz}{1 - sz + z^2} - \frac{2}{1 - z} \\ &= (s - 2) \left[z + (s + 2)z^2 + (s + 1)^2 z^3 \right. \\ &\quad \left. + (s + 2)s^2 z^4 + (s^2 + s - 1)^2 z^5 + \dots \right], \end{aligned} \quad (\text{D.5})$$

n	1	2	3	4	5	6	7	8	9	10	11
N_n	2	4	8	16	32	64	128	256	512	1024	2048
M_n	2	1	2	3	6	9	18	30	56	99	186

Table D1. N_n and M_n are the numbers of the period- n lattice states and orbits, respectively, for the $a = 6$ Hénon map.

n	1	2	3	4	5	6	7	8	9	10
M_n	1	2	5	10	24	50	120	270	640	1500
N_n^a	1	5	16	45	121	320	841	2205	5776	15125
$N_{n,0}^s$	1	5	4	15	11	40	29	105	76	275
$N_{n,1}^s$	1	1	4	3	11	8	29	21	76	55

Table D2. Lattice state and prime orbit counts for the $s = 3$ temporal cat. M_n is the number of period- n prime orbits (see Bird and Vivaldi [24]). N_n^a , $N_{n,0}^s$ and $N_{n,1}^s$ are numbers of lattice states that are invariant under group actions of H_n , $H_{n,0}$ and $H_{n,1}$ respectively.

which is indeed the generating function for $T_n(s/2)$, the Chebyshev polynomial of the first kind (103). Why Chebyshev? Essentially because $T_k(x)$ are also defined by a 3-term recurrence:

$$\begin{aligned} T_0(x) &= 1, \quad T_1(x) = x, \\ -T_{k+1}(x) + 2xT_k(x) - T_{k-1}(x) &= 0 \quad \text{for } k \geq 2. \end{aligned} \quad (\text{D.6})$$

Temporal Hénon. The problem of counting orbits for the Hénon map (52) was first addressed in 1979 by Simó [165]. For the complete horseshoe, $a = 6$ Hénon map repeller there are 2^n period- n lattice states, so

$$1/\zeta_{\text{AM}}(z) = \exp\left(-\sum_{n=1}^{\infty} \frac{2^n}{n} z^n\right) = 1 - 2z. \quad (\text{D.7})$$

The numbers of the shortest period lattice states and prime orbits are listed in table D1.

ϕ^4 field theory. The same as the temporal Hénon, with $2 \rightarrow 3$ replacement in (D.7).

Appendix D.2. Counting temporal cat lattice states using Kim-Lee-Park zeta function

As the symmetry of temporal cat is D_∞ , the number of lattice states for temporal cat given by the C_∞ Hill determinant (102) miscounts states related by reflections. In this case one uses the fundamental fact to count each type the time reversal invariant lattice states separately. As an example, consider temporal cat with $s = 3$. The

Hill determinants of the symmetry reduced orbit Jacobian matrices (C.5) count the corresponding lattice states:

$$\begin{aligned} N_n^a &= \left(\Lambda^{n/2} - \Lambda^{-n/2} \right)^2, \\ N_{n,0}^s &= \Lambda^{n/2} - \Lambda^{-n/2}, & n \text{ odd}, \\ N_{n,0}^s &= \sqrt{5} \left(\Lambda^{n/2} - \Lambda^{-n/2} \right), & n \text{ even}, \\ N_{n,1}^s &= \frac{1}{\sqrt{5}} \left(\Lambda^{n/2} - \Lambda^{-n/2} \right), & n \text{ even}. \end{aligned} \quad (\text{D.8})$$

Substitute into (179) to count symmetric lattice states:

$$\begin{aligned} h(t) &= \sum_{m=1}^{\infty} \left[N_{2m-1,0} t^{2m-1} + (N_{2m,0} + N_{2m,1}) \frac{t^{2m}}{2} \right] \\ &= \frac{\Lambda^{1/2} t}{1 - \Lambda t^2} - \frac{\Lambda^{-1/2} t}{1 - \Lambda^{-1} t^2} + \sqrt{\frac{9}{5}} \frac{\Lambda t^2}{1 - \Lambda t^2} - \sqrt{\frac{9}{5}} \frac{\Lambda^{-1} t^2}{1 - \Lambda^{-1} t^2}. \end{aligned} \quad (\text{D.9})$$

Using the definition of the Kim-Lee-Park zeta function (176–179), generating functions of the lattice state counts are

$$\begin{aligned} t \frac{\partial}{\partial t} \ln \zeta_a(t^2) &= \sum_{n=1}^{\infty} N_n^a t^{2n} \\ &= t^2 + 5t^4 + 16t^6 + 45t^8 + 121t^{10} + 320t^{12} + 841t^{14} \\ &\quad + 2205t^{16} + 5776t^{18} + 15125t^{20} + \dots, \end{aligned} \quad (\text{D.10})$$

and

$$\begin{aligned} h(t) &= \sum_{m=1}^{\infty} \left[N_{2m-1,0}^s t^{2m-1} + \frac{(N_{2m,0}^s + N_{2m,1}^s)}{2} t^{2m} \right] \\ &= t + 3t^2 + 4t^3 + 9t^4 + 11t^5 + 24t^6 + \\ &\quad 29t^7 + 63t^8 + 76t^9 + 165t^{10} + \dots, \end{aligned} \quad (\text{D.11})$$

in agreement with the numbers of lattice states with period up to 10 listed in the table D2. Kim-Lee-Park zeta function counts as advertised.

References

- [1] K. T. Alligood, T. D. Sauer, and J. A. Yorke, *Chaos, An Introduction to Dynamical Systems* (Springer, New York, 1996).
- [2] E. Allroth, “Ground state of one-dimensional systems and fixed points of 2n-dimensional map”, *J. Phys. A* **16**, L497 (1983).
- [3] A. M. Ozorio de Almeida and J. H. Hannay, “Periodic orbits and a correlation function for the semiclassical density of states”, *J. Phys. A* **17**, 3429 (1984).
- [4] S. Anastassiou, “Complicated behavior in cubic Hénon maps”, *Theoret. Math. Phys.* **207**, 572–578 (2021).
- [5] S. Anastassiou, A. Bountis, and A. Bäcker, “Homoclinic points of 2D and 4D maps via the parametrization method”, *Nonlinearity* **30**, 3799–3820 (2017).

- [6] S. Anastassiou, A. Bountis, and A. Bäcker, “Recent results on the dynamics of higher-dimensional Hénon maps”, *Regul. Chaotic Dyn.* **23**, 161–177 (2018).
- [7] V. I. Arnol’d and A. Avez, *Ergodic Problems of Classical Mechanics* (Addison-Wesley, Redwood City, 1989).
- [8] M. Artin and B. Mazur, “On periodic points”, *Ann. Math.* **81**, 82–99 (1965).
- [9] R. Artuso, E. Aurell, and P. Cvitanović, “Recycling of strange sets: I. Cycle expansions”, *Nonlinearity* **3**, 325–359 (1990).
- [10] R. Artuso, E. Aurell, and P. Cvitanović, “Recycling of strange sets: II. Applications”, *Nonlinearity* **3**, 361–386 (1990).
- [11] S. Aubry, “Anti-integrability in dynamical and variational problems”, *Physica D* **86**, 284–296 (1995).
- [12] S. Aubry and G. Abramovici, “Chaotic trajectories in the standard map. The concept of anti-integrability”, *Physica D* **43**, 199–219 (1990).
- [13] M. Baake, J. Hermisson, and A. B. Pleasants, “The torus parametrization of quasiperiodic LI-classes”, *J. Phys. A* **30**, 3029–3056 (1997).
- [14] E. Balkovsky, G. Falkovich, I. Kolokov, and V. Lebedev, “Intermittency of Burgers’ turbulence”, *Phys. Rev. Lett.* **78**, 1452–1455 (1997).
- [15] J. Barrow-Green, *Poincaré and the Three Body Problem* (Amer. Math. Soc., Providence RI, 1997).
- [16] A. Barvinok, *A Course in Convexity* (Amer. Math. Soc., New York, 2002).
- [17] A. Barvinok, *Lattice Points, Polyhedra, and Complexity*, tech. rep. (Univ. of Michigan, Ann Arbor MI, 2004).
- [18] A. Barvinok, *Integer Points in Polyhedra* (European Math. Soc. Pub., Berlin, 2008).
- [19] H. Bass, “The Ihara-Selberg zeta function of a tree lattice”, *Int. J. Math.* **3**, 717–797 (1992).
- [20] M. Beck and S. Robins, *Computing the Continuous Discretely* (Springer, New York, 2007).
- [21] J. M. Bergamin, T. Bountis, and C. Jung, “A method for locating symmetric homoclinic orbits using symbolic dynamics”, *J. Phys. A* **33**, 8059–8070 (2000).
- [22] J. M. Bergamin, T. Bountis, and M. N. Vrahatis, “Homoclinic orbits of invertible maps”, *Nonlinearity* **15**, 1603–1619 (2002).
- [23] O. Biham and W. Wenzel, “Characterization of unstable periodic orbits in chaotic attractors and repellers”, *Phys. Rev. Lett.* **63**, 819 (1989).
- [24] N. Bird and F. Vivaldi, “Periodic orbits of the sawtooth maps”, *Physica D* **30**, 164–176 (1988).
- [25] R. L. Bivins, J. D. Louck, N. Metropolis, and M. L. Stein, “Classification of all cycles of the parabolic map”, *Physica D* **51**, 3–27 (1991).

- [26] S. V. Bolotin and D. V. Treschev, “Hill’s formula”, *Russ. Math. Surv.* **65**, 191 (2010).
- [27] T. Bountis, H. W. Capel, M. Kollmann, J. C. Ross, J. M. Bergamin, and J. P. van der Weele, “Multibreathers and homoclinic orbits in 1-dimensional nonlinear lattices”, *Physics Letters A* **268**, 50–60 (2000).
- [28] T. Bountis and R. H. G. Helleman, “On the stability of periodic orbits of two-dimensional mappings”, *J. Math. Phys* **22**, 1867–1877 (1981).
- [29] T. Bountis and H. Skokos, *Complex Hamiltonian Dynamics* (Springer, Berlin, 2012).
- [30] A. Bridy and R. A. Pérez, “A count of maximal small copies in Multibrot sets”, *Nonlinearity* **18**, 1945–1953 (2005).
- [31] R. B. S. Brooks, R. F. Brown, J. Pak, and D. H. Taylor, “Nielsen numbers of maps of tori”, *Proc. Amer. Math. Soc.* **52**, 398–398 (1975).
- [32] A. Brown, “Equations for periodic solutions of a logistic difference equation”, *J. Austral. Math. Soc. Ser. B* **23**, 78–94 (1981).
- [33] K. M. Brucks, “MSS sequences, colorings of necklaces, and periodic points of $f(z) = z^2 - 2$ ”, *Adv. Appl. Math.* **8**, 434–445 (1987).
- [34] N. B. Budanur, K. Y. Short, M. Farazmand, A. P. Willis, and P. Cvitanović, “Relative periodic orbits form the backbone of turbulent pipe flow”, *J. Fluid Mech.* **833**, 274–301 (2017).
- [35] L. A. Bunimovich and Y. G. Sinai, “Spacetime chaos in coupled map lattices”, *Nonlinearity* **1**, 491 (1988).
- [36] O. Chavoya-Aceves, F. Angulo-Brown, and E. Piña, “Symbolic dynamics of the cubic map”, *Physica D* **14**, 374–386 (1985).
- [37] W. Y. C. Chen and J. D. Louck, “Necklaces, MSS sequences, and DNA sequences”, *Adv. Appl. Math.* **18**, 18–32 (1997).
- [38] B. V. Chirikov, “A universal instability of many-dimensional oscillator system”, *Phys. Rep.* **52**, 263–379 (1979).
- [39] W. G. Choe and J. Guckenheimer, “Computing periodic orbits with high accuracy”, *Computer Meth. Appl. Mech. and Engin.* **170**, 331–341 (1999).
- [40] F. Christiansen, P. Cvitanović, and V. Putkaradze, “Spatiotemporal chaos in terms of unstable recurrent patterns”, *Nonlinearity* **10**, 55–70 (1997).
- [41] D. Cimasoni, “The critical Ising model via Kac-Ward matrices”, *Commun. Math. Phys.* **316**, 99–126 (2012).
- [42] B. Clair, “The Ihara zeta function of the infinite grid”, *Electron. J. Combin.* **21**, P2–16 (2014).
- [43] G. A. T. F. da Costa, “The Feynman identity for planar graphs”, *Lett. Math. Phys.* **106**, 1089–1107 (2016).

- [44] R. Coutinho and B. Fernandez, “Extended symbolic dynamics in bistable CML: Existence and stability of fronts”, *Physica D* **108**, 60–80 (1997).
- [45] J. Cserti, “Application of the lattice Green’s function for calculating the resistance of an infinite network of resistors”, *Amer. J. Physics* **68**, 896–906 (2000).
- [46] J. Cserti, G. Széchenyi, and G. Dávid, “Uniform tiling with electrical resistors”, *J. Phys. A* **44**, 215201 (2011).
- [47] P. Cvitanović, “Invariant measurement of strange sets in terms of cycles”, *Phys. Rev. Lett.* **61**, 2729–2732 (1988).
- [48] P. Cvitanović, “Chaotic Field Theory: A sketch”, *Physica A* **288**, 61–80 (2000).
- [49] P. Cvitanović, “Recurrent flows: The clockwork behind turbulence”, *J. Fluid Mech. Focus Fluids* **726**, 1–4 (2013).
- [50] P. Cvitanović, “Counting”, in *Chaos: Classical and Quantum* (Niels Bohr Inst., Copenhagen, 2022).
- [51] P. Cvitanović, “Trace formulas”, in *Chaos: Classical and Quantum*, edited by P. Cvitanović, R. Artuso, R. Mainieri, G. Tanner, and G. Vattay (Niels Bohr Inst., Copenhagen, 2022).
- [52] P. Cvitanović, “Why cycle?”, in *Chaos: Classical and Quantum*, edited by P. Cvitanović, R. Artuso, R. Mainieri, G. Tanner, and G. Vattay (Niels Bohr Inst., Copenhagen, 2022).
- [53] P. Cvitanović, R. Artuso, R. Mainieri, G. Tanner, and G. Vattay, *Chaos: Classical and Quantum* (Niels Bohr Inst., Copenhagen, 2022).
- [54] P. Cvitanović, R. Artuso, L. Rondoni, and E. A. Spiegel, “Transporting densities”, in *Chaos: Classical and Quantum*, edited by P. Cvitanović, R. Artuso, R. Mainieri, G. Tanner, and G. Vattay (Niels Bohr Inst., Copenhagen, 2022).
- [55] P. Cvitanović, C. P. Dettmann, R. Mainieri, and G. Vattay, “Trace formulas for stochastic evolution operators: Weak noise perturbation theory”, *J. Stat. Phys.* **93**, 981–999 (1998).
- [56] P. Cvitanović, C. P. Dettmann, R. Mainieri, and G. Vattay, “Trace formulae for stochastic evolution operators: Smooth conjugation method”, *Nonlinearity* **12**, 939 (1999).
- [57] P. Cvitanović and Y. Lan, Turbulent fields and their recurrences, in *Correlations and Fluctuations in QCD : Proceedings of 10. International Workshop on Multiparticle Production*, edited by N. Antoniou (2003), pp. 313–325.
- [58] P. Cvitanović and H. Liang, *Spatiotemporal cat: A chaotic field theory*, In preparation, 2022.
- [59] P. Cvitanović and D. Lippolis, Knowing when to stop: How noise frees us from determinism, in *Let’s Face Chaos through Nonlinear Dynamics*, edited by M. Robnik and V. G. Romanovski (2012), pp. 82–126.

- [60] P. Cvitanović, N. Sørengaard, G. Palla, G. Vattay, and C. P. Dettmann, “Spectrum of stochastic evolution operators: Local matrix representation approach”, *Phys. Rev. E* **60**, 3936–3941 (1999).
- [61] J. A. De Loera, R. Hemmecke, J. Tauzer, and R. Yoshida, “Effective lattice point counting in rational convex polytopes”, *J. Symbolic Comp.* **38**, 1273–1302 (2004).
- [62] A. Deitmar, “Thara zeta functions of infinite weighted graphs”, *SIAM J. Discrete Math.* **29**, 2100–2116 (2015).
- [63] R. L. Devaney, *An Introduction to Chaotic Dynamical systems*, 2nd ed. (Westview Press, Cambridge, Mass, 2008).
- [64] R. L. Devaney and Z. Nitecki, “Shift automorphisms in the Hénon mapping”, *Commun. Math. Phys.* **67**, 137–146 (1979).
- [65] A. Dienstfrey, F. Hang, and J. Huang, “Lattice sums and the two-dimensional, periodic Green’s function for the Helmholtz equation”, *Proc. Roy. Soc. Ser A* **457**, 67–85 (2001).
- [66] X. Ding, H. Chaté, P. Cvitanović, E. Siminos, and K. A. Takeuchi, “Estimating the dimension of the inertial manifold from unstable periodic orbits”, *Phys. Rev. Lett.* **117**, 024101 (2016).
- [67] X. Ding and P. Cvitanović, “Periodic eigendecomposition and its application in Kuramoto-Sivashinsky system”, *SIAM J. Appl. Dyn. Syst.* **15**, 1434–1454 (2016).
- [68] E. J. Doedel, A. R. Champneys, T. F. Fairgrieve, Y. A. Kuznetsov, B. Sandstede, and X. Wang, *AUTO: Continuation and Bifurcation Software for Ordinary Differential Equations* (2007).
- [69] F. W. Dorr, “The direct solution of the discrete Poisson equation on a rectangle”, *SIAM Rev.* **12**, 248–263 (1970).
- [70] M. S. Dresselhaus, G. Dresselhaus, and A. Jorio, *Group Theory: Application to the Physics of Condensed Matter* (Springer, New York, 2007).
- [71] H. R. Dullin and J. D. Meiss, “Stability of minimal periodic orbits”, *Phys. Lett. A* **247**, 227–234 (1998).
- [72] H. R. Dullin and J. D. Meiss, “Generalized Hénon maps: the cubic diffeomorphisms of the plane”, *Physica D* **143**, 262–289 (2000).
- [73] D. S. Dummit and R. M. Foote, *Abstract Algebra* (Wiley, 2003).
- [74] E. N. Economou, *Green’s Functions in Quantum Physics* (Springer, Berlin, 2006).
- [75] S. Elaydi, *An Introduction to Difference Equations*, 3rd ed. (Springer, Berlin, 2005).
- [76] A. Endler and J. A. C. Gallas, “Conjugacy classes and chiral doublets in the Hénon Hamiltonian repeller”, *Phys. Lett. A* **356**, 1–7 (2006).
- [77] A. Endler and J. A. C. Gallas, “Reductions and simplifications of orbital sums in a Hamiltonian repeller”, *Phys. Lett. A* **352**, 124–128 (2006).

- [78] H. Faisst and B. Eckhardt, “Traveling waves in pipe flow”, *Phys. Rev. Lett.* **91**, 224502 (2003).
- [79] M. J. Feigenbaum and B. Hasslacher, “Irrational decimations and path-integrals for external noise”, *Phys. Rev. Lett.* **49**, 605–609 (1982).
- [80] A. L. Fetter and J. D. Walecka, *Theoretical Mechanics of Particles and Continua* (Dover, New York, 2003).
- [81] L. Flatto, J. C. Lagarias, and B. Poonen, “The zeta function of the beta transformation”, *Ergodic Theory Dynam. Systems* **14**, 237–266 (1994).
- [82] S. Friedland and J. Milnor, “Dynamical properties of plane polynomial automorphisms”, *Ergodic Theory Dynam. Systems* **9**, 67–99 (1989).
- [83] P. M. Gade and R. E. Amritkar, “Spatially periodic orbits in coupled-map lattices”, *Phys. Rev. E* **47**, 143–154 (1993).
- [84] G. Giacomelli, S. Lepri, and A. Politi, “Statistical properties of bidimensional patterns generated from delayed and extended maps”, *Phys. Rev. E* **51**, 3939–3944 (1995).
- [85] J. F. Gibson, *Channelflow: A spectral Navier-Stokes simulator in C++*, tech. rep., Channelflow.org (U. New Hampshire, 2019).
- [86] J. F. Gibson, J. Halcrow, and P. Cvitanović, “Visualizing the geometry of state-space in plane Couette flow”, *J. Fluid Mech.* **611**, 107–130 (2008).
- [87] S. Gnutzmann, T. Guhr, H. Schomerus, and K. Życzkowski, “Special issue in honour of the life and work of Fritz Haake”, *J. Phys. A* **54**, 130301 (2021).
- [88] C. Godsil and G. F. Royle, *Algebraic Graph Theory* (Springer, New York, 2013).
- [89] G. H. Golub and C. F. Van Loan, *Matrix Computations*, 4th ed. (J. Hopkins Univ. Press, Baltimore, MD, 2013).
- [90] J. Guckenheimer and B. Meloon, “Computing periodic orbits and their bifurcations with automatic differentiation”, *SIAM J. Sci. Comput.* **22**, 951–985 (2000).
- [91] M. N. Gudorf, *Spatiotemporal Tiling of the Kuramoto-Sivashinsky Equation*, PhD thesis (School of Physics, Georgia Inst. of Technology, Atlanta, 2020).
- [92] M. N. Gudorf, *Orbithunter: Framework for Nonlinear Dynamics and Chaos*, tech. rep. (School of Physics, Georgia Tech, 2021).
- [93] M. N. Gudorf, N. B. Budanur, and P. Cvitanović, *Spatiotemporal tiling of the Kuramoto-Sivashinsky flow*, In preparation, 2022.
- [94] D. Guido, T. Isola, and M. L. Lapidus, “Thara zeta functions for periodic simple graphs”, in *C*-algebras and Elliptic Theory II*, edited by D. Burghelea, R. Melrose, A. S. Mishchenko, and E. V. Troitsky (Birkhäuser, Basel, 2008), pp. 103–121.
- [95] V. Gurarie and A. Migdal, “Instantons in the Burgers equation”, *Phys. Rev. E* **54**, 4908–4914 (1996).

- [96] B. Gutkin, L. Han, R. Jafari, A. K. Saremi, and P. Cvitanović, “Linear encoding of the spatiotemporal cat map”, *Nonlinearity* **34**, 2800–2836 (2021).
- [97] B. Gutkin and V. Osipov, “Classical foundations of many-particle quantum chaos”, *Nonlinearity* **29**, 325–356 (2016).
- [98] M. C. Gutzwiller, *Chaos in Classical and Quantum Mechanics* (Springer, New York, 1990).
- [99] F. Haake, *Quantum Signatures of Chaos*, 3rd ed. (Springer, Berlin, 2010).
- [100] J. F. Heagy, “A physical interpretation of the Hénon map”, *Physica D* **57**, 436–446 (1992).
- [101] M. Hénon, “A two-dimensional mapping with a strange attractor”, *Commun. Math. Phys.* **50**, 94–102 (1976).
- [102] G. W. Hill, “On the part of the motion of the lunar perigee which is a function of the mean motions of the sun and moon”, *Acta Math.* **8**, 1–36 (1886).
- [103] B. Hof, C. W. H. van Doorne, J. Westerweel, F. T. M. Nieuwstadt, H. Faisst, B. Eckhardt, H. Wedin, R. R. Kerswell, and F. Waleffe, “Experimental observation of nonlinear traveling waves in turbulent pipe flow”, *Science* **305**, 1594–1598 (2004).
- [104] E. Hopf, “A mathematical example displaying features of turbulence”, *Commun. Pure Appl. Math.* **1**, 303–322 (1948).
- [105] G. Y. Hu and R. F. O’Connell, “Analytical inversion of symmetric tridiagonal matrices”, *J. Phys. A* **29**, 1511 (1996).
- [106] G. Y. Hu, J. Y. Ryu, and R. F. O’Connell, “Analytical solution of the generalized discrete Poisson equation”, *J. Phys. A* **31**, 9279 (1998).
- [107] Y. Ihara, “On discrete subgroups of the two by two projective linear group over p-adic fields”, *J. Math. Soc. Japan* **18**, 219–235 (1966).
- [108] S. Isola, “ ζ -functions and distribution of periodic orbits of toral automorphisms”, *Europhys. Lett.* **11**, 517–522 (1990).
- [109] A. K. Jiotsa, A. Politi, and A. Torcini, “Convective Lyapunov spectra”, *J. Phys. A* **46**, 254013 (2013).
- [110] W. Just, “Equilibrium phase transitions in coupled map lattices: A pedestrian approach”, *J. Stat. Phys.* **105**, 133–142 (2001).
- [111] B. Kastening, “Simplified transfer matrix approach in the two-dimensional Ising model with various boundary conditions”, *Phys. Rev. E* **66**, 057103 (2002).
- [112] G. Kawahara and S. Kida, “Periodic motion embedded in plane Couette turbulence: Regeneration cycle and burst”, *J. Fluid Mech.* **449**, 291 (2001).
- [113] J. P. Keating, “The cat maps: quantum mechanics and classical motion”, *Nonlinearity* **4**, 309–341 (1991).
- [114] Y.-O. Kim, J. Lee, and K. K. Park, “A zeta function for flip systems”, *Pacific J. Math.* **209**, 289–301 (2003).

- [115] H.-T. Kook and J. D. Meiss, “Application of Newton’s method to Lagrangian mappings”, *Physica D* **36**, 317–326 (1989).
- [116] Y. Lan and P. Cvitanović, “Variational method for finding periodic orbits in a general flow”, *Phys. Rev. E* **69**, 016217 (2004).
- [117] S. Lepri, A. Politi, and A. Torcini, “Chronotopic Lyapunov analysis. I. A detailed characterization of 1D systems”, *J. Stat. Phys.* **82**, 1429–1452 (1996).
- [118] S. Lepri, A. Politi, and A. Torcini, “Chronotopic Lyapunov analysis. II. Towards a unified approach”, *J. Stat. Phys.* **88**, 31–45 (1997).
- [119] J. Li and S. Tomsovic, “Exact relations between homoclinic and periodic orbit actions in chaotic systems”, *Phys. Rev. E* **97**, 022216 (2017).
- [120] M.-C. Li and M. Malkin, “Bounded nonwandering sets for polynomial mappings”, *J. Dynam. Control Systems* **10**, 377–389 (2004).
- [121] A. J. Lichtenberg and M. A. Lieberman, *Regular and Chaotic Dynamics*, 2nd ed. (Springer, New York, 2013).
- [122] W. J. Lick, *Difference Equations from Differential Equations* (Springer, Berlin, 1989).
- [123] D. A. Lind, “A zeta function for Z^d -actions”, in *Ergodic Theory of Z^d Actions*, edited by M. Pollicott and K. Schmidt (Cambridge Univ. Press, 1996), pp. 433–450.
- [124] D. Lippolis and P. Cvitanović, “How well can one resolve the state space of a chaotic map?”, *Phys. Rev. Lett.* **104**, 014101 (2010).
- [125] M. Lutzky, “Counting stable cycles in unimodal iterations”, *Phys. Lett. A* **131**, 248–250 (1988).
- [126] M. Lutzky, “Counting hyperbolic components of the Mandelbrot set”, *Phys. Lett. A* **177**, 338–340 (1993).
- [127] R. S. MacKay, *Renormalisation in Area-preserving Maps* (World Scientific, Singapore, 1993).
- [128] R. S. MacKay, “Indecomposable coupled map lattices with non-unique phase”, in *Dynamics of Coupled Map Lattices and of Related Spatially Extended Systems*, edited by J.-R. Chazottes and B. Fernandez (Springer, 2005), pp. 65–94.
- [129] R. S. MacKay and J. D. Meiss, “Linear stability of periodic orbits in Lagrangian systems”, *Phys. Lett. A* **98**, 92–94 (1983).
- [130] R. S. MacKay, J. D. Meiss, and I. C. Percival, “Transport in Hamiltonian systems”, *Physica D* **13**, 55–81 (1984).
- [131] P. C. Martin, E. D. Siggia, and H. A. Rose, “Statistical dynamics of classical systems”, *Phys. Rev. A* **8**, 423–437 (1973).
- [132] J. D. Meiss, “Symplectic maps, variational principles, and transport”, *Rev. Mod. Phys.* **64**, 795–848 (1992).

- [133] D. Micciancio and S. Goldwasser, *Complexity of Lattice Problems - A Cryptographic Perspective* (Springer, New York, 2002).
- [134] J. W. Mintmire, B. I. Dunlap, and C. T. White, “Are Fullerene tubules metallic?”, *Phys. Rev. Lett.* **68**, 631–634 (1992).
- [135] I. Montvay and G. Münster, *Quantum Fields on a Lattice* (Cambridge Univ. Press, Cambridge, 1994).
- [136] B. Mramor and B. Rink, “Ghost circles in lattice Aubry-Mather theory”, *J. Diff. Equ.* **252**, 3163–3208 (2012).
- [137] G. Münster, “Lattice quantum field theory”, *Scholarpedia* **5**, 8613 (2010).
- [138] G. Münster and M. Walzl, *Lattice gauge theory - A short primer*, 2000.
- [139] P. J. Myrberg, “Iteration der reellen Polynome zweiten Grades I”, *Ann. Acad. Sc. Fenn. A* **256**, 1–10 (1958).
- [140] P. J. Myrberg, “Iteration von quadratwurzeloperationen”, *Ann. Acad. Sc. Fenn. A* **259**, 1–10 (1958).
- [141] P. J. Myrberg, “Iteration der reellen Polynome zweiten Grades II”, *Ann. Acad. Sc. Fenn. A* **268**, 1–13 (1959).
- [142] P. J. Myrberg, “Sur l’itération des polynomes réels quadratiques”, *J. Math. Pures Appl.* **41**, 339–351 (1962).
- [143] P. J. Myrberg, “Iteration der reellen Polynome zweiten Grades III”, *Ann. Acad. Sc. Fenn. A* **336**, 1–13 (1963).
- [144] J. Nielsen, “Über die Minimalzahl der Fixpunkte bei den Abbildungstypen der Ringflächen”, *Math. Ann.* **82**, 83–93 (1920).
- [145] L. Onsager, “Crystal statistics. I. A Two-dimensional model with an order-disorder transition”, *Phys. Rev.* **65**, 117–149 (1944).
- [146] E. Ott, *Chaos and Dynamical Systems* (Cambridge Univ. Press, Cambridge, 2002).
- [147] J. P. Parker and T. M. Schneider, “Variational methods for finding periodic orbits in the incompressible Navier-Stokes equations”, *J. Fluid. Mech.* **941**, A17 (2022).
- [148] R. Peierls, “Zur Theorie des Diamagnetismus von Leitungselektronen”, *Z. Phys.* **80**, 763–791 (1933).
- [149] I. Percival and F. Vivaldi, “A linear code for the sawtooth and cat maps”, *Physica D* **27**, 373–386 (1987).
- [150] S. D. Pethel, N. J. Corron, and E. Boltt, “Deconstructing spatiotemporal chaos using local symbolic dynamics”, *Phys. Rev. Lett.* **99**, 214101 (2007).
- [151] H. Poincaré, “Sur les déterminants d’ordre infini”, *Bull. Soc. Math. France* **14**, 77–90 (1886).
- [152] H. Poincaré, *Les méthodes nouvelles de la mécanique céleste*, For a very readable exposition of Poincaré’s work and the development of the dynamical systems theory up to 1920’s see [15]. (Guthier-Villars, Paris, 1899).

- [153] A. Politi and A. Torcini, “Periodic orbits in coupled Hénon maps: Lyapunov and multifractal analysis”, *Chaos* **2**, 293–300 (1992).
- [154] A. Politi and A. Torcini, “Towards a statistical mechanics of spatiotemporal chaos”, *Phys. Rev. Lett.* **69**, 3421–3424 (1992).
- [155] A. Politi, A. Torcini, and S. Lepri, “Lyapunov exponents from node-counting arguments”, *J. Phys. IV* **8**, 263 (1998).
- [156] M. Pollicott, *Dynamical zeta functions*, in *Smooth Ergodic Theory and Its Applications*, Vol. 69, edited by A. Katok, R. de la Llave, Y. Pesin, and H. Weiss (2001), pp. 409–428.
- [157] C. Pozrikidis, *An Introduction to Grids, Graphs, and Networks* (Oxford Univ. Press, Oxford, UK, 2014).
- [158] P. Ren, T. Aleksić, D. Emms, R. C. Wilson, and E. R. Hancock, “Quantum walks, Ihara zeta functions and cospectrality in regular graphs”, *Quantum Inf. Process.* **10**, 405–417 (2010).
- [159] A. Rényi, “Representations for real numbers and their ergodic properties”, *Acta Math. Acad. Sci. Hung.* **8**, 477–493 (1957).
- [160] V. Rosenhaus and M. Smolkin, *Feynman rules for wave turbulence*, 2022.
- [161] O. E. Rössler, “An equation for continuous chaos”, *Phys. Lett. A* **57**, 397–398 (1976).
- [162] H. J. Rothe, *Lattice Gauge Theories - An Introduction* (World Scientific, Singapore, 2005).
- [163] S. Saito, “A proof of Terras’ conjecture on the radius of convergence of the Ihara zeta function”, *Discrete Math.* **341**, 990–996 (2018).
- [164] I. Sato, “Bartholdi zeta functions of group coverings of digraphs”, *Far East J. Math. Sci.* **18**, 321–339 (2005).
- [165] C. Simó, “On the Hénon-Pomeau attractor”, *J. Stat. Phys.* **21**, 465–494 (1979).
- [166] B. Simon, “Almost periodic Schrödinger operators: A review”, *Adv. Appl. Math.* **3**, 463–490 (1982).
- [167] S. Smale, “Differentiable dynamical systems”, *Bull. Amer. Math. Soc.* **73**, 747–817 (1967).
- [168] J. Stephenson and D. T. Ridgway, “Formulae for cycles in the Mandelbrot set II”, *Physica A* **190**, 104–116 (1992).
- [169] D. Sterling and J. D. Meiss, “Computing periodic orbits using the anti-integrable limit”, *Phys. Lett. A* **241**, 46–52 (1998).
- [170] D. G. Sterling, H. R. Dullin, and J. D. Meiss, “Homoclinic bifurcations for the Hénon map”, *Physica D* **134**, 153–184 (1999).
- [171] G. Sterling D., *Anti-integrable Continuation and the Destruction of Chaos*, PhD thesis (Univ. Colorado, Boulder, CO, 1999).

- [172] S. H. Strogatz, *Nonlinear Dynamics and Chaos* (Westview Press, Boulder, CO, 2014).
- [173] R. Sturman, J. M. Ottino, and S. Wiggins, *The Mathematical Foundations of Mixing* (Cambridge Univ. Press, 2006).
- [174] T. Sunada, *Topological Crystallography* (Springer, Tokyo, 2013).
- [175] A. Terras, *Zeta Functions of Graphs: A Stroll through the Garden* (Cambridge Univ. Press, 2010).
- [176] M. Toda, *Theory of Nonlinear Lattices* (Springer, Berlin, 1989).
- [177] D. Treschev and O. Zubelevich, “Hill’s formula”, in *Introduction to the Perturbation Theory of Hamiltonian Systems* (Springer, Berlin, 2009), pp. 143–162.
- [178] D. Viswanath, “The Lindstedt-Poincaré technique as an algorithm for finding periodic orbits”, *SIAM Rev.* **43**, 478–496 (2001).
- [179] D. Viswanath, “Symbolic dynamics and periodic orbits of the Lorenz attractor”, *Nonlinearity* **16**, 1035–1056 (2003).
- [180] D. Viswanath, “The fractal property of the Lorenz attractor”, *Physica D* **190**, 115–128 (2004).
- [181] D. Wang and Y. Lan, A reduced variational approach for searching cycles in high-dimensional systems, 2022.
- [182] Wikipedia contributors, Index of a subgroup — Wikipedia, The Free Encyclopedia, 2022.
- [183] S. V. Williams, X. Wang, H. Liang, and P. Cvitanović, Nonlinear chaotic lattice field theory, In preparation, 2022.
- [184] A. P. Willis, Openpipeflow: Pipe flow code for incompressible flow, tech. rep., Openpipeflow.org (U. Sheffield, 2014).
- [185] U. Wolff, “Triviality of four dimensional ϕ^4 theory on the lattice”, *Scholarpedia* **9**, 7367 (2014).
- [186] H. W. Wyld, “Formulation of the theory of turbulence in an incompressible fluid”, *Ann. Phys.* **14**, 143–165 (1961).
- [187] F.-G. Xie and B. L. Hao, “Counting the number of periods in one-dimensional maps with multiple critical points”, *Physica A* **202**, 237–263 (1994).
- [188] D. Zhou, Y. Xiao, and Y.-H. He, “Seiberg duality, quiver gauge theories, and Ihara’s zeta function”, *Int. J. Mod. Phys. A* **30**, 1550118 (2015).